EUROPEAN Journal of Molecular Biotechnology

Has been issued since 2013.
ISSN 2310-6255. E-ISSN 2409-1332
2015. Vol.(8). Is. 2. Issued 4 times a year

The journal is registered by Federal Service for Supervision of Mass Media, Communications and Protection of Cultural Heritage (Russia). Registration Certificate **ПИ № ФС77-55114** 26.08.2013.

Journal is indexed by: **CiteFactor** – Directory of International Reseach Journals (Canada), **Cross Ref** (UK), **EBSCOhost Electronic Journals Service** (USA), **Global Impact Factor** (Australia), **International Society of Universal Research in Sciences** (Pakistan), **Journal Index** (USA), **Electronic scientific library** (Russian Federation), **Open Academic Journals Index** (Russian Federation), **Sherpa Romeo** (Spain), **ULRICH's WEB** (USA), **Universal Impact Factor** (Australia).

Postal Address: 26/2 Konstitutcii, Office 6
354000 Sochi, Russian Federation

Website: http://ejournal8.com/
E-mail: ejm2013@mail.ru

Founder and Editor: Academic Publishing House *Researcher*

Passed for printing 16.06.15.
Format 21 × 29,7/4.
Enamel-paper. Print screen.
Headset Georgia.
Ych. Izd. l. 4,5. Ysl. pech. l. 4,2.

Circulation 500 copies. Order № 8.

European Journal of Molecular Biotechnology

2015

Is. 2

Европейский журнал молекулярных биотехнологий

2015

№ 2

Европейский журнал молекулярных биотехнологий

Издается с 2013 г. ISSN 2310-6255. E-ISSN 2409-1332
2015. № 2 (8). Выходит 4 раза в год.

Журнал зарегистрирован Федеральной службой по надзору в сфере массовых коммуникаций, связи и охраны культурного наследия (Российская Федерация). Свидетельство о регистрации средства массовой информации ПИ № ФС77-55114 от 26.08.2013 г.

Журнал индексируется в: **CiteFactor** – Directory of International Reseach Journals (Канада), **Cross Ref** (Великобритания), **EBSCOhost Electronic Journals Service** (США), **Global Impact Factor** (Австралия), **International Society of Universal Research in Sciences** (Пакистан), **Journal Index** (США), **Научная электронная библиотека** (Россия), **Open Academic Journals Index** (Россия), **Sherpa Romeo** (Испания), **ULRICH's WEB** (США), **Universal Impact Factor** (Австралия).

Адрес редакции: 354000, Российская Федерация, г. Сочи, ул. Конституции, д. 26/2, оф. 6
Сайт журнала: http://ejournal8.com/
E-mail: ejm2013@mail.ru

Учредитель и издатель: ООО «Научный издательский дом "Исследователь"» - Academic Publishing House *Researcher*

Подписано в печать 16.06.15.
Формат 21 × 29,7/4.
Бумага офсетная.

Печать трафаретная.
Гарнитура Georgia.
Уч.-изд. л. 4,5. Усл. печ. л. 4,2.
Тираж 500 экз. Заказ № 8.

CONTENTS

Published in the Russian Federation
European Journal of Molecular Biotechnology
Has been issued since 2013.
ISSN: 2310-6255
E-ISSN 2409-1332
Vol. 8, Is. 2, pp. 56-62, 2015

DOI: 10.13187/ejmb.2015.8.56
www.ejournal8.com

UDC 577.29

Isolation of Promoters and Fragments of Genes Controlling Endosperm Development Without Fertilization in Arabidopsis and Engineering of the Antisense Constructions*

Grigory A. Gerashchenkov
Gulnar R. Yasybaeva
Nataliya A. Rozhnova
Aleksey V. Chemeris

Institute of Biochemistry and Genetics of Ufa Research Centre of RAS, Russian Federation

Corresponding author: Grigory Alekseevich Gerashchenkov
E-mail**:** apomixis@anrb.ru

Abstract

Apomixis is asexual seed reproduction without both meiosis and fertilization based on the complex developmental processes such as apomeiosis, parthenogenesis and specific endosperm development. This investigation is aimed at engineering of apomixis in *Arabidopsis thaliana* with sexual seed reproduction. The fragments of known genes of endosperm formation MEA, FIE, FIS2 and gene of apomeiosis DYAD (as control) were isolated using Q5 high fidelity DNA polymerase. These gene fragments of interest at the antisense orientation were fused with isolated constitutive and meiosis specific promoters of Arabidopsis at NcoI sites. The fused promoter-gene fragment modules were cloned in pCambia1301 at SalI cites. The engineered constructions will be used for the floral dip transformation of Arabidopsis and down regulation of these genes at engineering of apomixis.

Keywords: *Arabidopsis thaliana*, apomixis, endosperm formation, *MEA, FIE, FIS2*.

Introduction

Apomixis (from Greek apo, without + mixis, mixture) is asexual seed reproduction of floral plants at which germs arise without both meiosis and fertilization [1 – 4]. In fact apomixis is a natural system of maternal genome cloning by seeds. Applied usage of apomixis promises the economic and social benefits exceeding a prize from the "green revolution" which solved a hunger problem in many developing countries. So, only the profit on world production of apomictic rice is estimated more than at $2.0 billion in a year [4].

Already the first apomictic experiments of G. Mendel showed that there are objects for which general principles of inheritance don't work (see experiments with Hieracium plants). The molecular nature of an apomixis still remains unclear [5 – 7]. As it is established so far, it occurs in

* The article is published in accordance with collective decision of the Editorial Board and the Organizing Committee of the 19th international conference "Biology of the XXI century" (Pushchino, April 2015).

the case of specific abnormal alteration of normal course of meiosis. That is why apomixis may be result of the sophisticated deregulation of classical sexual seed reproduction. The first attempt of engineering of apomixis de novo in Arabidopsis plants with sexual reproduction proved to have promising prospects [8].

Probably the construction of transgene plants with differently expressed genes of apomictic triad (sporogenesis, gametogenesis and an endosperm formation) under the control the cell-specific promoters will allow to construct prototype of apomixis at many agricultural forms with sexual reproduction [7]. **This approach could allow understanding** how genome works upon transition from amphimixis to apomixis in floral plants. The goal of work is the creation of genetically engineered constructions with genes involving in the endosperm formation in Arabidopsis plants.

Materials and methods

1. Biological material

The selection of model objects is very important at the investigations of reproductive systems of floral plants in general and the apomixis in particular [9]. Extensive molecular and genetic resources (completely sequenced genome, mutants ets) are available for Arabidopsis thaliana that facilitates search of the genes participating in the control of apomixis. there The plants of Arabidopsis thaliana of the ecotypes Ler2n, Col 0 (2n) and Wass were in the focus of researches.

2. Methods of molecular biology

Total DNA was extracted from sprouts and leaves of plants by salt extraction method [10]. The screening of perspective promoter and gene candidates was performed from literary data [4, 11]. The analysis of nucleotide sequences and selection of primers carried out with usage of Genbank data and other Resources of PubMed (http://www.ncbi.nlm.nih.gov**).** Promoters and fragments of genes were isolated by means of HiFi Q5 polymerase (NEB). 1% agarose gel-electrophoresis of DNA fragments were carried out in 1x TAE buffer. The subsequent cleaning of DNA preparations was carried out using special kits for cleaning of DNA (Cytokin, Russia) and Quantum PrepTM Freeze'N Squeeze DNA Gel Extraction Spin Columns (BioRad). Restrictase FastDigestTM NcoI (Fermentas) was used to create NcoI sticky ends at promoters and antisense fragments of genes. The fusion of promoters and antisense fragments of genes at NcoI ends was carried out using T4 DNA ligase (Fermentas) or (NEB). The alloyed constructions were amplified by HiFi Q5 polymerase (NEB) and fractioned in agarose gel slab for the subsequent cleaning. Resrictase FastDigestTM SalI (Fermentas) was used for the creation of sticky ends and following cloning of the constructions in pCambia1301 plasmid. Further selection of plasmids and control of inserts were carried out. Nucleotide sequence analysis of DNA preparations was carried out at Beckman Coultier or AppliedBiosystems 3500 analyzers. Thus, in our work we used the following promoters: constitutive (as positive control) – *pMEF1* and *pUBQ* promoters [12], meiosis specific – *pAtDMC1* and *pMS5* promoters [13], ovule specific – *pAGL11* promoter [14], and also gene fragments in the antisense orientation – *DYAD* [15], *MEA* [16], *FIE* [17] and *FIS2* [18].

Results

At first the selection of the most perspective candidate genes of autonomous endosperm development was carried out as it discussed in the articles [4, 11]. Summary of these genes are in Tab.1. Our work is devoted to creation of recombinant plasmids on the basis of the binary vector pCambia 1301 for genetic transformation of plants. Genes *DYAD, SERK* and fragments of genes of interest (*DYAD, FIE, MEA, FIS2*) under constitutive and ovule specific promoters were cloned in the T-DNK field of pCambia 1301. The scheme of vector constructions is submitted in Fig. 1.

Table 1: Genes candidates used in work

##	**Elements of apomictic triad**	**Genes**	**Gene product / function**
I	Apomeiosis	*DYAD (SWI1)*	Meiosis specific chromatin associated protein (phospholipase C), participates in chromosome non-disjunction
II	Parthenogenesis	*SERK1* (Somatic embryogenesis receptor kinase)	Serin-treonin protein kinase, initiates a somatic embryogenesis
III	Autonomous endosperm development	1. *FIE* (Fertilization-independent endosperm) 2. *MEA/ MEDEA* (Maternal embryogenesis control protein) 3. *FIS2* (Fertilization-independent seed 2)	Proteins of Polycomb system, repress development of the central cell in ovule

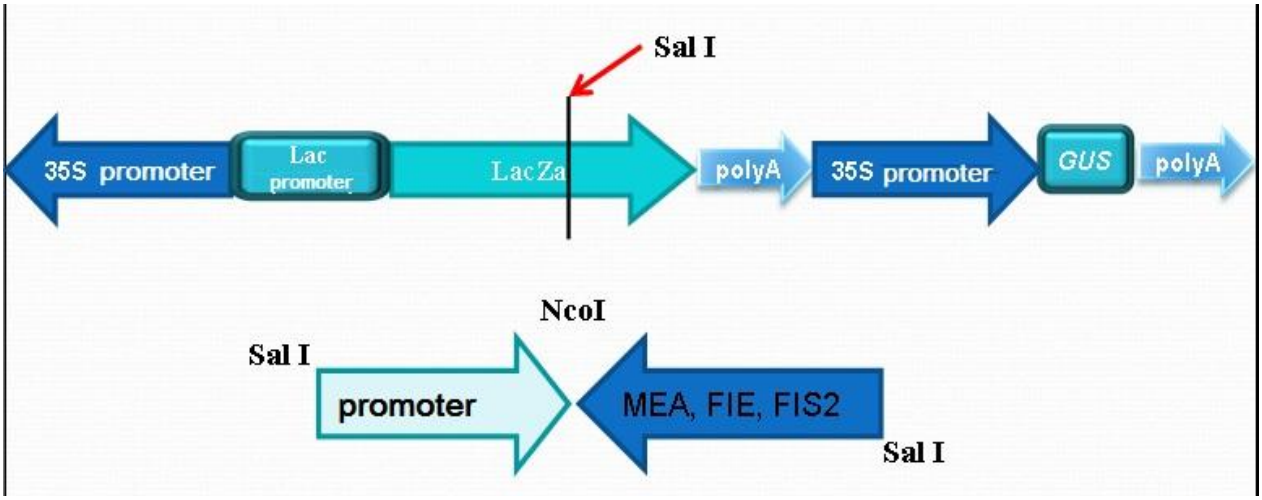

Fig. 1. The scheme of isolation and cloning of promoters and fragments of genes in the antisense orientation

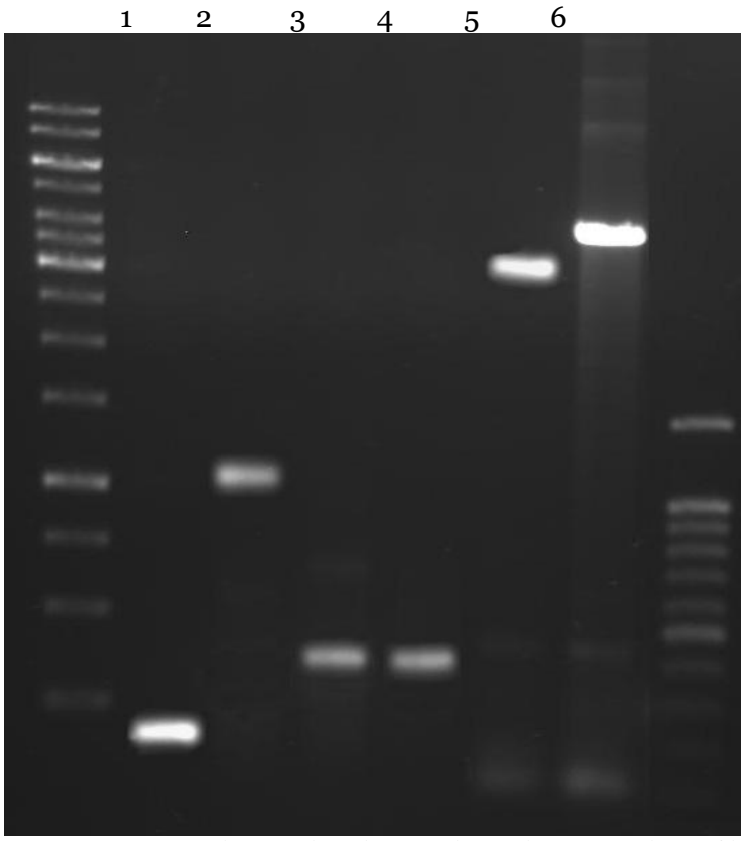

Fig. 2. The electrophoresis separation of isolated fragments of genes.
Fragments of genes are in the antisense orientation:
1 - *DYAD* (0.2 kb); 2 - *MEA* (1.0 kb), 3 - *FIE* (0.4 kb); 4 - *FIS2* (0.4 kb). Full size gene in sense orientation: 5 – *DYAD* (3.0 kb); 6 - *SERK* (4.0 kb)

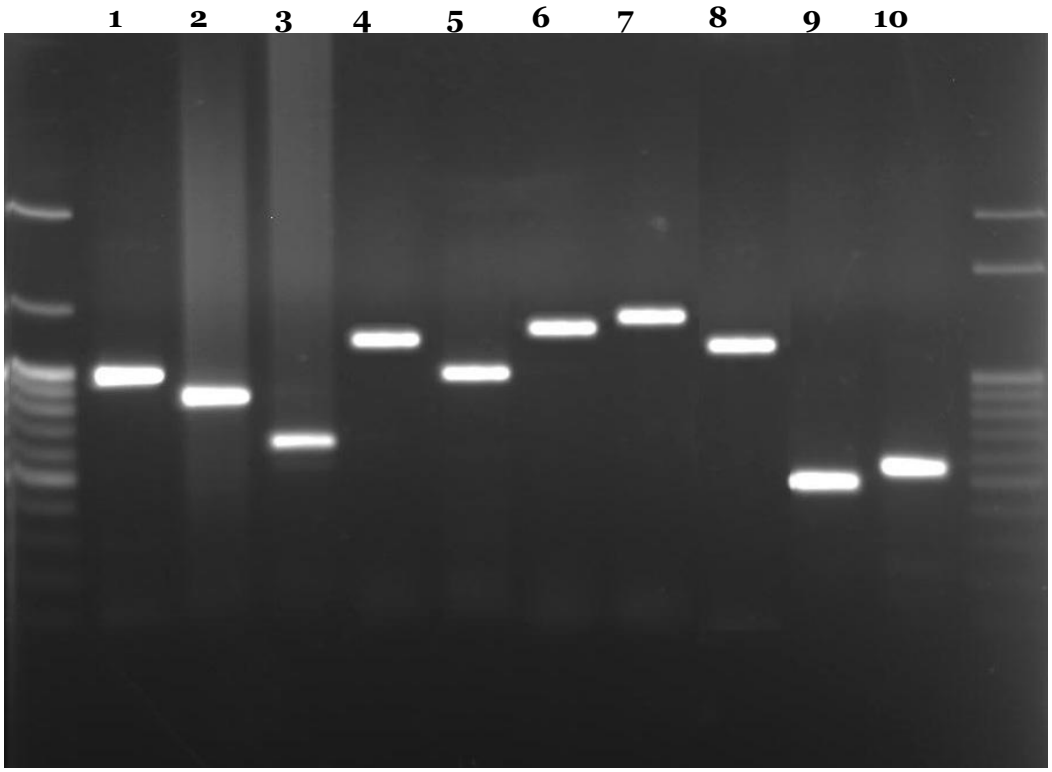

Fig. 3. The electrophoresis separation of isolated promoters
Promoters: 1 - p1 (*pEF1a*), 2 - p2 (*pUBQ*), 3 - p4 (*pMS5*), 4 - p11 (*pRKD1*), 5 - p10 (*pDD45*), 6 - p7 (*pAt5g40260*), 7 - p8 (*pAt5g40260*), 8 - p11 (*pRKD1*), 9 - p9 (*pEC1*), 10 - p13 (*pRKD2p*)

Table 2: The scheme of fused constructions including promoters and fragments of genes in the antisense orientation

NN, names, and sizes	**Genes**			
Promoters	**1) *DYAD*, 0.2 kb**	**2) *MEA*, 1.0 kb**	**3) *FIE*, 0.4 kb**	**4) *FIS2*, 0.4kb**
1) *pEF1a*, 1.0 kb	1.2 kb	2.0 kb	1.4 kb	1.4 kb
2) *pUBQ*, 0.9 kb	1.1 kb	1.9 kb	1.3 kb	1.3 kb
3) *pDMC1*, 3.0 kb	3.2 kb			
4) *pMS5*, 0.6 kb	**0.8 kb**	**1.6 kb**	**1.0 kb**	**1.0 kb**

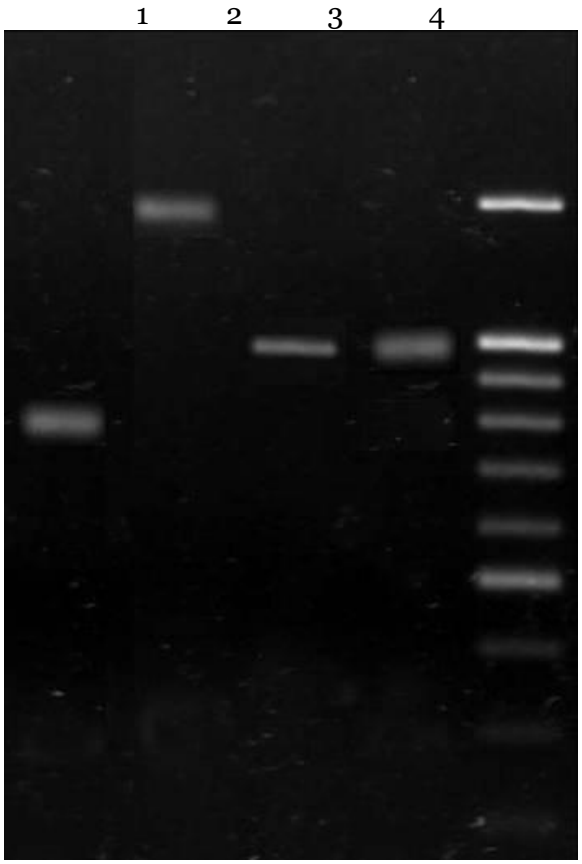

Fig. 4. The electrophoresis separation of constructions containing fragments of genes in the antisense orientation under pMS5 promoter

The created constructions with the fragments of genes in the antisense orientation:
1 – *pMS5_DYAD* (0.2 + 0.6 = 0.8 kb); 2 - *pMS5_MEA* (1.0 + 0.6 = 1.6 kb) ; 3 - *pMS5 _FIE* (0.4 + 0.6 = 1.0 kb); 4 - *pMS5 _FIS2* (0.4 + 0.6 = 1.6 kb).

The control DNA sequencing the cloned elements validated correct assemblies of the constructions.

Discussion

The idea of apomixis engineering de novo due to the deregulation of the genes involved in sexual process at plants (first of all in arabidopsis) was stated in 1993 [19]. It is known that apomictic ways don't function independently from a classical sexual way of seed plants, and, therefore, the genes controlling apomixis can't be entirely new in the function, and, most likely, are subjected to regulatory changes [20]. We need take into account classical model plants, such as arabidopsis and corn, have no apomixis, and however have abundance of forms and lines reminding apomixis ("miming apomixis"). Availability of information about some genes involved in functioning of an apomictic triad – apomeiosis, parthenogenesis and endosperm formation (see Table 1.) create fine prerequisites for the creation of apomictic prototype at arabidopsis.

So, the group of d'Erfurth managed to create in the lab a MiMe genotype of arabidopsis for which meiosis is entirely replaced with a mitosis due to a combination of three various genes involved in meiosis [9]. The simultaneous suppression of *OSD1/TAM, At-Spo11-1* and *Atrec8* genes leads to formation of male and female gametes. Thus artificial mutants of MiMe only demonstrate a sign of apomeiosis (the first elements of an apomictic triad) and aren't capable to a parthenogenesis. Thus, MiMe genotype plants bring forth offspring with the doubled set of chromosomes, and special schemes of crossings are necessary for lowering of the ploidy level. We will note that artificial MiME system of arabidopsis isn't known at natural apomicts. Thus, the engineering of apomixis de novo is an excellent alternative to unsuccessful attempts cloning genes of apomixis.

The strategy of our researches is to place the genes of interest under the transcriptional control of cell-, tissue-, and/or organ- specific promoter, for example, the promoter, specifically expressed in an ovule (ovule-specific promoter). It is known that arabidopsis genes of *FERTILIZATION-INDEPENDENT ENDOSPERM (FIE)* [17], *MEDEA (MEA)* [16] and *FERTILIZATION-INDEPENDENT SEED2 (FIS2)* [18] suppress development of endosperm. Perhaps, the suppression of these genes could initiate the process of the autonomous endosperm development. As a result of this work, we created the genetically engineered constructions containing the key genes in the antisense orientation for down regulation of their expression and following the fertilization-independent seed development (see Fig.1 – 4).

In our lab work we faced with the task to clone genes of *FIE, MEA* and *FIS2* in antisense orientation in binary vector of pCambia 1301 under various promoters. We described the received results in this article. In further work we should introduce vector constructions into arabidopsis plants and to estimate how their work in various lines (especially in mutants with different deviations of developments). The comparative cytogenetic analysis will be used for this purpose. Ploidy levels of control and transgenic plants will be studied too.

The nature of inheritance of transgene constructions and deviation from splitting in progeny of transgene plants will be investigated. Discussions about prospects of use of these or those elements of future constructions for engineering of apomixis is proceeding up to now [4, 6]. However messages except works of d'Erfurth group practically are out [8]. A few references (given in article) show common progress in this field and importance of our results.

Conclusion

All efforts to use of biotechnological of advantages of apomixis assume the transfer of an apomixis in crops. In this direction three key strategy may be useful [21]: (1) a direct introgression of apomixis in agricultural plants by means of traditional schemes of selection; (2) genetic transformation of agricultural plants by means of transfer of the alien genes controlling an expression of an apomixis; and (3) artificial deregulation of own genes controlling sexuality. The recent works performed at Arabidopsis, corn and rice allowed to perform identification of apomixis-like mutants and the corresponding genes [4, 6, 7, 11].

In this investigation we reported about the cloning of *DYAD* gene fragment (as control) and *FIE, MEA* and *FIS2* fragments of genes in the antisense orientation under constitutive and cell- and meiosis specific promoters in binary vectors of pCambia 1301 for the down regulation of the genes of interest controlling autonomous endosperm development. The fused constructions will be used for the production of transgene arabidopsis plants by floral dip method.

Acknowledgements

This work was supported by Russian Foundation of Basic Research (grant No. 14-04-97089) and Bashkirian Acadamy of Sciences (grant No. 40/55-P).

References:

1. Khohlov SS (1967) Apomixis: classification and distribution at angiosperm plants. *Progress of modern genetics,* 1, pp. 43–105.

2. Petrov DF (1988) Apomixis is in nature and experiment. Novosibirsk: *Science (Nauka).* 216 p.

3. Gerashchenkov G, Rozhnova N (2004) Genetic control of gametophytic apomixis: current status of knowledge. *Proceedings of the Latvian Academy of Sciences,* 58 (B, 5/6) , pp. 167–174.

4. Barcaccia G, Albertini E (2013) Apomixis in plant reproduction: a novel perspective on an old dilemma. *Plant Reprod,* 26(3) , pp. 159–179.

5. Bhat V, Dwivedi KK, Khurana JP, Sopry SK (2005) Apomixis: An enigma with potential applications, *Curr. Sci.* 89, pp. 1879–1893.

6. Hand ML and Koltunow AMG (2014) The Genetic Control of Apomixis: Asexual Seed Formation. *Genetics*, pp. 197: 441–450.

7. Arnaud R and Vielle-Calzada J-P (2015) Meiosis, unreduced gametes, and parthenogenesis: implications for engineering clonal seed formation in crops. *Plant Reprod.,* 28(2), pp. 91–102. DOI 10.1007/s00497-015-0262-6

8. d'Erfurth I, Jolivet S, Froger N, Catrice O, Novatchkova M, Mercier R (2009) Turning meiosis into mitosis. *PLoS Biol.* 7, e1000124.

9. Gerashchenkov G, Rozhnova N, Zarjanova L, Gorbunova V, Tyrnov V, and Zavalishina A (1999) Focus on the Saratov collection of Zea mays L. to detect RAPD-markers of parthenogenesis in AT-1 line of maize with the autonomous development of embryo. *Apomixis Newsletter,* 11, pp. 26–31.

10. Aljanabi S M and Martinez I (1997) Universal and rapid salt-extraction of high quality genomic DNA for PCR-based techniques. *Nucleic Acids Res.* 25(22), pp. 4692–4693.

11. Nagaya S, Kawamura K, Shinmyo A and Kato K (2010) The HSP Terminator of Arabidopsis thaliana Increases Gene Expression in Plant Cells. *Plant Cell Physiol.* 51(2), pp. 328–332.

12. Li J, Farmer AD, Lindquist IE, Dukowic-Schulze S, Mudge J, Li T, Retzel EF, Chen C (2012) Characterization of a set of novel meiotically-active promoters in Arabidopsis. *BMC Plant Biology,* 12, p.104.

13. Nain V, Verma A, Kumar N, Sharma P, Ramesh B, Kumar PA (2008) Cloning of an ovule specific promoter from Arabidopsis thaliana and expression of beta-glucuronidase. Indian J Exp Biol, 46(4), pp. 207-211.

14. Ravi M, Marimuthu MPA and Siddiqi I (2008) Gamete formation without meiosis in Arabidopsis. *Nature,* 451, pp. 1121–1125.

15. Grossniklaus U, Vielle-Calzada JP, Hoeppner MA, Gagliano WB (1998) Maternal control of embryogenesis by MEDEA, a polycomb group gene in Arabidopsis. *Science,* 280, pp. 446–450.

16. Ohad N, Yadegari R, Margossian L, Hannon M, Michaeli D, Harada JJ, Goldberg RB, and Fisher RL (1999) Mutations in FIE, a WD polycomb group gene, allow endosperm development without fertilization. *Plant Cell,* 11, pp. 407–415.

17. Luo M, Bilodeau P, Koltunov A, Dennis ES, Peacock WJ and Chaudhury AM (1999) Genes controlling fertilization-independent seed development in Arabidopsis thaliana. *Proc. Natl. Acad. Sci. of USA*. 96, pp. 296–301.

18. Pupilli F, Barcaccia G (2011) Cloning plants by seeds: Inheritance models and candidate genes to increase fundamental knowledge for engineering apomixis in sexual crops. *J. Biotechnol,* doi:10.1016/j.jbiotec.2011.08.028.

19. Chaudhury AM and Peacock JW (1993) Approaches to isolating apomictic mutants in *Arabidopsis thaliana*: Prospects and progress. In *Apomixis: Exploiting Hybrid Vigor in Rice*, G.S. Khush, ed (Manila, The Philippines: International Rice Research Institute), pp. 66–71.

20. Tucker MR, Araujo AC, Paech NA, Hecht V, Schmidt ED, Rossell JB, De Vries SC, Koltunow AM (2003) Sexual and apomictic reproduction in Hieracium sub-genus pilosella are closely interrelated developmental pathways. *Plant Cell,* 15, pp. 1524–1537.

21. Drews GN, Koltunow AM (2011) The female gametophyte. *Arabidopsis Book*. 9:e0155. doi: 10.1199/tab.0155. Epub 2011 Dec 26.

Published in the Russian Federation
European Journal of Molecular Biotechnology
Has been issued since 2013.
ISSN: 2310-6255
E-ISSN 2409-1332
Vol. 8, Is. 2, pp. 63-79, 2015

DOI: 10.13187/ejmb.2015.8.63
www.ejournal8.com

UDC 553.9: 470.22

Studying the Mechanism of Phototransformation of Light Signal by Various Mammal and Bacterial Photoreceptor Pigments – Rhodopsin, Iodopsin and Bacteriorhodopsin

[1] Ignat Ignatov
[2] Oleg Mosin

[1] The Scientific Research Center of Medical Biophysics (SRC MB), Bulgaria
Professor, D.Sc., director of SRC MB
1111, Sofia, N. Kopernik street, 32
E-mail: mbioph@dir.bg
[2] Moscow State University of Applied Biotechnology, Russian Federation
Senior research Fellow of Biotechnology Department, Ph. D. (Chemistry)
103316, Moscow, Talalihina ulitza, 33
E-mail: mosin-oleg@yandex.ru

Abstract

This review article outlines the structure and function of mammal and bacterial photoreceptor pigments (rhodopsin, iodopsin, bacteriorhodopsin) and their aspects of bio-nanotechnological usage. On an example of bacteriorhodopsin is described the method of its isolation from purple membranes of photo-organotrophic halobacterium *Halobacterium halobium ET 1001* by cellular autolysis by distilled water, processing of bacterial biomass by ultrasound at 22 KHz, alcohol extraction of low and high-weight molecular impurities, cellular RNA, carotenoids and lipids, the solubilization with 0,5 % (w/v) SDS-Na and subsequent fractionation by methanol and gel filtration chromatography on Sephadex G-200 Column balanced with 0,09 *M* Tris-buffer (*pH* = 8,35) with 0,1 % (w/v) SDS-Na and 2,5 mM EDTA. Within the framework of the research the mechanism of color perception by the visual retina analyzer having the ability to analyze certain ranges of the optical spectrum as colors, was studied along with an analysis of the additive mixing of two or more colors. It was shown that at the mixing of electromagnetic waves with different wavelengths, the visual analyzer perceives them as the separate or average wave length corresponding to the mixing color.

Keywords: vision, rhodopsin, iodopsin, bacteriorhodopsin, additive colour mixing.

Introduction

Vision (the visual perception) is a process of psycho-physiological processing of the images of surrounding objects, carried out by the visual system, which allows get an idea of the size, shape and color of surrounding objects, their relative position and distance between them. By means of this mechanism the mammals can receive 90 % of all incoming visual information to the brain.

The function of the visual system is carried out through various interrelated complex structures designated as retina visual analyzer, consisting of a peripheral part (retina, optic nerve, optical tract) and the central department of combining stem and subcortical centers of the midbrain, as well as the visual cortex of the cerebral hemispheres. It is known that the human eye can perceive only light waves of a certain length – from $\lambda = 380$ to $\lambda = 770$ nm.

The light rays from treated subjects pass through the optical system of the eye (cornea, lens and vitreous body) and onto the retina, wherein the light-sensitive photoreceptor cells (rods and cones) are located. Light incidented on the photoreceptors, triggers a cascade of biochemical reactions of visual pigments (in particular, the most studied of them is the mammal retina pigment, rhodopsin responsible for the perception of electromagnetic radiation in the visible range), and in turn, – the occurrence of nerve impulses, which are transmitted through the following retinal neurons and further to the optic nerve. The optic nerve in turn carries the nerve impulses into the lateral geniculate body – subcortical center of vision, and thence to the cortical center, located in the occipital lobe of the brain, where the visual image is formed.

Over the last decade new data have been obtained, revealing the molecular basis of visual perception. The visual molecules of mammals (rhodopsin, iodopsin) and halobacteria (bacteriorhodopsin), involved in the light perception, were identified and the mechanism of their action recently was cleared up quite completely.

The structural research of rhodopsin and its affiliated chromophore proteins of eukaryotic and prokaryotic origin (iodopsin, bacteriorhodopsin) and the analysis of their functioning have been carried out in the Scientific Research Center of Medical Biophysics (Bulgaria) throughout the last 20 years. These studies have been aimed at finding new effective methods based on bio-nanotechnology for better treatment of ophthalmic diseases.

The purpose of the research was the studying of basic biochemical mechanisms associated with visual perception of light by the mammal phototransforming pigment rhodopsin and some nano- and biotechnological applications of visual phototransforming pigments as trans-membrane protein bacteriorhodopsin, extracted from purple membranes of photo-organorotrophic halobacterium *Halobacterium halobium ET 1001*.

Material and Methods

Biological objects

As a producer of bacteriorhodopsin (BR) was used a carotenoid strain of extreme photo-organorotrophic halobacterium *Halobacterium halobium ET 1001*, obtained from Moscow State University (Russia). The strain was modified by selection of individual colonies on solid (2 % (w/v) agarose) media with peptone and 4,3 *M* NaCl.

Growth conditions

BR (yield 8–10 mg from 1 g of raw biomass) was obtained in synthetic (SM) medium (g/l): *D*,*L*-alanine – 0,43; *L*-arginine – 0,4; *D*,*L*-aspartic acid – 0,45; *L*-cysteine – 0,05; *L*-glutamic acid – 1,3; *L*-lycine – 0,06; *D*,*L*-histidine – 0,3; *D*,*L*-isoleucine – 0,44; *L*-leucine – 0,8; *L*-lysine – 0,85; *D*,*L*-methionine – 0,37; *D*,*L*-phenylalanine – 0,26; *L*-proline – 0,05; *D*,*L*-serine – 0,61; *D*,*L*-threonine – 0,5; *L*-tyrosine – 0,2; *D*,*L*-tryptophan – 0,5; *D*,*L*-valine – 1,0; AMP – 0,1; UMP – 0,1; NaCl – 250; $MgSO_4 \cdot 7H_2O$ – 20; KCl – 2; NH_4Cl – 0,5; KNO_3 – 0,1; KH_2PO_4 – 0,05; K_2HPO_4 – 0,05; Na^+-citrate – 0,5; $MnSO_4 \cdot 2H_2O$ – $3 \cdot 10^{-4}$; $CaCl_2 \cdot 6H_2O$ – 0,065; $ZnSO_4 \cdot 7H_2O$ – $4 \cdot 10^{-5}$; $FeSO_4 \cdot 7H_2O$ – $5 \cdot 10^{-4}$; $CuSO_4 \cdot 5H_2O$ – $5 \cdot 10^{-5}$; glycerol – 1,0; biotin – $1{,}0 \cdot 10^{-4}$; folic acid – $1{,}5 \cdot 10^{-4}$; vitamin B_{12} – $2 \cdot 10^{-5}$. The growth medium was autoclaved for 30 min at 0,5 atm, the *pH* value was adjusted to 6,5–6,7 with 0,5 *M* KOH. Bacterial growth was performed in 500 ml Erlenmeyer flasks (volume of the reaction mixture 100 ml) for 4–5 days at +35 °C on Biorad shaker ("Birad Labs", Hungary) under intense aeration and monochromatic illumination (3 lamps × 1,5 lx). All further manipulations for BR isolation were carried out with the use of a photomask lamp equipped with an orange light filter.

Isolation of purple membranes (PM)

Biomass (1 g) was washed with distilled water and pelleted by centrifugation on T-24 centrifuge ("Carl Zeiss", Germany) (1500 g, 20 min). The precipitate was suspended in 100 ml of dist. H_2O and kept for 3 h at +4 °C. The reaction mixture was centrifuged (1500 g, 15 min), the

pellet was resuspended in 20 ml dist. H_2O and disintegrated by infrasound sonication (22 kHz, 3 times × 5 min) in an ice bath (0 °C). The cell homogenate after washing with dist. H_2O was resuspended in 10 ml of buffer containing 125 mM NaCl, 20 mM $MgCl_2$, and 4 mM Tris-HCl (*pH* = 8,0), then 5 mg of RNA-ase (2–3 units of activity) was added . The mixture was incubated for 2 h at +37 °C. Then 10 ml of the same buffer was added and kept for 10–12 h at 4 °C. The aqueous fraction was separated by centrifugation (1500 g, 20 min), the PM precipitate was treated with 50 % (v/v) ethanol (5 times × 7 ml) at +4 °C followed by separation of the solvent. This procedure was repeated 6 times to give colorless washings. The protein content in the samples was determined spectrophotometrically on DU-6 spectrophotometer ("Beckman Coulter", USA) by the ratio D_{280}/D_{568} ($\varepsilon_{280} = 1{,}1 \cdot 10^5$; $\varepsilon_{568} = 6{,}3 \cdot 10^4$ $M^{-1} \cdot cm^{-1}$) [1]. PM regeneration is performed as described in [2]. Yield of PM fraction was 120 mg (80–85%).

Isolation of BR

The fraction of PM (in H_2O) (1 mg/ml) was dissolved in 1 ml of 0,5 % (w/v) sodium dodecyl sulfate (SDS-Na), and incubated for 5–7 h at +37 °C followed by centrifugation (1200 g, 15 min). The precipitate was separated, than methanol was added to the supernatant in divided portions (3 times × 100 ml) at 0 °C. The reaction mixture was kept for 14–15 h in ice bath at +4 °C and then centrifuged (1200 g, 15 min). Fractionation procedure was performed three times, reducing the concentration of 0,5 % SDS-Na to 0,2 and 0,1 %. Crystal protein (output 8–10 mg) was washed with cold ^2H_2O (2 times × 1 ml) and centrifuged (1200 g, 15 min).

Purification of BR

Protein sample (5 mg) was dissolved in 100 ml of buffer solution and placed on a column (150×10 mm), stationary phase – Sephadex G-200 ("Pharmasia", USA) (specific volume packed beads – 30–40 units per 1 g dry. Sephadex) equilibrated with buffer containing 0,1 % (w/v) SDS-Na and 2,5 mM ETDA. Elution proceeded by 0,09 M Tris-HCl buffer containing 0,5 *M* NaCl, *pH* = 8,35 at a flow rate of 10 ml/cm^2h. The combined protein fraction was subjected to freeze-drying, in sealed glass ampoules (10×50 mm) and stored in frost camera at -10 °C.

Quantitative analysis of the protein

The process was performed in 12,5% (w/v) polyacrylamide gel (PAAG) containing 0,1 % (w/v) SDS-Na. The samples were prepared for electrophoresis by standard procedures (LKB protocol, Sweden). Electrophoretic gel stained with Coomassie blue R-250 was scanned on a CDS-200 laser densitometer (Beckman, USA) for quantitative analysis of the protein.

Absorption spectrometry

Absorption spectra of pigments were recorded on programmed DU-6 spectrophotometer ("Beckman Coulter", USA) at λ = 280 nm and λ = 750 nm.

IR-spectroscopy

IR-spectra were registered on Brucker Vertex IR spectrometer ("Brucker", Germany) (a spectral range: average IR – 370–7800 cm^{-1}; visible – 2500–8000 cm^{-1}; the permission – 0,5 cm^{-1}; accuracy of wave number – 0,1 cm^{-1} on 2000 cm^{-1}) and Thermo Nicolet Avatar 360 Fourier-transform IR.

Color analyzing

Colors were analyzed by using chromatic color analyzer "Tsvetan" ("Photopribor", Cherkassk, Ukraine). Operating relative absorbance, % from -80 to 70; measurement error, ±5 %; response time, from 0,4 sec to 63,0 sec; overall dimensions, 300 mm.

Scanning electron microscopy

The structural studies were carried out with using scanning electrom microscopy (SEM) on JSM 35 CF (JEOL Ltd., Corea) device, equiped with X-ray microanalyzer "Tracor Northern TN", SE detector, thermomolecular pump, and tungsten electron gun (Harpin type W filament, DC

heating): working pressure – 10^{-4} Pa (10^{-6} Torr); magnification – 300000; resolution – 3,0 nm; accelerating voltage – 1–30 kV; sample size – 60–130 mm.

Results and Discussion

Practical aspects of molecular basis of vision

The process of perception of light has a definite localization in photoreceptor light-sensitive cells of the retina. The retina in its structure is a multilayer layer of nervous tissue that is sensitive to light, which lines the inside of the back of the eyeball. Pigmented retina located at the membrane referred to as retinal pigmented epithelium (RPE), which absorbs light passing through the retina. This prevents the reverse reflection of the light through the retina and does not allow the vision to disperse.

Light enters through the eye and creates a complex of biochemical reactions in the photoreceptor cells of the retina. Photoreceptor cells are divided into two types that due to their characteristic form are designated as rods and cones [3]. Rods are receptors of light of low intensity; they arranged in a colored layer of the retina, in which is synthesized photochromic protein rhodopsin, responsible for color perception. Cones on the contrary contain a group of visual pigments (iodopsin), and adapted to distinguish different colors. Rods can persive black and white images in the dim light, cones – to carry out color vision in bright light. Human retina contains approximately 3 million of cones and 100 million of rods. Their dimensions are very small – the length of about 50 mm, the diameter from 1 to 4 μm.

Electrical signals generated by the rods and cones, are handled by other retina cells – bipolar and ganglion cells before they are transmitted to the brain via the optic nerve [4]. Additionally, there are two intermediate layers of neurons. Horizontal cells transmit messages back and forth between the photoreceptor cells, bipolar cells and each other. Amacrine cells of the retina are linked to bipolar cells, ganglion cells, as well as with each other. Both types of these intermediate neurons play a major role in the processing of visual information at the level of the retina before it is transmitted to the brain for final processing.

Cones are approximately 100 times less sensitive to light than rods, but much better perceive the rapid movement. The wand can be stimulated by a single photon. Cascade of molecular interactions enhances this “quantum” of information into a chemical signal, which is then perceived by the nervous system. The degree of enhancement signal varies depending on ambient light: rods are more sensitive under low than inder bright light. As a result, they operate effectively in a wide range of ambient light. Sensory system of rods is packed up in clearly distinguishable cellular substructure that can be easily selected and investigated *in vitro* in isolated state. This property makes them as indispensable convenient objects for further structural-functional studies, as well as studies of photoreceptor pigments (rhodopsin, iodopsin) and the mechanism of their action. These mammal photoreceptor pigments are used as basic models for comparative studying the mechanism of light perception by the bacterial photoreceptor pigment bacteriorhodopsin (BR), isolated from purple membranes of halobacterium *Halobacterium halobium ET 1001*, since the mechanisms of perception of light by eukaryots and halobacteria have some similar reactions.

Rhodopsin and its structural and functional properties

Rhodopsin [5] is one of the most important integral mammal photoreceptor proteins of rod retina cells, which absorbs a photon and creates a biochemical response constituting a first step in a chain of events that provide vision. Rhodopsin consists of two components – a colorless protein opsin and a chromophore component 11-*cis*-retinal residue, acted as the light acceptor (Fig. 1). The absorption of a light photon by 11-*cis*-retinal “turns on” the enzymatic activity of opsin and further photosensitive biochemical cascade of reactions that are responsible for vision [6].

Rhodopsin belongs to the group of the G-protein-coupled receptors (GPCR-receptors) of the retibylidene protein family responsible for transmembrane signaling mechanism based on the interaction with intracellular membrane G-proteins – universal intermediaries in the transmission of hormonal signals from the cell membrane receptors to effector proteins, causing the final cellular response. The establishment of the spatial structure of rhodopsin is so important because rhodopsin as the “originator” of the family of GPCR-receptors is a “model” for the structure and function of other receptors that it is extremely important from fundamental scientific and practical points of view [7].

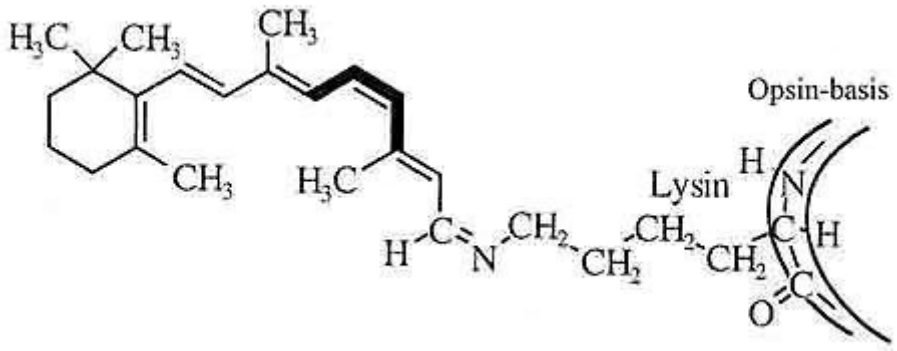

Figure 1. Configuration of photosensitive chromophore of rhodopsin in the basic (unexcited) phase (at the double bond is marked 11-*cis*-configuration)

The spatial structure of rhodopsin was defined by using X-ray diffraction and NMR spectroscopy, while the molecular structure of related to rhodopsin transmembrane chromoprotein bacteriorhodopsin (BR) [8] having a similar structure, performing the functions of ATP-dependent translocase in cell membranes of halophilic microorganisms pumped protons across the cytoplasmic membrane of the cell and is involved in the anaerobic photosynthetic phosphorylation (non-green synthesis), was determined as early as 1990. On the contrary, the complete structure of rhodopsin remained unknown until 2003 [9]. The opsin fragment of the rhodopsin molecule has 348 amino acid residues in a polypeptide chain that is formed by seven transmembrane α-helix segments situated across the membrane and joined with short non-helix sections [10]. The N-terminus of α-helix is located in the extracellular region, while the C-terminus – in the cytoplasmic region. The 11-*cis*-retinal residue is connected to one of the α-helixes, located near the middle of the membrane, so that its long axis is parallel to the membrane surface (Fig. 2). It was also determined the dislocation of 11-*cis*-retinal aldimine bond with ε-amino group of Lys-296 residue being located in the seventh α-helix. Thus, 11-*cis*-retinal is mounted in the center of a complex highly organized protein in the cellular membrane comprising rods. This rigid structure provides a photochemical "adjustment" of retinal residue, affecting its absorption spectrum. The free 11-*cis*-retinal in a dissolved form has an absorption maximum in the ultraviolet region – at a wavelength of 380 nm, while rhodopsin absorbs green light at 500 nm [11]. This shift in the wavelength of light is important from a functional point of view; it is aligned with the spectrum of light that enters into the retina.

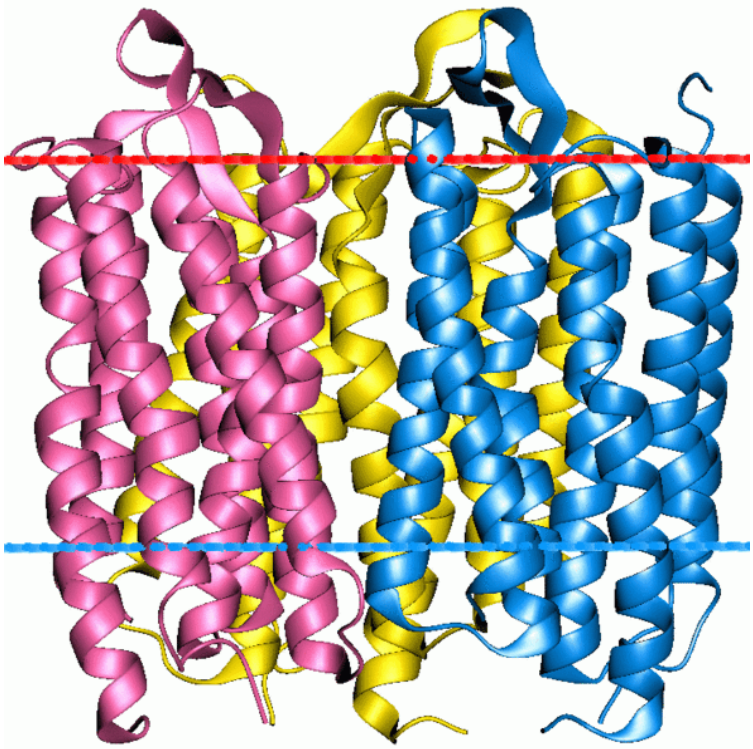

Figure 2. The structure of rhodopsin according to computer modeling data

The absorption spectrum of rhodopsin is defined by specific properties of the chromophore – 11-*cis*-retinal residue and opsin fragment. This range in vertebrates has two characteristic peaks – one in the ultraviolet (λ = 278 nm) due to the opsin fragment, and the other – in the visible region (λ = 500 nm) corresponds to absorption of the chromophore (Fig. 3). Further transformation of rhodopsin under the action of light to the final stable product consists of a series of very fast intermediate stages. Investigating the absorption spectra of intermediates of rhodopsin in retina extracts at low temperatures at which these products are stable, allows evaluate in the detail the photochemical changes of rhodopsin [12].

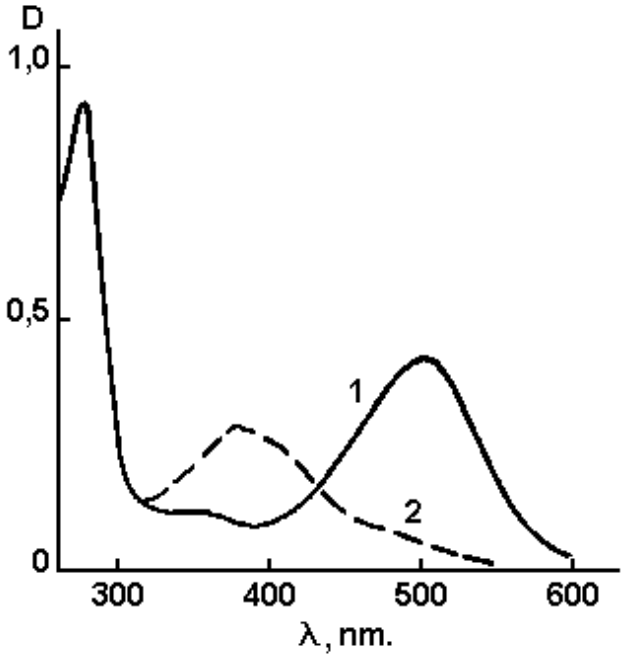

Figure 3. Absorption spectrum of rhodopsin from the frog *Rana temporaria* (in water extract): 1 – rhodopsin (restored pigment); 2 – yellow indicator (discolored pigment)

Upon absorption of light photon it is occurred isomerization of 11-*cis*-retinal into 11-*trans*-retinal (quantum yield, 0,67), that induces a conformational change in the protein and activates photopsin and promotes its binding to G-protein transducin, which triggers a second messenger cascade [13]. Subsequent cycles of the photochemical reactions of rhodopsin lead to a local depolarization of the membrane and the stimulation of the nerve impulse propagates along the nerve fiber due to changes in ion transport in the photoreceptor (Fig. 4). Subsequently rhodopsin is restored (regenerated) with participation of retinal isomerase through the following steps, shown on Fig. 4: 11-*trans*-retinal → 11-*trans*-retinol → 11-*cis*-retinol → 11-*cis*-retinal, the latter is connected with opsin to form rhodopsin.

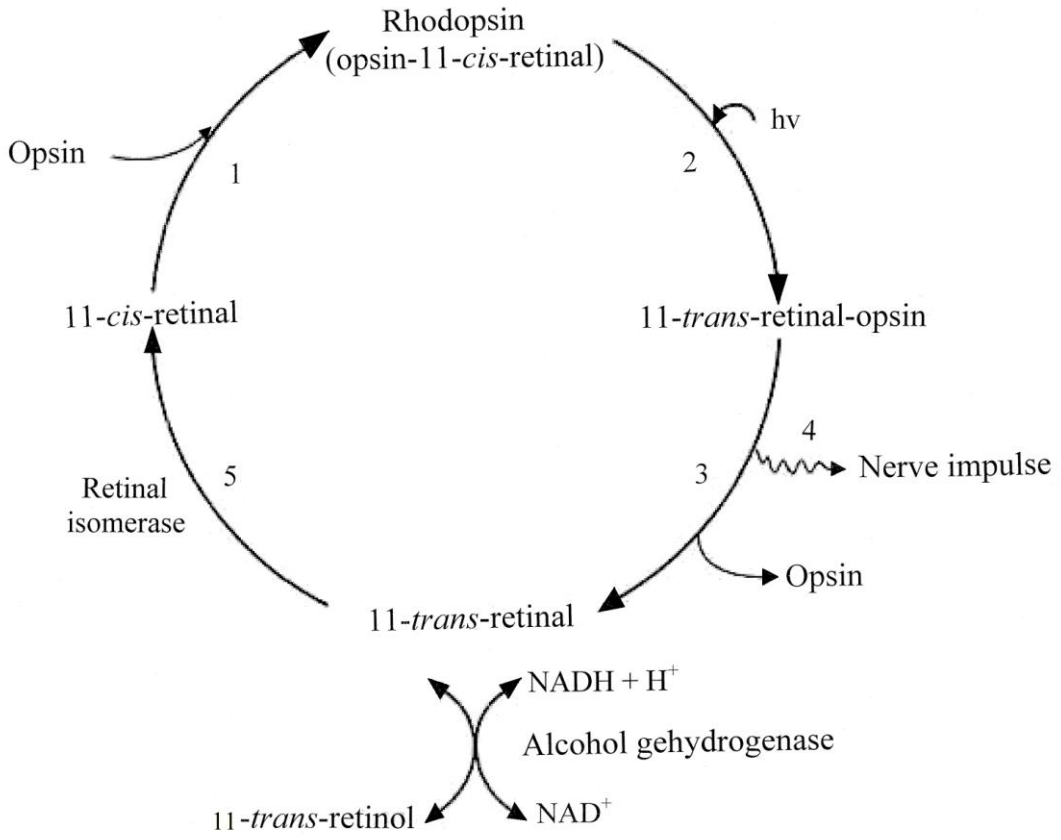

Figure 4. Photocycle scheme of rhodopsin: 1 – 11-*cis*-retinal in the dark links with protein opsin to form rhodopsin; 2 – under light illumination occurs photoisomerization of 11-*cis*-retinal into 11-trans-retinal; 3 – 11-*trans*-retinal-opsin complex splits into 11-*trans*-retinal and opsin; 4 – local depolarization of the membrane and the occurrence of a nerve impulse propagates along the nerve fiber; 5 – regeneration of the original pigment.

Bacteriorhodopsin and its applications

Bacteriorhodopsin (BR), named by analogy to the visual apparatus of mammalian chromoprotein rhodopsin, was isolated from the cell membrane of an extreme photo-organotrophic halobacterium *Halobacterium halobium* in 1971 by D. Osterhelt and W. Stohenius. This photo-transforming trans-membrane protein with the molecular weight ~26,5 kDa is a chromoprotein determining the purple-red culour of halophilic bacteria, contained as chromophore group an equimolar mixture of 13-*cis*-and 13-*trans*-retinol C20-carotenoid, bound by Schiff base (as in the visual animal pigments) with Lys-216 residue of the protein.

In its structure and location in the cell membrane BR refers to integral transmembrane proteins, penetrating the cell membrane, which is divided into three fractions: yellow, red and purple. Purple fraction comprising on 75% (w/w) of cell membrane consists from carotenoids, phospholipids (mostly phosphoglycerol diesters with a small amount of nonpolar lipids and isoprenoids) forms natural two-dimensional crystals which can be investigated using electron

microscopy diffraction methods as X-ray scattering [15]. These methods have established the existence in the BR molecule seven α-helical protein segments, while in the middle are symmetrically located a retinal residue (Fig. 5).

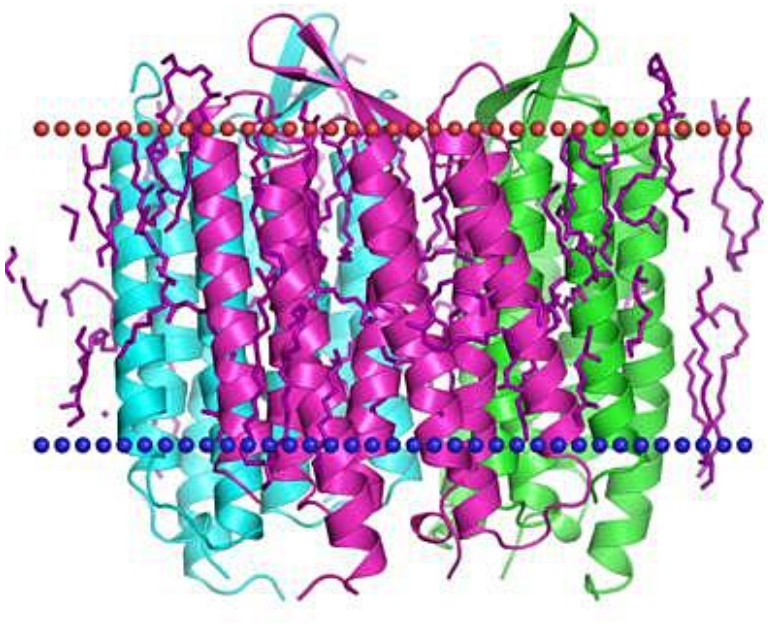

Figure 5. The structure of BR from PM of halophilic bacterium *H. halobium* according to computer modeling data

Polypeptide chain of BR consists of 248 amino acid residues, 67% of which are hydrophobic, formed with the aromatic amino acids, and 33% – hydrophilic residues of aspartic and glutamic acids, arginine and lysine [16]. These residues play important structural and functional role in the spatial orientation of the α-helical segments of the BR molecule, arranged in PM in an orderly manner forming trimers with an average diameter ~0,5 μm and a thickness 5–6 nm; each trimmer is surrounded by six others so that to form a regular hexagonal lattice [17]. The BR molecule arranged in a direction perpendicular to the plane of the cell membrane. Hydrophobic domains represent transmembrane segments and hydrophilic domains protruding from the cell membrane, connecting the individual α-helical intramembranous segments of the BR molecules.

BR acts as a light-dependent proton pump, pumping protons across the cell membrane that generates an electrochemical gradient of H^+ on the surface of the cell membrane, which energy is used by the cell for the synthesis of ATP in the anaerobic photosynthetic phosphorylation. The mechanism of ATP synthesis is called "non-chlorophyll photosynthesis", in contrast to the plant photosynthesis with the participation of chlorophyll. In this mechanism, at absorbtion of a light photon BR molecule became decolorized by entering into the cycle of photochemical reactions, resulting in the release of a proton to the outside of the membrane, and the absorption of proton from intracellular space. By the absorption of a light photon is occured reversible isomerization of 13-*trans*-BR (λ_{max} = 548 nm) (the quantum yield 0,03 at +20 °C) into 13-*cis*-BR (λ_{max} = 568 nm) [18], initiating a cascade of photochemical reactions lasting from 3 ms to 1 ps with the formation of transitional intermediates J, K, L, M, N, and O, followed by separation of H^+ from the retinal residue of BR and its connection from the side of cytoplasm (Fig. 6). As a result, between the internal and external surface of the membrane forms a concentration gradient of H^+, which leads that illuminated halobacteria cells begin to synthesize ATP, i.e. convert light energy into energy of chemical bonds. This process is reversible and in the dark flows in the opposite direction. In this way the BR molecule behaves as a photochromic carrier with a short relaxation

time – the transition from the excited state to the ground state. Optical characteristics of BR vary depending on the method of preparation of PM and the polymer matrix.

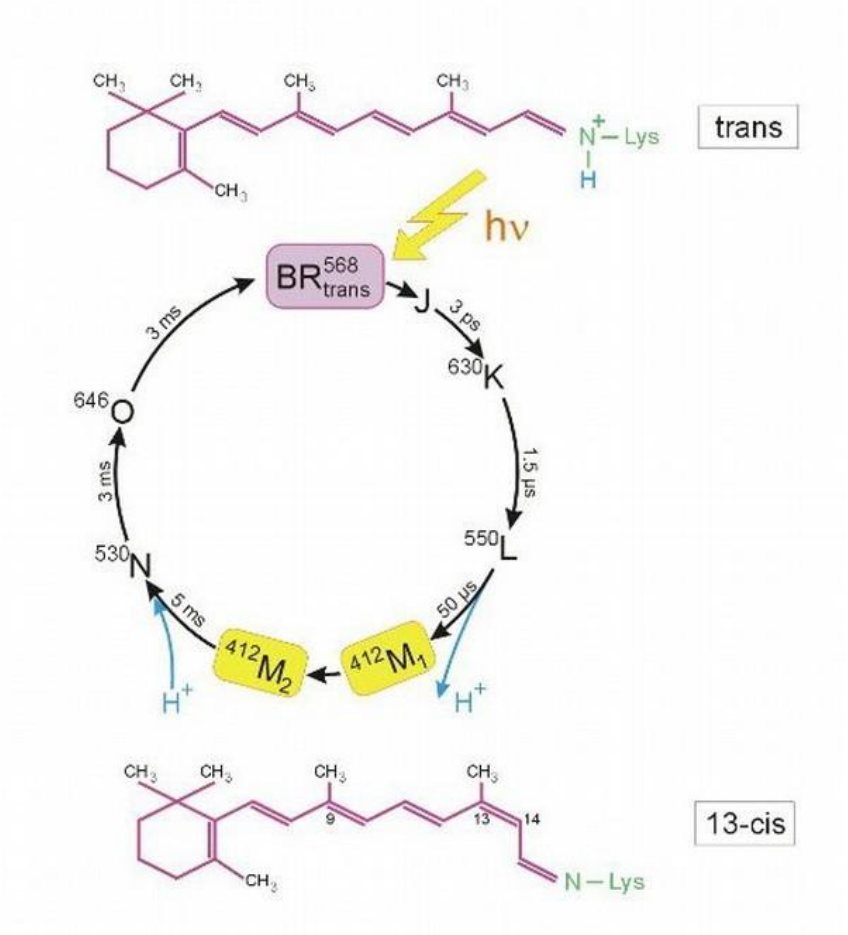

Figure 6. Photocycle scheme of BR (aqueous solution, pH = 7,2, t = +20 °C). Latin numbers J, K, L, M, N, O denote the spectral intermediates of BR. M_1 and M_2 represent spectral intermediants of meta- bacteriorhodopsin with the protonated and deprotonated aldimine bond. The superscripts correspond to the position of the absorption maximum of the photocycle intermediates (nm)

BR is the focus of bio-and nanotechnology because of its high sensitivity and resolution, and is used in molecular bioelectronics as natural photochromic material for light-controlled electrical regulated computer modules and optical systems [19, 20]. In addition, BR is very attractive as a model for studies related to the research of functional activity and structural properties of photo-transforming membrane proteins in the native and photo-converting membranes [21].

Nanofilms produced using the BR-containing purple membranes (PM) of halobacteria were first obtained and studied in this country in the framework of the project “Photochrome”, when it was demonstrated effectiveness and prospects for the use of BR as photochromic material for holographic recording. The main task for the manufacture of BR-containing nanofilms is the orientation of PM between the hydrophobic and hydrophilic media. Typically, to improve the characteristics of the BR-containing films use multiple layers of PM that are applied to the surface of the polymeric carrier and dried up, preserving their natural structure. The best results are achieved in the manufacture of nanofilms based on gelatin matrix [22]. This allows achieve high concentration of BR (up to 50 %) in nanofilms and avoid aggregation of membrane fragments and destruction of BR in the manufacturing process [23]. Embedded in a gelatin matrix PM fragments are durable (~10^4 h) and resistant to solar light, the effects of oxygen, temperatures greater than +80 °C (in water) and up to +140 °C (in air), *pH* = 1–12, and action of most proteases [24]. Dried PM are stacked on top of each other, focusing in the plane of the matrix, so that a layer with 1 μm thickness contains about 200 monolayers [25]. When illuminated such nanofilms exert the electric potential 100–200 mV, which coincides with the membrane potential of living cells [26]. These

factors are of great practical importance for integration of PM into polymeric nanomatrix with keeping photochemical properties.

Technology for preparation of BR consists in growing of halobacteria on liquid synthetic growth media (with 15–20 % (w/w) NaCl) with amino acids, or on natural growth media with peptons – mixtures of polypeptides and amino acids derived from the partial hydrolysis product or powdered milk, animal meat by proteolytic enzymes (pepsin, trypsin, chymotrypsin), or protein-vitamin concentrate of yeast [27]. The subsequent isolation of BR from purple membranes is carried out by a combination of physical, chemical and enzymatic methods [28]. Under optimal growing conditions (incubation period 4–5 days, temperature +35 ^{o}C, illumination with monochromatic light at λ = 560 nm) in cells are synthesized the purple carotenoid pigment, characterized as BR by the spectral ratio of protein and chromophore fragments D_{280}/D_{568} = 1,5:1,0 in the molecule.

Within the framework of the research we described an effective method for isolation of BR from PM of photo-organotrophic halobacterium *H. halobium* consisted by cellular autolysis by distilled water, processing of bacterial biomass by ultrasound at 22 KHz, llocation of PM fraction, purification of PM from low and high-molecular weight impurities, cellular RNA, carotenoids and lipids, PM solubilization in 0,5 % (w/v) solution of the ionic detergent SDS-Na to form a microemulsion with the subsequent fractionation of the protein by methanol [29]. The protein is localized in the PM; the release of low molecular weight impurities and intracellular contents is reached by osmotic shock of cells with distilled water in the cold after the removal of 4,3 *M* NaCl and the subsequent destruction of the cell membrane by ultrasound at 22 kHz. For the destruction of cellular RNA the cellular homogenate was treated with Rnase I. Fraction PM along with the desired protein in a complex with lipids and polysaccharides also contained impurity of related carotenoids and proteins. Therefore, it was necessary to use special methods of fractionation of the protein without damaging its native structure and dissociation.

BR being a transmembrane protein intricately penetrates bilipid layer in form of seven α-helices; the use of ammonium sulfate and other conventional agents to salting out did not give a positive result for isolation of the protein. The resolving was in the translation of the protein to a soluble form by the colloidal dissolution (solubilization) in an ionic detergent. Using as the ionic detergent SDS-Na was dictated by the need of solubilization of the protein in a native, biologically active form in complex with 13-*trans*-retinal, because BR solubilized in 0,5 % (v/v) SDS-Na retains a native α-helical configuration [30]. Therefore, there is no need the use organic solvents as acetone, methanol and chloroform for purification of lipids and protein, and precipitation and delipidization are combined in a single step, which significantly simplifies the further fractionation. A significant advantage of this method is that the isolated protein in complex with lipids and detergent molecules was distributed in the supernatant, and other high molecular weight impurities – in unreacted precipitate, easily separated by centrifugation. Fractionation of solubilized in 0,5 % (w/v) SDS-Na protein and its subsequent isolation in crystalline form was achieved at 0 ^{o}C in three steps precipitating procedure with methanol, reducing the concentration of detergent from 0,5; 0,25 and 0,1 % (w/v) respectively. The final stage of BR purification involved the separation of the protein from low-molecular-weight impurities by gel-permeation chromatography on dextran Sephadex G-200 Column balanced with 0,09 M Tris-HCl buffer (*pH* = 8,35) with 0,1 % (w/v) SDS-Na and 2,5 mM EDTA (output of the protein 8–10 mg).

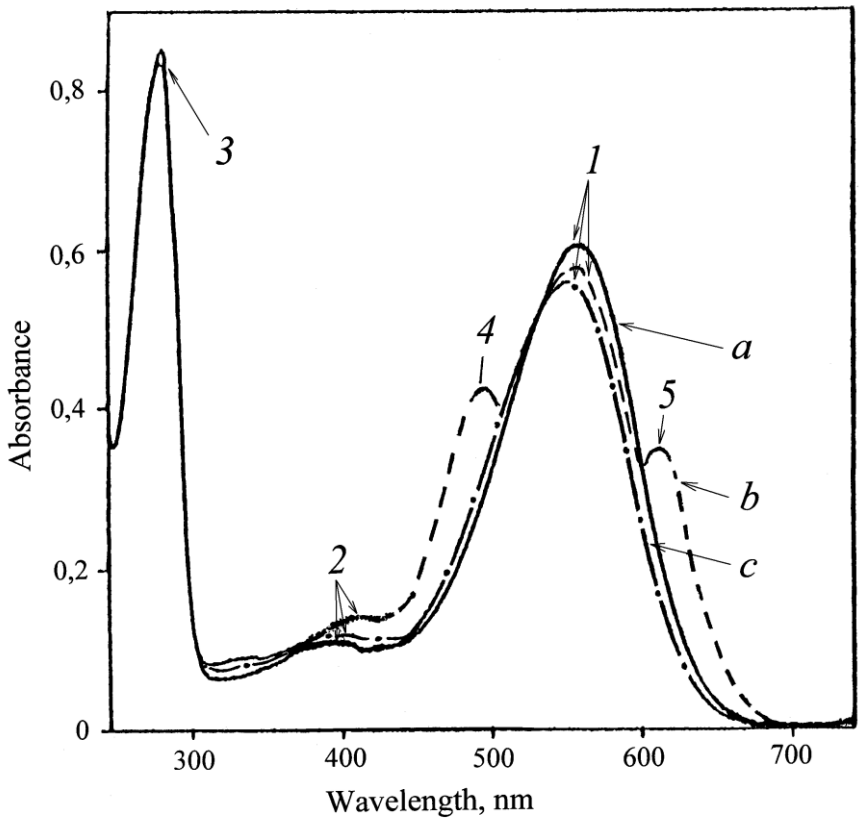

Figure 7. The absorption spectra of the PM (50% (v/v) ethanol) at various stages of processing: (a) – natural BR; (b) – PM after intermediate treatment; (c) – PM purified from carotenoids. The bandwith (1) is the spectral form of BR^{568}, (2) – impurity of spectral form of meta-bacteriorhodopsin (M^{412}), (3) – the total absorption bandwith of aromatic amino acids, (4) and (5) – extraneous carotenoids. As a control used the native BR

Absorption spectra of PM purified from carotenoids (4) and (5) (chromatographic purity 80–85 %) are shown in Figure 7 at various processing stages (*b*) and (*c*) relative to the native BR (*a*). Formation of retinal-protein complex in the BR molecule leads to a bathochromic shift in the absorption spectrum of PM (Fig. 8*c*) – the main bandwith (1) with the absorption maximum at λ = 568 nm caused by the light isomerization of the chromophore by the C13=C14 bond is determined by the presence of 13-*trans*-retinal residue in BR^{568}; additional low-intensity bandwith (2) at λ = 412 nm characterizes a minor impurity of a spectral form of *meta*-bacteriorhodopsin (M^{412}) (formed in the light) with deprotonated aldimine bond between 13-*trans*-retinal residue and protein; the total bandwith (3) with λ = 280 nm is determined by the absorption of aromatic amino acids in the polypeptide chain of the protein (for native BR D_{280}/D_{568} = 1,5 : 1,0).

The final stage of BR purification involved the separation of the protein from low-molecular-weight impurities by gel-permeation chromatography (GPC). For this purpose the fractions containing BR were passed twice through a chromatography column with dextran Sephadex G-200 balanced with 0,09 M Tris-buffer (pH = 8,35) containing 0,1% (w/v) SDS-Na and 2,5 mM EDTA. Elution was carried out at 20±25 °C with 1 mM Tris-HCl buffer (pH = 7,6) at 10 ml/cm²·h. The data on purification of BR of phospholipids and carotenoids are shown in Table 1. 84% of phospholipids was removed by five washes (65, 70 and 76% was removed by 1st, 2nd and 3nd wash respectively). The total endogenous phospolipid removal on the BR peak was 92% relative to the native PM.

Table 1: Summary results for the isolation and purification of BR by various methods

Sample	**PM content, mol PM/mol BR**	**Phospholipid and carotenoid removal, %**	**BR yield*, %**
PM fraction	20,5	–	–
PM washed with EtOH			
1 wash	16,9	65	93
2 wash	15,1	70	90
3 wash	14,5	76	88
4 wash	13,6	81	84
5 wash	13,2	84	80
BR crystallised from MeOH	12,9	86	75
BR from GPC on Sephadex G-200	10,2	92	86

* Notes: Percentage yield is indicated in mass.% relative to BR solubilized in 0,5% SDS-Na before concentration.

The method for protein fractionation made it possible to obtain 8–10 mg of BR from 1 g of bacterial biomass. The homogeneity of BR was confirmed by electrophoresis in 12,5% (w/v) PAAG with 0,1% (w/v) SDS-Na and the regeneration of apomembranes with 13-*trans*-retinal.

Iodopsin

Iodopsin is a violet, light-sensitive pigment of the retinal cone cells, responsible for the light and color vision in mammals, the close analogue of rhodopsin. This pigment consists of a protein named photopsin linked with the chromophore, a retinal residue. According to the three-component theory of vision, it is believed that there has to be three types of this pigment and accordingly – three types of cones that are sensitive to blue, green and red light correspondingly. Evidently, there should be three types of cones – S, M, L types, each of which contains only their photosensitive pigment, corresponding to a specific opsin.

It is now established that this group of pigments comprises the isomorphic pigments, slightly different in composition and absorption spectra. Various opsins are different by amino acids in the molecule, and absorb light at several different wavelengths as do retinal-related molecules.

Iodopsin consists of three pigments – hlorolab, eritrolab and tsianolab. With the densitometry method W. Rushton studied the coefficient of light absorption in the photo layers of the retina with different wavelengths [31]. The hlorolab pigment absorbs the light rays corresponding to yellow-green (450–630 nm absorption band), the eritrolab – yellow and red (λ = 500-700 nm), and the third predicted pigment tsianolab – blue-green (λ = 500–700 nm) parts of the visible spectrum [32]. However, other different types of cones containing the only one pigment have not still yet been found.

The applying of intensive adapting yellow, purple and blue background, allowed get three different threshold curves in absorption spectra of iodopsin [33]. Making a correction for light absorption by the front media of the eye (lens and macular pigment yellow), G. Wald indicates as the maximums of the three pigments the peaks corresponding to the wavelengths: λ = 430, 540 and 575 nm, which correspond to the photoreceptors cones of the retina that produce basic bio-signals – S, M, L (Table 2).

Table 2: The maximums of tsianolab, hlorolab and eritrolab pigments in absorption spectra and the sensitivity range [33]

Type of cones/photopigment (opsin)	**Designation**	**Sensitivity range**	**Maximum sensitivity**
S-cones/tsianolab (OPN1SW)	β	400–500 nm	420–440 nm
M-cones/hlorolab (OPN1MW)	γ	450–630 nm	534–545 nm
L-cones/eritrolab (OPN1LW)	ρ	500–700 nm	564–580 nm

It should be noted, however, that this interpretation does not fit correctly into the very basis of three-component hypothesis of color, as eritrolab and hlorolab have a sensitivity to the entire visible spectrum, and according to the three-component hypothesis they should be the narrow channeled, and their spectra sensitivity must comply strictly to the certain regions of the spectrum. In addition their maximums do not correspond to red and green colors (as postulated by the three-component hypothesis); their actual spectral maxima correspond to eritrolab – yellow-red (orange) and hlorolab – yellow-green region of the spectrum.

The basic principles of the mechanism of color vision

It is established that the retina has three types of cone cells – S, M and L cells, having a different sensitivity to different parts of the visible range of the spectrum (Fig. 8). The cone cells of S type have a spectral range from λ = 400 nm to λ = 500 nm with a maximum peak at λ = 420–440 nm, the cone cells of M type – from λ = 450 nm to λ = 630 nm with a maximum peak at λ = 534–555 nm, while the cone cells of L type – from λ = 500 nm to λ = 700 nm with a maximum peak at λ = 564–580 nm. As the curves of the sensitivity of the cone cells overlap, it is impossible for the monochromatic light to stimulate only one type of cone cells. The other types of cone cells react though to a lesser degree. The set of all possible values of the color combinations causing a visual reaction determines the human color space. The human brain generally can discern approximately 10 million of different colors.

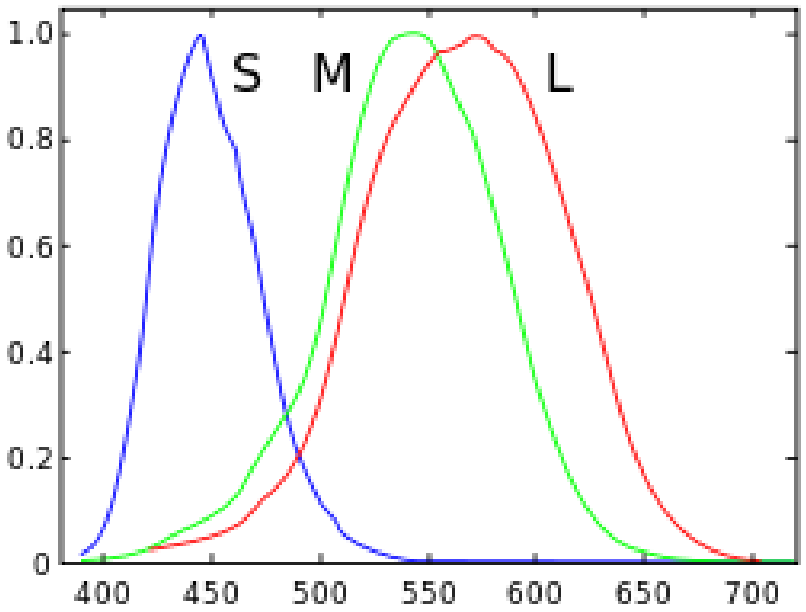

Figure 8. The spectra of blue, green, and red rays in S, M and L points on the graphs of electromagnetic waves, which cones emit as the brightest ray signals rays of these points, from all the beams of monochromatic waves of substantive focused points with lengths in nm.

The electromagnetic wave spectrum stimulates the different types of cone cells from the three types S, L and M to a different degree. Thus, the red light stimulates the L cone cells more than the

M cone cells. On the contrary, the blue light stimulates the S cone cells in the strongest way. The yellow-green light provides a strong stimulation to the L and M cone cells, and a weaker stimulation to the S cone cells. The brain then combines the information from all types of cone cells for different wavelengths and analyzes them as different colours.

The additive mixing of colors

The analysis of the activity of the three types of cones – S, L and M in the perception of different colors also shows how the brain "deciphers" the different colors. The foundation of this colour analysis, shown in Figure 10, was made by M. Marinov and I. Ignatov in 2008. The maximum of the spectral sensitivity of the visual analyzer corresponds to the light green colour corresponds to 560 nm in spectra (Fig. 9). However, it is not clear whether the green colour perceived by brain is a combined mixing effect of the yellow and blue colors, or whether it corresponds to a wavelength of the green color from the visible spectrum. The human brain can register the colors, i.e. the green colour as a spectrometer, with certain lengths of the electromagnetic waves. It can also register the green colour as a mixture of yellow and blue. However, the full perception of colours by the visual analyzer cannot be defined by a spectrometer.

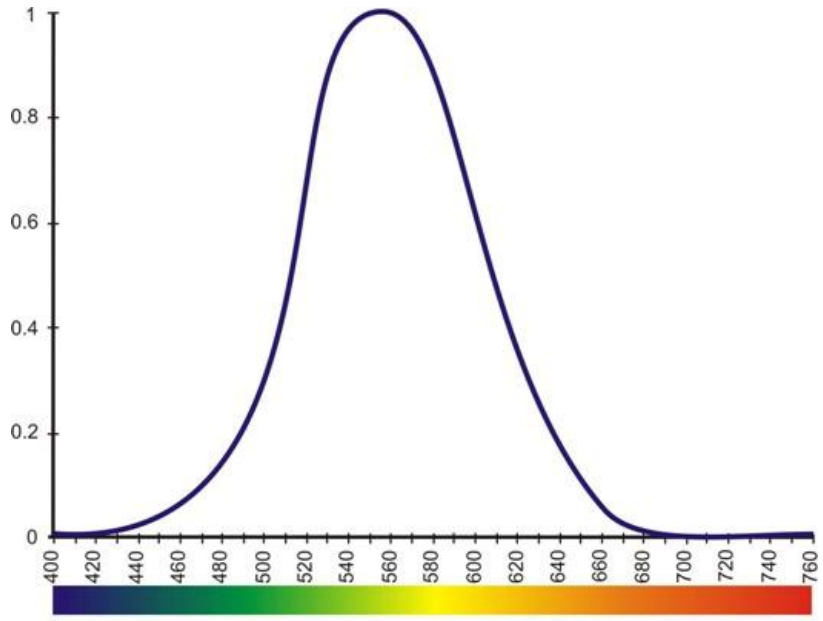

Figure 9. The maximum of the spectral sensitivity of the visual analyzer on the graphs of the electromagnetic waves (M. Marinov and I. Ignatov, 2008)

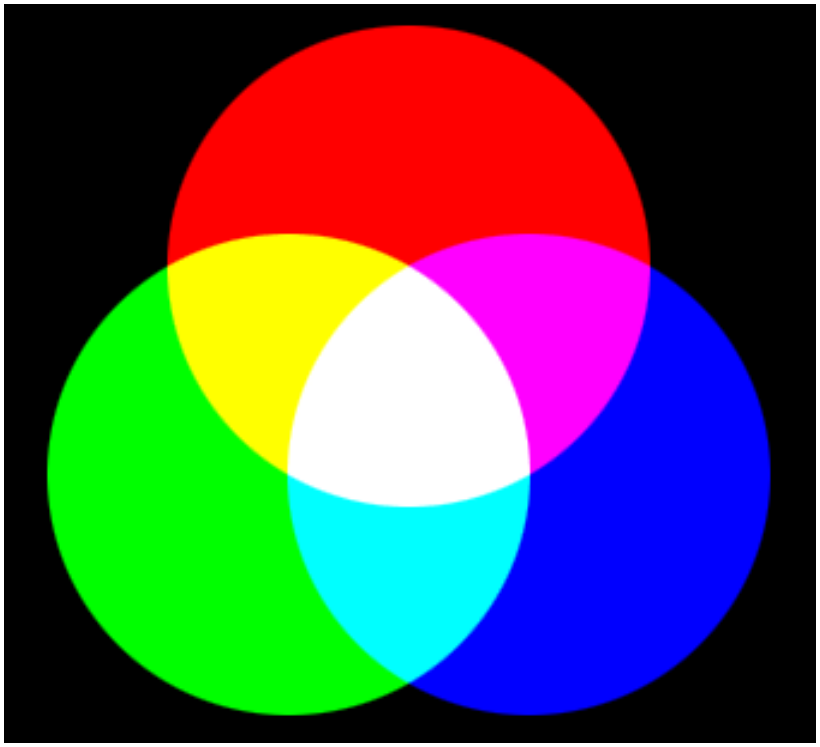

Figure 10. Additive physical mixing of different colours by the visual analyzer (M. Marinov and I. Ignatov, 2008)

As an example via the mixing of electromagnetic waves that correspond to green and red colour, the medium yellow colour is obtained. In the mixing process of green and red, no medium colour is obtained; the brain therefore perceives it as the yellow colour [34]. When there is an emission of electromagnetic waves that correspond to green and red colour, the brain adopts an "average decision" – the yellow colour (Fig. 10). Analogously, for the yellow and blue colour, the brain adopts an "average decision" – the green colour. This means that a spectral mixing of colours is observed between the blue-yellow and green-red pairs [35]. In its turn, green and blue colours are perceived as the cyan colour. The vision sensitivity furthermore is at its lowest for the violet, blue and red color. The mixing of electromagnetic waves that correspond to the blue and red colour is perceived as the violet colour. In the mixing of electromagnetic waves that correspond to more colors, the brain does not perceive them as separate or average, but as a white colour. Thus, the spectral notion of colour is not determined solely by the wavelength. The analysis is being performed by brain, and the notion of colour is at its essence a product of our consciousness.

Conclusions

The mechanism of color perception by the visual analyzer has been studied using a photoreceptive chromo-protein rhodopsin as a basic model. A further research into the function of rhodopsin and other retina affiliated chromo-proteins as iodopsin will allow investigate in detail the mechanism of visual perception of light for better treatment of functional eye diseases in ophthalmology. It should be noted that rhodopsin up till now remains to be the most studied model chromoprotein of all GPCR-receptor family. This allowed us to us to carry out the comparative analysis and better analyze the functional properties of another analogous trans-membrane bacterial chromoprotein – bacteriorhodopsin isolated from purple membranes of halobacterium *H. Halobium ET 1001* in semi-preparative quantities, and study its structural-functional parameters and applications in bio-nanotechnologies.

Acknowledgements

The authors wish to thank Parashkeva Tzaneva (Bulgarian Academy of Science) for her cooperation in the research. Also authors would like to commemorate the memory of Prof. Marin Marinov (1928–2009) – the initiator of the research of color vision in Bulgaria.

References:

1. Neugebauer D.Ch. Recrystallization of the purple membrane *in vivo* and *in vitro* / D.Ch. Neugebauer, H.P. Zingsheim, D. Oesterhelt // Journal Molecular Biology. 1978. Vol. 123. P. 247–257.

2. Rudiger M. Reconstitution of bacteriorhodopsin from the apoprotein and retinal studied by Fourier-transformed infrared spectroscopy / M. Rudiger, J. Tittor, K. Gerwert, D. Oesterhelt // Biochemistry. 1997. Vol. 36. P. 4867–4874.

3. Hubel D. Eye, Brain and Vision. Scientific American Library Series (Book 22), 2nd edition, New York: W.H. Freeman Publ., 1995. 256 p.

4. Hogan M.J. Histology of the Human Eye / M.J. Hogan, J.A. Alvarado, J.E. Weddell. Philadelphia: WB Saunders Co., 1970. 115 p.

5. Nathans J. Molecular genetics of human color vision: the genes encoding blue, green, and red pigments / J. Nathans, D. Thomas, D.S. Hogness // Science. 1986. Vol. 232, № 47. P. 193–202.

6. Liang Y. Rhodopsin signaling and organization in heterozygote rhodopsin knockout mice / Y. Liang, D. Fotiadis, T. Maeda // J. Biol. Chem. 2004. Vol. 279. P. 48189–48196.

7. Palczewski K., Kumasaka T., Hori T. Crystal structure of rhodopsin: a G-protein-coupled receptor // Science. 2000. Vol. 289. P. 739–745.

8. Henderson R. Model for the structure of bacteriorhodopsin based on high-resolution electron cryo-microscopy / K. Palczewski, T. Kumasaka, T. Hori // J. Mol. Biol. 1990. Vol. 213, № 4. P. 899–929.

9. Palczewski K. G-protein-coupled receptor rhodopsin / K. Palczewski // Annu. Rev. Biochem. 2006. Vol. 75. P. 743–767.

10. Ovchinnikov Yu.A. Visual rhodopsin: Whole amino acid sequence and topology in membrane / Yu.A. Ovchinnikov, N.G. Abdulaev, M.Yu. Feigina, I.D. Artamonov, A.S. Bogachuk // Bioorganic. Chemistry. 1983. № 10. P. 1331–1340.

11. Hargrave P.A. The structure of bovine rhodopsin / P.A. Hargrave, J.H. McDowell, D.R. Curtis // Biophys. Struct. Mech. 1983. Vol. 9. P. 235–244.

12. Schertler G.F. Projection structure of frog rhodopsin in two crystal forms / G.F. Schertler, P.A. Hargrave // Proc. Natl. Acad. Sci. U.S.A. 1995. Vol. 92. P. 11578–11582.

13. Lipkin V.M. Visual system. mechanisms of transmission and amplification of the visual signal in eye retina / V.M. Lipkin // Soros Educational Journal. 2001. Vol. 7, № 9. P. 2–8 [in Russian].

14. Oesterhelt D. Rhodopsin - like protein from the purple membrane of *Halobacterium halobium* / D. Oesterhelt, W. Stoeckenius // Nature. 1971. Vol. 233, № 89. P. 149–160.

15. Lanyi J.K. X-ray diffraction of bacteriorhodopsin photocycle intermediates / J.K. Lanyi // Molecular Membrane Biology. 2004. Vol. 21, № 3. P. 143–150.

16. Jap B.K. Peptide-chain secondary structure of bacteriorhodopsin / B.K. Jap, M.F. Maestre, S.B. Hayward, R.M. Glaeser // Biophys J. 1983. Vol. 43, № 1. P. 81–89.

17. Nonella M. Structure of Bacteriorhodopsin and in situ isomerization of retinal: A molecular dynamics study / M. Nonella, A. Windemuth, K. Schulten // Journal Photochem. Photobiol. 1991. Vol. 54, № 6. P. 937–948.

18. Zimanyi L. Pathway of poton uptake in the bacteriorhodopsin photocycle / L. Zimanyi, Y. Cao, R. Needleman, M. Ottolenghi, J.K. Lanyi // Biochemistry. 1993. Vol. 32. P. 7669–7678.

19. Vought B.W. Molecular electronics and hybrid computers / B.W. Vought, R.R. Birge R.R. (Eds.) in: Wiley Encyclopedia of Electrical and Electronics Engineering. NY: Wiley-Interscience, 1999. 490 p.

20. Hampp N. Bacteriorhodopsin and its potential in technical applications / N. Hampp, D. Oesterhelt. in: Nanobiotechnology / Ch. Niemeyer, C. Mirkin (eds.). Weinheim: Wiley-VCH-Verlag, 2004. 167 p.

21. Wang W.W. Bioelectronic imaging array based on bacteriorhodopsin film / W.W. Wang, G.K. Knopf, A.S. Bassi // IEEE Transactions on Nanobioscience. 2008. Vol. 7, № 4. P. 249–256.

22. Shuguang W.U. Bacteriorhodopsin encapsulated in transparent sol-gel glass: a new biomaterial / W.U. Shuguang, L.M. Ellerby, J.S. Cohan // Chem. Mater. 1993. Vol. 5. P. 115–120.

23. Weetall H. Retention of bacteriorhodopsin activity in dried sol-gel glass / H. Weetall // Biosensors & Bioelectronics. 1996. Vol. 11. P. 325–333.

24. Downie J. Long holographic lifetimes in bacteriorhodopsin films / J. Downie, D.A. Timucin, D.T. Smithey, M. Crew // Optics Letters. 1998. V. 23, № 9. P. 730–732.

25. Korposh S.O. Films based on bacteriorhodopsin in sol-gel matrices / S.O. Korposh, M.Y. Sichka, I.I. Trikur // Proc. of SPIE. 2005. Vol. 5956. Paper Number 595616. P. 312–320.

26. Seitz A. Kinetic optimization of bacteriorhodopsin films for holographic interferometry / A. Seitz, N. Hampp // J. Phys. Chem. B. 2000. Vol. 104, № 30. P. 7183–7192.

27. Mosin O.V. The inclusion of deuterated aromatic amino acids in the molecule of bacteriorhodopsin *Halobacterium halobium* / O.V. Mosin, D.A. Skladnev, V.I. Shvets // Applied Biochemistry and Microbiology. 1999. Vol. 35, № 1. P. 34–42.

28. Mosin O.V. Biosynthesis of transmembrane photo transforming protein bacteriorhodopsin labeled with deuterium on residues of aromatic acids [2,3,4,5,6-$^{2}H_{5}$]Phe, [3,5-$^{2}H_{2}$]Tyr and [2,4,5,6,7-$^{2}H_{5}$] / O.V. Mosin, V.I. Shvez, D.A. Skladnev, I. Ignatov // Nauchnoe priborostroenie. 2013. Vol. 23, № 2. P. 14–26 [in Russian].

29. Mosin O.V. The photo-transforming photochrome protein bacteriorhodopsin derived from photoorganoheterotrophic halobacterium *Halobacterium halobium* / O.V. Mosin, I. Ignatov // Nanoengineering. 2013. Vol. 1. P. 14–21 [in Russian].

30. Mosin O.V. The natural photo-transforming photochrome transmembrane protein nanomaterial bacteriorhodopsin from purple membranes of halobacterium *Halobacterium halobium* / O.V. Mosin, I. Ignatov // Journal of Nano and Microsystem Technique. 2013. Vol. 7. P. 47–54 [in Russian].

31. Rushton W.A.H. In: Visual problems of colour / N.P.L. Sump. (Ed.) London: Her Majesty's Stationary Office, 1958. Vol. 1. P. 71–101.

32. Wyszecki G. Color Science: Concepts and Methods, Quantitative Data and Formulae (2nd ed.) / G. Wyszecki G., W.S. Stiles. New York: Wiley–IS&T Series in Pure and Applied Optics, 1982. 935 p.

33. Wald G. The receptors of human color vision // Science. 1964. Vol. 145 (3636). P. 1007–116.

34. Ignatov I. Process of perception of light and evolution of sight at the higher animals and humans / I. Ignatov, O.V. Mosin // Naukovedenie. 2013. № 3. P. 1–19 [in Russian], [Online] Available: URL: http://naukovedenie.ru/PDF/98tvn313.pdf (May-June 2013).

35. Ignatov I. Color Kirlian spectral analysis. Color observation with visual analyzer / I. Ignatov, M. Marinov // Euromedica, 2008. 32 p.

Published in the Russian Federation
European Journal of Molecular Biotechnology
Has been issued since 2013.
ISSN: 2310-6255
E-ISSN 2409-1332
Vol. 8, Is. 2, pp. 80-87, 2015

DOI: 10.13187/ejmb.2015.8.80
www.ejournal8.com

UDC 577

Molecular Characterization of Some Productive Traits in Mesopotamian Buffaloes (*Bubalus bubalis*)

Da´ad Ali Hussain

University of Baghdad, Iraq
Genetic Engineering and Biotechnology Institute for Postgraduate Studies
Dr.

Abstract

One of these major genes is growth hormone and growth hormone receptor (GH, GHR) genes which are related to production and reproduction traits in livestock. Associations were analysed between the bovine growth hormone (GH) as well as growth hormone receptor (GHR) combined with their genotypes (GH/*Alu*I& GHR/*Alu*I). There is extensive literature on the genetic polymorphism of GH and GHR in cattle, but perusal of literature has indicated paucity of information on these two genes in buffalo.

This study aimed to evaluate the genetic polymorphism within growth hormone and its receptor genes in Iraqi buffalo using PCR-RFLP technique. Genomic DNA extracted from 100 healthy buffaloes and amplified using primers that were designed from the cattle GH and GHR gene sequences.

All tested buffalo DNA amplified fragments at 428bp for GH 5th exon. The digestion with *AluI* endonuclease gave three types of genotypes. The Distribution of the three genotypes and allele frequency was calculated according to Hardy-Weinberg equation, were LL=94 (94.09%), LV=6 (5.82%) and VV=0 (0.09%), so that most of buffaloes was homozygous (LL) due to the presence of the restriction site at position 52^53 (AG^CT) and less heterozygous was for the valine allele as compared with leucine allele homozygous.

The amplified fragments of GHR gene obtained from all tested buffalo DNA at 342-bp were digested with *Alu*I endonuclease. The result showed that all tested buffaloes are genotyped as GG for GHR gene, where amplified fragments were digested into two digested fragments at 241and 101-bp due to the presence of *Alu*I restriction site at position (AG^CT).

Keywords: Buffalo, GH, GHR, PCR-RFLP.

Introduction

Authorized national livestock sector development is largely determined by the ownership, preservation and utilization of biological resources such as livestock animals that have been developed and are still maintained subsistence (Andreas *et al.*, 2010). Improvement of important livestock through selective breeding has received more attention so that annual optimum selective breeding programs may achieve improvement in most of the economic traits of different farm animals (Pawar *et al.*, 2007). Buffalo (*Bubalus bubalis*) is one large ruminant that has its own

advantages for development because it can survive with low quality of feed, tolerant to local parasites and high productivity of meat and milk (Andreas *et al.*, 2010).

Tambasco *et al.*, (2003) have proposed candidate gene strategy. In other words, the genetic variation of gene is affecting the physiological pathways and phenotype. Several studies reported that the candidate genes have influenced for preweaning growth traits such as growth hormone and growth hormone receptor genes (Ge *et al.,* 2003; Kim *et al.,* 2004).

The growth hormone gene is located on 19th chromosome and it is a major regulation gene for postnatal growth and metabolism in mammals. The growth hormone receptor gene is located on 20th chromosome and it is a mediation gene of the biological actions of growth hormone on target cells. Several studies proved that the genetic polymorphism of growth hormone and growth hormone receptor genes correlated with preweaning growth traits (Stasio *et al.,* 2002; Hale *et al.,* 2000). In other words, the genetic polymorphism for both genes was found responsible to improve economic traits.

The studies on candidate genes in beef cattle from other countries are carried out on growth (Tambasco *et al.,* 2003; Kim *et al.,* 2004). The mutation of growth hormone gene on promoter or on the 5th exon depicted one of changing phenotype since polypeptide chains that are translated from converting DNA. For example, the mutation on the 5th exon. This substitution illustrated low body weight and average daily milk production (Lucy *et al.,* 1998). Studies concern with correlation between growth hormone receptor gene and growth were focused on mutations on promotor region, few studies reported the effect of exon nine mutations on economic traits (Hale *et al.*, 2000).

The objective of this study was to detect the genetic polymorphism within growth hormone and growth hormone receptor genes in Mesopotamian buffalo using PCR-RFLP technique.

Materials and methods:

Genomic DNA extraction:

The total numbers of blood samples were taken from *vena jugularis* of 100 different sex pubered local buffaloes and were accomplished by reserving them in EDTA tubes at -20˚C (Miller *et al.*, 1988). Genomic DNA was extracted from whole blood samples with isolation kit, QIA®mini, (QIAGENE, Germany). Moreover, the DNA concentration was estimated and the samples were diluted to 30ng/µl in TE at least 24 hours prior to the reaction.

Polymerase chain reaction (PCR):

Amplification of GH and GHR fragments were done by using polymerase chain reaction–restriction fragment length polymorphism (PCR-RFLP) methods. A 428 bp (GH gene), as well as 342 bp (GHR gene), were amplified by PCR using forward and reverse primers according to Balogh *et al.*, (2009) and Di Stasio *et al.,* (2005) (Table1).

Reagents used for amplification of both target fragments were performed in a 25 µl reaction mixtures(Promiga, USA), containing(2x PCR reaction buffer, 3 mM MgCl2, 400 µM dNTPs, 10 U Tag DNA polymerase), 5 µl template genomic DNA, while GH primer 1.3 µl and GHR was 1.25 µl, so far, the sterile water was 12.4, 12.5 µl respectively.

The reaction was cycled for 1 min. at 94°C, 2 min at an optimized annealing temperature that was determined for each primer (Table 1) and 2 min. at 72°C for 30 cycles.

The PCR products were electrophoresed on 1.5% agarose gel stained with ethidium bromide at constant voltage (10v/cm) for 30 minutes to test the amplification success (Othman *et al.*, 2012).

Table 1: The sequences and information of primers used in this study

The primer	5′ -------- 3′	PCR (35 cycles)	product size	R.E	References
GH	CGGACCGTGTCTATGAGAAGCTGAAG GTTCTTGAGCAGCGCGTCGTCA	94°C 1 min 53°C 2 min 72°C 2 min	428 bp	*Alu*I	Balogh *et al.* (2009)

GHR	GCT AAC TTC ATC GTG GAC AAC CTA TGG CAT GAT TTT GTT CAG	94°C 1 min 53°C 2 min 72°C 2 min	342 bp	*Alu*I	Di Stasio *et al* (2005)

Restriction fragment length polymorphism (RFLP) technique:

The PCR products for the two tested fragments were digested with the restriction enzyme *Alu*I. The restriction mixture for each sample was prepared by adding 2 µl of 10 × restriction buffers to 7 units of the appropriate restriction enzyme and 0.2 µl BSA; the volume was completed to 20 µl by sterile water. This restriction mixture was mixed with PCR product (~10µl) and incubated at 37˚c for 3 hours in water bath. The digested PCR products were electrophoresed on 3% agarose gel at 50 v for 2hours, staining with ethidium promide to detect the different genotypes of the two tested sequences by UV- transilluminator and finally documented in gel doc system (Otaviano *et al*, 2005).

Results and discussion

Growth hormone (GH) actions on target cells depend on the GH receptor (GHR) (Burton *et al.*, 1994). The GH binding to GHR causes its dimerization, activation of the GHR-associated JAK2 tyrosine kinase, and tyrosyl phosphorylation of both JAK2 and GHR (Zhu *et al.*, 2001). These events activate a variety of signaling molecules, including MAP kinases, protein kinase C, and STAT transcription factors (Maj *et al.*, 2004).

The primers GH, GHR were amplified with DNA fragment, which is used as a template for PCR reaction. The PCR amplification was confirmed by running 7µl of PCR product along with 100bp DNA marker in 1.5 agarose gel. The amplified PCR products (GH, GHR) were visualized as a single band of expected size under the UV with the marker, which were 428bp for GH and 342bp for GHR (Figure 1 and 2).

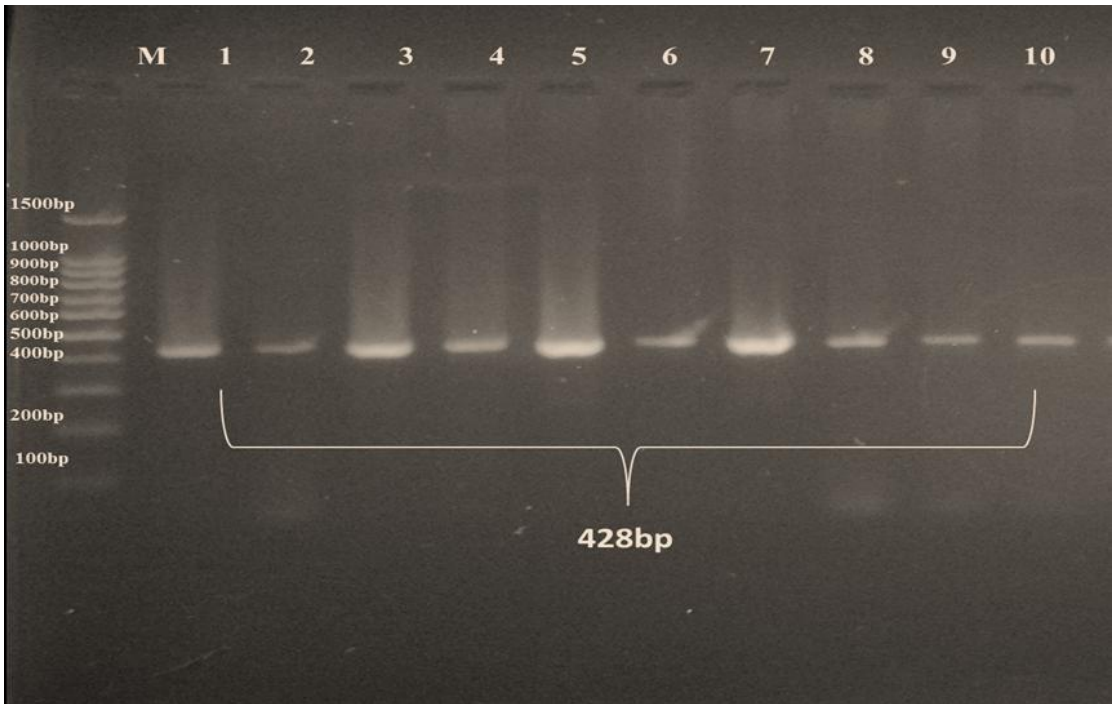

Figure (1): PCR products of bovine GH gene with size of 428 bp, amplified with primer GH1. The product was electrophoresis on 1.5% agarose gel at5 volt/cm2 for 1hour.Lane M DNA ladder (100-1000), Lane (1-10) PCR products was visualized under U.V light after stain with Ethidium Bromide.

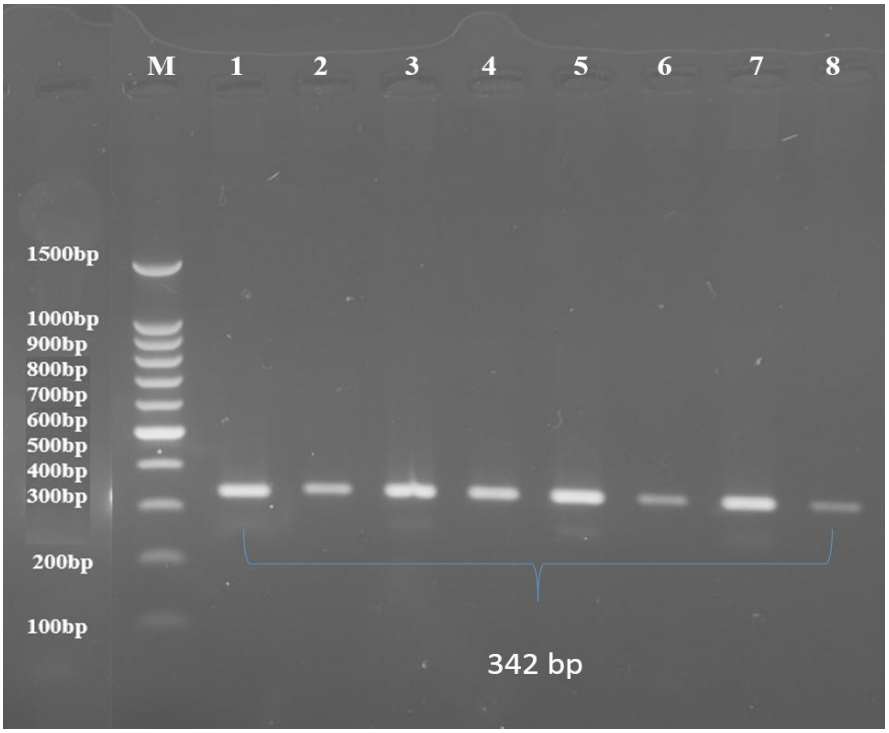

Figure (2): PCR products of bovine GHR gene with size of 342 bp, amplified with primer GHR. The product was electrophoresis on 1.5% agarose gel at5 volt/cm² for 1hour.Lane M DNA ladder (100-1000), Lane (1-8) PCR products was visualized under U.V light after stain with Ethidium Bromide.

The PCR amplified fragments (428bp) of the primer GH that located on the 5th exon at the position 2141, which consider the single SNP were lay on the coding region. We can easily differentiate between 2 different genotypes, LL with four fragments of 265, 96, 51 and 16bp, LV with five digested fragments at 265, 147, 96, 51 and 16 bp. VV genotype (265, 147 and 16 bp) were not observed (Figure 3). Most of buffalo animals investigated in this study are genotyped as LL, as a result of the presence of the restriction site at position 52^53 (AG^CT) for the PCR product, this result supported by Balgh *et al.* (2009) and Andreas *et al.* (2010) through their studying on GH/ *Alu*I gene polymorphisms in Indonesian buffalo. In contrary, this result was partially disagree with Moravčíková *et al.* (2012), with the presence of VV genotype through their studying on GH/ *Alu*I gene polymorphisms in Slovak cattle, otherwise the digested give more than band this may be hard to detect this is may be due to product size which consider large and has to more than one restriction site for the same enzyme.

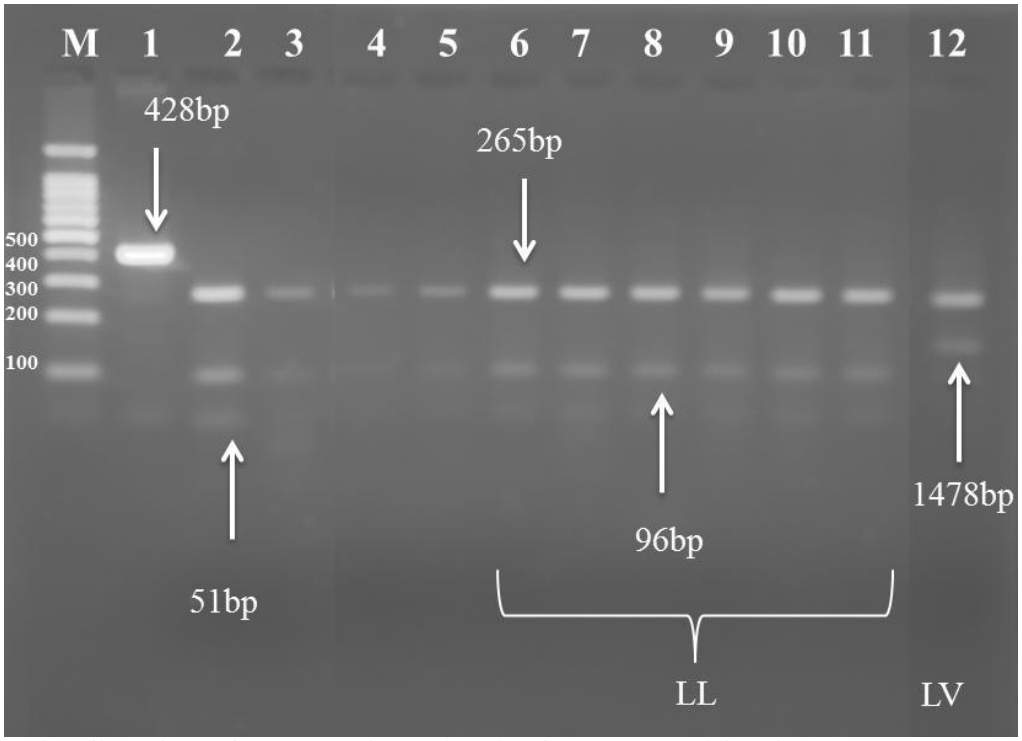

Figure (3): The digestion of PCR products (428) of GH gene with *AluI* enzyme. The product was electrophoresis on 3% agarose gel at 5 volt/cm2 for 1.5 hour, Visualized under U.V light after stain with Ethidium Bromide. Lane M DNA ladder (100-1000), Lane (1): PCR products of the GH gene with size of 428 bp, Lane 2-11: the digested form which represented the dominant LL genotype. Lane 12: digested form which represented the dominant heterogeneous LV genotype.

Distribution of the three genotypes and allele frequency was calculated according to Hardy-Weinberg equation as shown in table (2), Were LL=94 (94.09%), LV=6 (5.82%) and VV=0 (0.09%), so that most of buffaloes was homozygous (LL) and less heterozygous was for the valine allele as compared with leucine allele homozygous (Hussain *et al.*, 2014) . However Kovacs *et al.* (2006) have obtained same result. On the basis of statistical analyses it can be found that LL genotyped dams produced milk with significantly higher milk fat and protein percent. The same association between LL genotype of GH gene with higher milk fat and protein percent was reported by Reis *et al.*, (2001), Sadeghi *et al.*, (2008) and Jakaria *et al.*, (2009).

The mutation of GH 5th exon loci in buffalo were very low. This was indicated by the value of one genotype percentage. A limited number of males in the population, and the high inbreeding frequency can cause low diversity in buffalo.

It can be concluded that the diversity of GH gene in Iraqi buffalo was very low and showed no polymorphisms were detected in these genes. Most buffaloes tested had LL genotype for locus GH 5th exon loci.

Table 2: The genotype of buffalo GH genotypes and allele frequency calculated according to Hardy-Weinberg equation distribution among samples.

Genotypes	**LL**	**LV**	**VV**
Observed	94	6	0
Expected *H-W Freq.*	94.09 94.09%	5,82 5.82%	0.09 0.09%
Allele Frequencies	L= 194 (97%) V= 6 (3%)		
	P-Value =0.7571		

In cattle, a single gene located on chromosome 20 encodes the GHR (Menon *et al.*, 2001). The gene coding for bovine GHR consists of 9 exons (from 2 to 10) in the translated part and of a long 5'-noncoding region (Maj *et al.*, 2004). So far, the primers used in this study (Table 1) flanked a 342-bp fragment from exon 9 of Iraqi buffalo GHR gene. The amplified fragments obtained from all tested buffalo DNA (100 animals) at 342-bp.

Depending on the presence or absence of the restriction site at position 101^102 (AG^CT) in these amplified fragments, we can easily differentiate between 3 different genotypes. AA with undigested one fragment at 342-bp, GG with two digested fragments at 241-and 101-bp and AG with three digested fragments at 342-, 241- and 101-bp.

All buffalo animals investigated in this study are genotyped as GG where all tested buffalo DNA amplified fragments were digested with *Alu*I endonuclease and gave two digested fragments at 241- and 101-bp (Figure 4) due to the presence of restriction site at position 101^102 (AG^CT**)**.

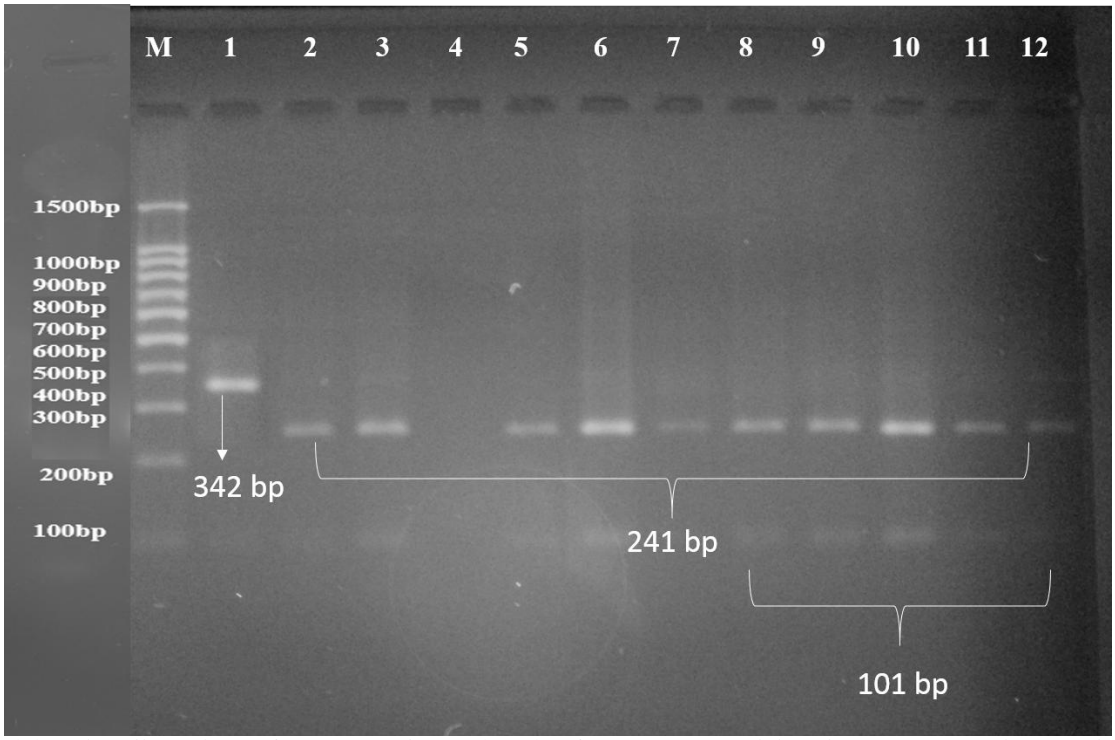

Figure (4): The digestion of PCR products (342) of GHR gene with *AluI* enzyme. The product was electrophoresis on 3% agarose gel at 5 volt/cm^2 for 1.5 hour, Visualized under U.V light after stain with Ethidium Bromide. Lane M DNA ladder (100-1000), Lane (1): the undigested PCR products of the GHR gene with size of 342bp, which represented recessive AA genotype, Lanes 2 to 12: the digested form which represented the dominant GG genotype.

These results supported by Andreas *et al.*, (2010) and Othman *et al.*, (2012), while Some studies showed the substitution at position 256 in cattle (Genbank accession number AY053546), from A to G. These changes caused a loss of enzyme recognition sites of *Alu*I, so that produced fragment of the length 298 bp, known as the AG genotype (Ge *et al.*, 2000; Di Stasio *et al.*, 2005). Genotype found in buffalo in this research was GG genotype (Figure4).

Genetic diversity based on molecular marker GH *Alu*I and GHR *Alu*I loci in buffalo were very low.

Dybus and Grzesiak (2006) showed that the GHRH *Hae*III and GH *Msp*I genes in buffalo from Banten Province were Polymorphic. Low diversity in buffalo can be caused by a 100-limited number of males in the population, and the high inbreeding frequency.

Conclusion

In conclusion, it can be concluded that the diversity of GH *Alu*I and GHR *Alu*I genes in Iraqi buffalo was very low and showed no polymorphisms were detected in these genes. All buffaloes tested had LL genotype for locus GH *Alu*I and GG genotype for locus GHR *Alu*I.

References:

1. Andreas E, Sumantri, Nuraini H, Farajallah A. Anggraeni A. 2010. Identification of GH/ *ALUI* genes polymorphisms in Indonesian buffalo. J. Indones. *Trop. Anim. Agric.*, 35: 215-221.
2. Burton JL, McBride BW, Block E, Glimm DR. 1994. A review of bovine growth hormone. *Can. J. Anim. Sci.* 74: 167-201.
3. Balogh, O., Kovacs, K., Kulcsar, M., Gaspardy, A., Febel, H., Zsolnai, A., Fesus, L., Delavaud, C., Chilliard, Y., Gilbert, R. O. & Gy. Huszenicza (2009) Interrelationship of growth hormone AluI polymorphism and hyperketonemia with plasma hormones and metabolites in the beginning of lactation in dairy cows. Livestock Sci. 123:180-186.
4. Dybus A, Grzesiak W. 2006. GHRH/HaeIII gene polymorphism and its associations with milk production traits in Polish Black-and-White cattle. *Arch. Tierz. Dummerstorf*, 49: 434-438.
5. Ge W, Davis ME, Hines HC, Irvin KM. 2000. Rapid communication: single nucleotide polymorphisms detected in exon 10 of the bovine growth hormone receptor gene. *J. Anim. Sci.* 78:2229–2230.
6. Ge W, Davis ME, Hines HC, Irvin KM, Simmen RCM. 2003. Association of single nucleotide polymorphisms in the growth hormone and growth hormone receptor genes with blood serum insulin-like growth factor I concentration and growth traits in Angus cattle. *J. Anim. Sci.* 81: 641-648.
7. Hale CS, Herring WO, Shibuya H, Lucy MC, Lubahn DB, Keisler DH, Johnson GS. 2000. Decreased growth in Angus steers with a short TGmicrosatellite allele in the P1 promoter of the growth hormone receptor gene. *J. Anim. Sci.* 78: 2099-2104.
8. Hussain DA, Ghareeb AM, Salo WH. 2014. Evaluation of DNA polymorphism in bovine growth hormone gene by PCR-RFLP method. *I.J.S.N.* 5(3): 407-411.
9. Jakaria R, Noor R, Martojo H, Duryadi D, Tappa B. 2009 Identification of growth hormone (Gh) gene MspI and AluI Loci Polymorphism in beef cattle. In the 1st International Seminar on Animal Industry 2009, Bogor, Indonesia, pp. 42-46.
10. Kim NK, Seo YW, Kim GH, Joh JH, Kim OH, Chung ER, Lee CS. 2004. A previously unreported DraI polymorphism within the regulatory region of the bovine growth hormone gene and association with growth traits in Korean Hanwoo cattle. *Anim. Gent.* 35: 142-167.
11. Kmiec M, Kowalewska-Luczak I, Kulig H, Terman A, Wierzbicki H, Lepczynski A. 2007. Associations between GHRH/HaeIII restriction polymorphism and milk production traits in a herd of dairy cattle. *J. Anim. Vet. Adv.* 6(11), 1298-1303.
12. Kovacs K, Volgyi- Csik J, Zsolnai A, Gyorkos I, Fesus L. 2006 Associations between the AluI polymorphism of growth hormone gene and production and reproduction traits in a Hungarian Holstein-Friesian bull dam population. *Arch. Tierz. Dummerstorf* 49: 236-249.
13. Lucy MC, Johnson GS, Shibuya H, Boyd CK, Herring WO. 1998. Rapid communication: polymorphic (GT)n microsatellite in the bovine somatotropin receptor gene promoter. *J. Anim. Sci.* 76: 2209-2210.
14. Moravčíková, N. & Trakovická, A. (2012) SNP analysis of the bovine growth hormone and leptin genes by PCR-RFLP method. J. M. B. F. S., 1: 679-688
15. Maj A, Oprzdek J, Oprzdek A, Dymnicki I, Zwierzchowski L. 2004. Polymorphism in the 5'-noncoding region of the bovine growth hormone receptor gene and its association with meat production traits in cattle. *Anim. Res.* 53,503-514.
16. Otaviano AR, Tonhati H, Sena JA Muooz A. 2005. Kappa-casein gene study with molecular markersin female buffaloes (*Bubalus bubalus*). *Genet.Mol.Biol.* 28: 237-241.
17. Othman EO, Abdel-Samad MF, Abo El Maaty NA, Sewify KM. 2012. Evaluation of DNA polymorphism in Egyption buffalo growth hormone and its receptor genes. *J. Appl. Biol. Sci.* 6: 37-42.
18. Pawar RS, Tajane KR, Joshi CG, Rank DN, Bramkshtri BP. 2007. Growth hormone gene polymorphism and its association with lactation yield in dairy cattle. *Indian J. Anim.* Sci. 77: 884-888.

19. Sadeghi M, Shahr-e-Babak MM, Rahimi G, Javaremi AN. 2008. Association between gene polymorphism of bovine growth hormone and milk traits in the Iranian Holstein Bulls. *Asian J. Anim. Sci*. 2:1–6.

20. Stasio LD, Sartore S, Albera A. 2002. Lack of association of GH1 and POU1F1 gene variants with meat production traits in Piemontese cattle. *Anim. Gent*. 33: 61-64.

21. Tambasco DD, Paz CCP, Tambasco-Studart M, Pereira AP, Alencar MM, Freitas AR, Coutinho LL, Packer IU, Regitano LCA. 2003. Candidate genes for growth traits in beef cattle cross Bos taurus x Bos indicus. *J. Anim. Breed. Genet*. 120: 51-56.

22. Zhu T, Goh ELK, Graichen R, Ling L, Lobie PE. 2001. Signal transduction via the growth hormone receptor. *Cell. Signal*. 13, 599-616.

Published in the Russian Federation
European Journal of Molecular Biotechnology
Has been issued since 2013.
ISSN: 2310-6255
E-ISSN 2409-1332
Vol. 8, Is. 2, pp. 88-102, 2015

DOI: 10.13187/ejmb.2015.8.88
www.ejournal8.com

UDC 577.37 + 537.86

Metabolism, Physiology and Biotechnological Applications of Halobacteria

[1] Oleg Mosin
[2] Ignat Ignatov

[1] Moscow State University of Applied Biotechnology, Russian Federation
Senior research Fellow of Biotechnology Department, Ph. D. (Chemistry)
103316, Moscow, Talalihina ulitza, 33
E-mail: mosin-oleg@yandex.ru
[2] The Scientific Research Center of Medical Biophysics (SRC MB), Bulgaria
Professor, D. Sc., director of SRC MB.
1111, Sofia, N. Kopernik street, 32
E-mail: mbioph@dir.bg

Abstract

Halophiles (*lat.* "salt-loving") is the taxonomic group of extreme aerobic obligate Gram-negative microorganisms that live in conditions of high salinity – in the seas, salt lakes, saline soils etc. These microorganisms are known to reddish patina on products, preserved with using large quantities of salt (NaCl). Halophiles were isolated for the first time at the beginning of the XX century from the marine flora estuary mud, but their systematic study was started only at the end of the second decade of the XX century. The internal environment of the human body is not suitable for existence of halobacteria, since none of them are known to have pathogenic forms. Halobacteria have great practical potential for using in molecular bioelectronics and bio-nanotechnology due to their unique ability to convert the energy of sunlight into electrochemical energy of protons H^+ due to the presence in their cells a special photo transforming retinal containing integral protein – bacteriorhodopsin, the mechanism of action of which has been currently studied in detail. This article describes the characteristics of the metabolism and physiology of halophilic bacteria, as well as a method of biosynthesis and preparation of bacteriorhodopsin from purple membranes of cells of the extreme photoorganotrophic halobacterium *Halobacterium halobium*.

Keywords: halobacteria, bacteriorhodopsin, purple membranes, biosynthesis.

Introduction

The halophiles, related according to the taxonomic classification to the ancient archaea *Archebacteria* genera are single-celled microorganisms with no marked nucleus and expressed membrane organelles, occupy a special place among other microorganisms [1]. These are the only microorganisms that can exist in environments with a high salt content – on salt crystals in the coastal strip, on the salt marsh, in the salt brine etc. (Figure 1). In the Dead Sea (Israel), for example, the salt concentration reaches 26–27 %, in some years, rising to 30 %, whereas at 35 % NaCl precipitates from the salt solution into the sediment [2]. Biochemical apparatus of the cell,

enzymes and ribosomes of halophilic bacteria due to the peculiar cell osmoregulation system and the structure of the cell wall, consisting of proteins and amino sugars, is not only insensitive to such high salt concentrations, but on the contrary needs NaCl and functions effectively only in saturated solutions with 15–20 % of NaCl [3]. For maintainance of cell stability of halophiles primarily NaCl is required. Wherein, Na^+ cations interact with the negatively charged cell wall of halobacteria imparting the necessary stiffness. Inside the cell, the concentration of NaCl is low. Potassium cations (K^+), in conjunction with chlorine anions (Cl^-) are needed to maintain the ionic equilibrium inside and outside of the cells, to stabilize enzymes and other cellular membrane structures of halobacteria. While removing the halobacteria from salinity environment, their cell wall is dissolved and the cytoplasmic membrane disintegrates into smaller fragments.

The family of halobacteria (lat. *Halobacteriaceae)* includes about 20 genera, including *Halobacterium*, *Halococcus*, *Haloarcula*, *Natrococcus*, *Natrobacterium* and others. Extremely halophilic forms of halobacteria are referred to the genera of *Halobacterium* and *Halococcus* (15–32 % NaCl), whereas less halophilic forms – to the genera of *Haloarcula*, *Natronobacterium* and *Natronococcus* (5–20 % NaCl). Members of the halobacteria family are presented by coccoid or rod-shaped forms, as well as by mobile or stationary forms of microorganisms, most of which are painted Gram-positively. Some halobacteria have gas vacuoles for keeping the buoyancy control. The halobacteria usually do hot form spores. According to the nutrition type halobacteria are predominantly aerobic microorganisms, e.g. they require oxygen for the growth, but they also can tolerate the very low oxygen content in growth media (hemoorganotrophs) [4]. Furthermore, halobacteria can use a wide range of organic compounds for the growth as amino acids, carbohydrates and organic acids. They possess a few changes in biochemical pathways of assimilation of sugars via complete citric acid cycle. With a lack of oxygen halobacteria are able to evolve the photoorganotrophic pathway by synthesizing the photo-transforming membrane protein bacteriorhodopsin (BR), which allows use solar energy for the growth.

The halobacteria are oftnen refered as organisms “living on the edge of physiological capabilities”. They have virtually no competitors that could exist under the same conditions, and therefore halophiles freely evolved throughout the evolution of life on Earth. The interesting fact is that some modern bacteria under the growth in extreme conditions acquire the features of halophiles and other ancient archaebacteria by losing the more rigid upper layer in the cell membrane. It is assumed that archaebacteria had lost this layer under the influence of high salt concentrations. The changes in the structure of their cell membranes are caused by the need to ensure the necessary protection for the cells from aggressive external environment. The process of formation of adaptive protective systems in halobacteria demanded the synthesis of specific substances and cellular systems, which do never almost occur in other microorganisms.

Halobacteria have lived on Earth since the Archean age – 3,0–3,5 billion years, almost without changing. Fossilized remains of these organisms are found in ancient rocks aged 2,7 billion years and in Precambrian formations. The oldest of these bacterial remains were found in Isuan green-stone belt in the west of Greenland, where there have been the oldest on Earth, sedimentary rocks formed 3,8 billion years ago. It is possible that the archaebacteria were the first forms of life on Earth in the first period of its evolution [5]. One of the main arguments in favor of this hypothesis is the fact that the representatives of numerous species of archaebacteria use as the sole carbon source for the biosynthesis of components of the cell biomass a mixture of amino acids, i.e., they are heterotrophs.

It is argued that the archaea, bacteria and eukaryotes are submitted by three separate taxonomic lines which were early separated from the ancestral group of microorganisms [6]. Perhaps it was occurred even before the evolution of the cell, wherein the lack of the cell membrane made it impossible to unlimited transfer and exchange of genes that is why the ancestors of the three domains are differed in lockable sets of genes. It is very likely that the common ancestor of archaea and bacteria was a thermophile, it gives a reason to us to assume that low temperatures were “extreme environment” for archaea, and organisms adapted to them, appeared a little later. Indicating the relationship between these three domains is a crucial for understanding the origin of life. The majority of metabolic pathways, which involves most of the genes are similar in bacteria and archaea, whereas the genes responsible for the expression of other genes are very similar in archaea and eukaryotes. According to the cellular structure the archaea are closest to Gram-positive bacteria: their cells are covered with the plasma membrane, the additional outer

membrane, characteristic for Gram-negative bacteria is absent; the cell walls are of varying composition and as a rule are usually thick.

Table 1 below shows some of the main features of the archaea, characteristic or inherent to other domains, to demonstrate their relationship.

Table 1: The general features characteristic of bacteria, archaea and eukaryotes

Typical for archaea and bacteria	Typical for archaea and eukaryotes	Typical only for archaea
The absence of the nucleus and membrane organelles	The absence of peptidoglycan (murein)	The structure of the cell wall (cell walls of some archaea contain psevdomurein)
Ring chromosome	DNA is associated with histone protein	The cell membrane lipids contain ether linkage bond
Genes are combined into operons	Translation of protein begins with the methionine residue	The structure of flagellin
No introns and RNA processing	Similar RNA polymerase and other components of the transcription	The structure of the ribosome (some signs closer to the bacteria, while some others - with eukaryotes)
Polycistronic mRNA	Similar mechanisms of replication and repair of DNA	The structure and metabolism of tRNA
Cell size (more than 100 times less than in eukaryotes)	A similar ATPase (type V)	No fatty acid synthase

The genetic apparatus of the archaea is represented by a single circular chromosome with the size of 5751492 bp found in *Methanosarcina acetivorans*, having the largest known gene among the archaea [7]. On the contrary in *Nanoarchaeum equitans* 1/10 the size of the genome composes 490 885 bp, having the smallest known genome among the archaea; it contains only 537 genes, encoding different proteins [8]. The archaea also contains smaller molecules of DNA, known as plasmids. Probably the plasmids can be transferred via contact between the cells, in a process similar to bacterial conjugation.

However, evolutionary relationship between archaea and eukaryotes remains to be unclear. Besides the similarities in the structure and functions of cells, there are similarities at the genetic level. It was found that a group of archaea – *Crenarchaeota* are closer to eukaryotes than to other types of archaea – *Euryarchaeota* [9] The most common is a hypothesis that the ancestor of eukaryotes early separated from the archaea, and eukaryotes appeared as a result of the merger of archaea and eubacteria; the later became the cytoplasm and the nucleus of the new merged cell [10]. This hypothesis explains the various genetic similarities, but has some difficulty in explaining the cell structure.

The recent information on the genetic diversity of the archaea is fragmentary, and the total number of species could not be evaluated fully. Comparative analysis of the 16S structures of rPHK

of archaea allowed assuming the existence of 18–20 phylogenetic groups of the archaea [11]. Numerous of these groups are known only from a single sequence of rRNA, which suggests that the limits of the diversity of these organisms remain to be unclear. Many halobacteria have never been cultured under laboratory conditions, which makes their identification difficult.

The aim of the research was the investiging of the metabolism and physiology of extreme halophilic bacteria *Halobacterium halobium* and searching for new biotechnological applications of the synthesized by this bacterium photo-transforming integral membrane protein bacteriorhodopsin (BR).

Material and methods

Bacterial objects

As a BR producer was used a carotenoid strain of extreme photo-organotrophic halobacterium *Halobacterium halobium* ET 1001, obtained from Moscow State University (Russia). The strain was modified by selection of individual colonies on solid (2% (w/v) agarose) media with peptone and 4.3 M NaCl.

Growth conditions

BR (yield 8–10 mg from 1 g biomass) was obtained in synthetic (SM) medium (g/l): *D,L*-alanine – 0,43; *L*-arginine – 0,4; *D,L*-aspartic acid – 0,45; *L*-cysteine – 0,05; *L*-glutamic acid – 1,3; *L*-lycine – 0,06; *D,L*-histidine – 0,3; *D,L*-isoleucine – 0,44; *L*-leucine – 0,8; *L*-lysine – 0,85; *D,L*-methionine – 0,37; *D,L*-phenylalanine – 0,26; *L*-proline – 0,05; *D,L*-serine – 0,61; *D,L*-threonine – 0,5; *L*-tyrosine – 0,2; *D,L*-tryptophan – 0,5; *D,L*-valine – 1,0, AMP – 0,1; UMP – 0,1; NaCl – 250; $MgSO_4 \cdot 7H_2O$ – 20; KCl – 2; NH_4Cl – 0,5; KNO_3 – 0,1; KH_2PO_4 – 0,05; K_2HPO_4 – 0,05; Na^+-citrate – 0,5; $MnSO_4 \cdot 2H_2O$ – $3 \cdot 10^{-4}$; $CaCl_2 \cdot 6H_2O$ – 0,065; $ZnSO_4 \cdot 7H_2O$ – $4 \cdot 10^{-5}$; $FeSO_4 \cdot 7H_2O$ – $5 \cdot 10^{-4}$; $CuSO_4 \cdot 5H_2O$ – $5 \cdot 10^{-5}$; glycerol – 1,0; biotin – $1 \cdot 10^{-4}$; folic acid – $1{,}5 \cdot 10^{-4}$; vitamin B_{12} – $2 \cdot 10^{-5}$. The growth medium was autoclaved for 30 min at 0,5 atm, the pH value was adjusted to 6,5–6,7 with 0,5 *M* KOH. Bacterial growth was performed in 500 ml Erlenmeyer flasks (volume of the reaction mixture 100 ml) for 4–5 days at 35 °C on Biorad shaker ("Birad Labs", Hungary) under intense aeration and monochromatic illumination (3 lamps × 1,5 *lx*). All further manipulations for BR isolation were carried out with the use of a photomask lamp equipped with an orange light filter.

Isolation of purple membranes (PM)

Biomass (1 g) was washed with distilled water and pelleted by centrifugation on T-24 centrifuge ("Carl Zeiss", Germany) (1500 g, 20 min). The precipitate was suspended in 100 ml of dist. H_2O and kept for 3 h at 4 °C. The reaction mixture was centrifuged (1500 g, 15 min), the pellet was resuspended in 20 ml dist. H_2O and disintegrated by infrasound sonication (22 kHz, 3 times × 5 min) in an ice bath (0 °C). The cell homogenate after washing with dist. H_2O was resuspended in 10 ml of buffer containing 125 mM NaCl, 20 mM $MgCl_2$, and 4 mM Tris-HCl (pH = 8.0), then 5 mg of RNA-ase (2–3 units of activity) was added. The mixture was incubated for 2 h at 37 °C. Then 10 ml of the same buffer was added and kept for 10–12 h at 4 °C. The aqueous fraction was separated by centrifugation (1500 g, 20 min), the PM precipitate was treated with 50 % (v/v) ethanol (5 times × 7 ml) at 4 °C followed by separation of the solvent. This procedure was repeated 6 times to give a colorless washings. The protein content in the samples was determined spectrophotometrically on DU-6 spectrophotometer ("Beckman Coulter", USA) by the ratio D_{280}/D_{568} ($\varepsilon_{280} = 1{,}1 \cdot 10^5$; $\varepsilon_{568} = 6{,}3 \cdot 10^4$ $M^{-1} \cdot cm^{-1}$) [12]. PM regeneration is performed as described in the article [13]. Yield of PM fraction – 120 mg (80–85 %).

Isolation of BR

Fraction PM (in H_2O) (1 mg/ml) was dissolved in 1 ml of 0,5 % (w/v) sodium dodecyl sulfate (SDS-Na), and incubated for 5–7 h at 37 °C followed by centrifugation (1200 g, 15 min). The precipitate was separated, than methanol was added to the supernatant in divided portions (3 times × 100 ml) at 0 °C. The reaction mixture was kept for 14–15 h in ice bath at 4 °C and then centrifuged (1200 g, 15 min). Fractionation procedure was performed three times, reducing the

concentration of 0,5 % SDS-Na to 0,2 and 0,1 %. Crystal protein (output 8–10 mg) was washed with cold ^2H_2O (2 times × 1 ml) and centrifuged (1200 g, 15 min).

Purification of BR

Protein sample (5 mg) was dissolved in 100 ml of buffer solution and placed on a column (150 × 10 mm), stationary phase – Sephadex G-200 ("Pharmasia", USA) (specific volume packed beads – 30–40 units per 1 g dry of Sephadex) equilibrated with buffer containing 0,1 % (w/v) SDS-Na and 2,5 mM ETDA. Elution proceeded by 0,09 M Tris-buffer containing 0,5 M NaCl, pH = 8,35 at a flow rate of 10 ml/cm^2 · h. Combined protein fraction was subjected to freeze-drying, in sealed glass ampoules (10 × 50 mm) and stored in frost camera at -10 ^{0}C.

Quantitative analysis of the protein

The procedure was performed in 12,5 % (w/v) polyacrylamide gel (PAAG) containing 0,1 % (w/v) SDS-Na. The samples were prepared for electrophoresis by standard procedures (LKB protocol, Sweden). Electrophoretic gel stained with Coomassie blue R-250 was scanned on a CDS-200 laser densitometer (Beckman, USA) for quantitative analysis of the protein.

Absorption spectra

Absorption spectra of pigments were recorded on the programmed DU-6 spectrophotometer ("Beckman Coulter", USA) at λ = 280 nm and λ = 750 nm.

Scanning electron microscopy

The structural studies were carried out with using scanning electrom microscopy (SEM) on JSM 35 CF (JEOL Ltd., Corea) device, equiped with X-ray microanalyzer "Tracor Northern TN", SE detector, thermomolecular pump, and tungsten electron gun (Harpin type W filament, DC heating); working pressure: 10^{-4} Pa (10^{-6} Torr); magnification: 100000, resolution: 3,0 nm, accelerating voltage: 1–30 kV; sample size: 60–130 mm.

Results and Discussion

The structure of BR

The mechanism of converting the solar energy into the chemical energy of ATP used by halobacteria is different from the classic photosynthetic mechanism realized by plants and green algae containing chlorophyll. For this purpose halobacteria use a special chromophore protein with a molecular weight of 26 kDa, designated bacteriorhodopsin (BR) by analogy with the photo-sensitive protein of mammalian visual apparatus – rhodopsin providing visual perception in animals and humans [14]. BR was firstly isolated in 1971 from the cell membrane of extreme photoorganotrophic halobacteria *Halobacterium halobium*, inhabiting saline geothermal lakes and seas, including the Dead Sea (Israel) [15]. This photo-transforming protein is represented by a chromoprotein associated by aldimine bond with the amino acid residue lysine-216. As a chromophore group the BR contains an equimolar mixture of 13-*cis*- and 13-*trans-retinal* – an analogue of vitamin A defining purple-red color of colonies of halobacteria. Along with the BR the cell membrane of halophiles contains other carotenoid pigments, the main of which bakterioruberin, causes the colorage of halobacteria from pink to red and red-orange [16]. The presence of these pigments has to the halophiles an important meaning as a means of protection against excessive solar radiation, as their habitats are characterized by high luminosity, and these pigments are able to delay radiation.

The cell membrane of halophiles also contains two sensory rhodopsins, which provide positive and negative phototaxis in cells [17]. These proteins absorb different wavelengths of light, causing a cascade of signals that eventually control the flagella of halobacteria. For example, the absorption of a photon of red light leads to the generation of a signal on which halobacteria begin to move toward the light source. By the absorption of a photon of blue light, it is occurred the opposite reaction. The maximum optical effect is achieved in both cases at wavelengths of λ = 565 and λ = 370 nm, respectively [18]. Thus, the photosensor reaction provides the optimal for the cell spatial orientation. Cells leave areas, which penetrates detrimental shortwave solar radiation and by means of flagella or gas vacuoles are concentrated in a favorable light condition area. This mechanism provides optimal conditions for the growth and vital function of halobacteria.

Furthermore, the cell membrane of halovacteria contains another membrane protein, halorhodopsin serving as a light-dependent pump of chlorine ions (Cl^-), the main function of which is the transport of Cl^- into the cell [19]. Life in environments with high concentrations of NaCl has resulted in the development in halobacteria an effective system of active transport of Na^+ and K^+, whereby Na^+ is pumped out the cell and K^+, on the contrary, is pumped into the cell. As a result, the Na^+ content in the cytoplasm is maintained at a low level.

Despite the similarity of the mechanism of action of BR with the visual animal protein – rhodopsin, the amino acid sequence of BR differs from the animal rhodopsin that suggests their independent evolutionary origins. This is confirmed by the fact that the BR molecule forms 13-*cis, trans*- configuration rather than 11-*cis, trans*-configuration as in the animal rhodopsin [20]. However, the conformation of BR indicates that the protein belongs along with the rhodopsin to the family of transport G-proteins that involved in a large number of biochemical signal processes in the cell.

According to the structure and location in the cell membrane BR refers to integral transmembrane proteins, penetrating the entire thickness of the cell membrane of halophiles, which is divided into three main fractions: yellow, red and purple. The purple fraction, containing 75 % of BR, carotenoid and phospholipid (mainly phospho glycerol with a small amount of non-polar lipids and isoprenoids) and water forms natural two-dimensional crystals that can be investigated with using electron microscopy techniques and diffraction analysis – X-ray scattering and the scattering of electrons and neutrons on the surface of PM crystals [21]. These methods proved the existence in the BR molecule 7 α-helical protein segments in the middle of which is symmetrically located the chromophore moiety as a retinal residue (Figure 1).

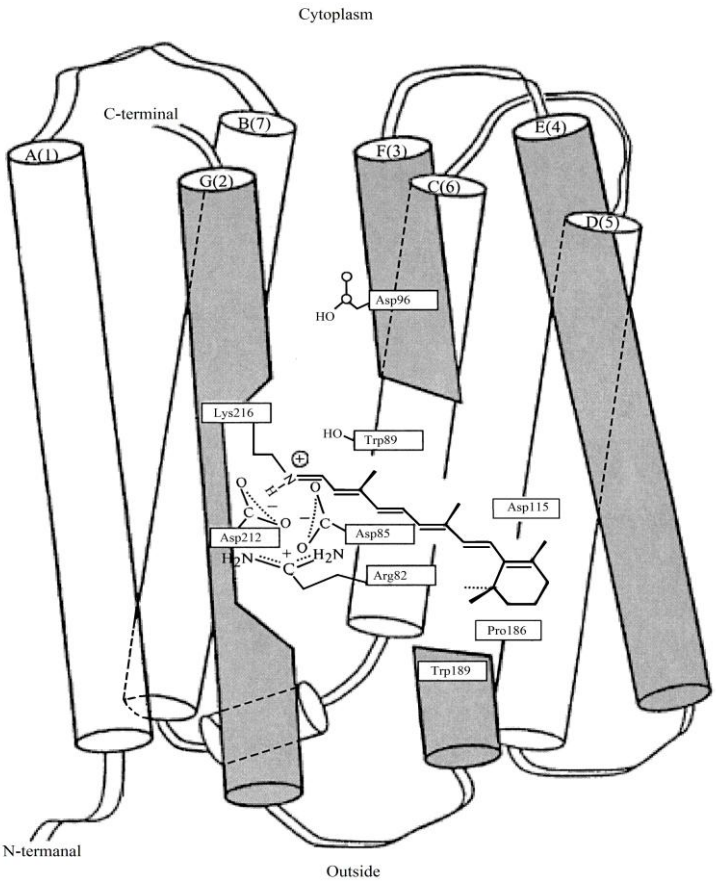

Figure 1. Location of the protein moiety of the BR and the retinal residue in the cell membrane of halobacteria *Halobacterium halobium* according to computer simulation [20]: protein fragments of the BR molecules in the form of 7 penetrating the cell membrane α-helical segments are indicated in Latin characters; dark color designated the segments responsible for binding the retinal residue to the protein part of the BR molecule.

The polypeptide chain of BR consists of 248 amino acid residues, 67 % of which are hydrophobic [22], while 33 % – hydrophilic residues formed by aspartic and glutamic acids, arginine and lysine (Figure 2a). These residues play an important structural and functional role in the spatial orientation of α-helical segments of the BR molecule, which is organized in the purple membrane in an orderly manner in the form of trimmers with an average diameter of about 0,5 mm and a thickness of 5–6 nm. Each trimmer is surrounded by six others so that a proper hexagonal crystal lattice is formed (Figure 2b). The individual BR molecule consists of 7 α-helix segments arranged in the direction perpendicular to the plane of the cytoplasmic membrane (Figure 2c). Hydrophobic domains represent transmembrane segments, whereas hydrophilic domains protrude from the membrane and connect the individual intra membranous α-helical segments of protein segments in the BR molecule [23].

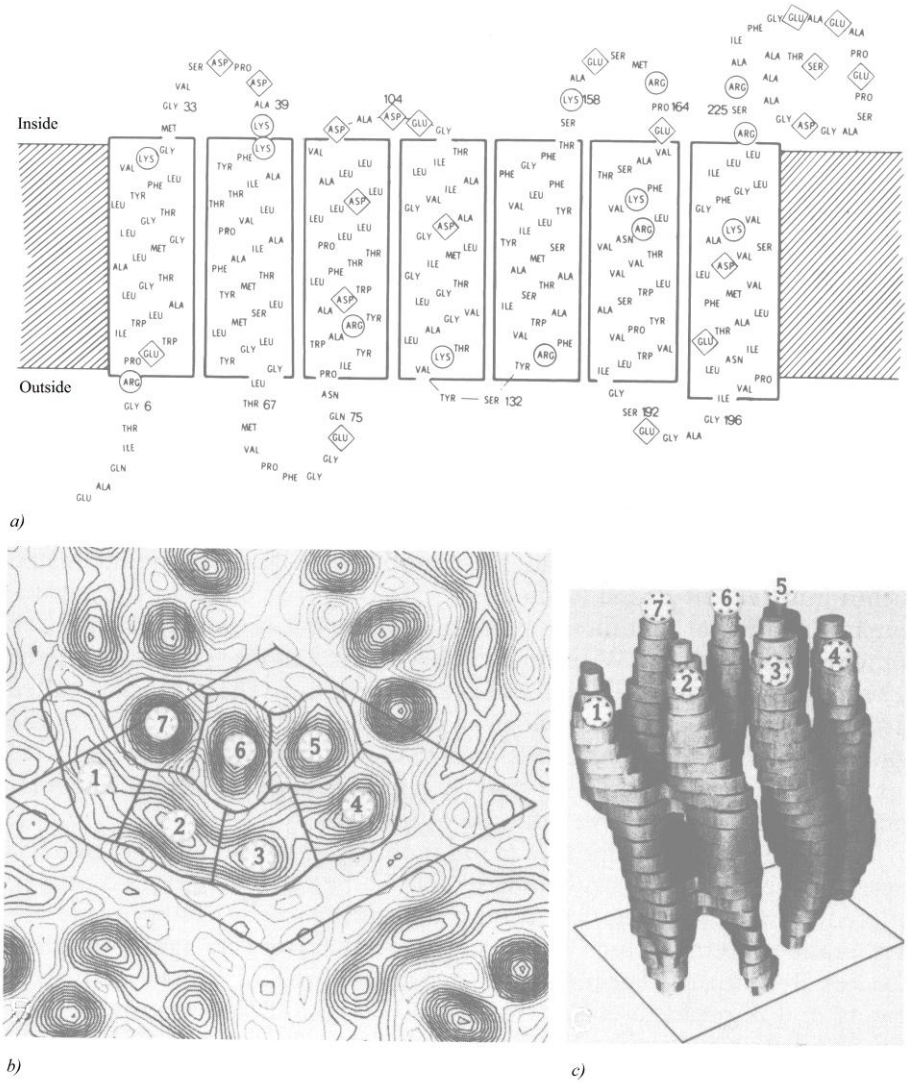

Figure 2. The structure of the BR molecule according to diffraction analysis [21]: a) – the primary structure of the BR molecule: amino acids indicated in Latin characters, circles and rhombs show the functionally important amino acids responsible for spatial orientation of α-helical segments of the protein residue of BR and formation of channels for the transfer of protons H^+ across the cell membrane; b) – electron density map of PM (a single molecule of the protein is encircled in the center). Numbers 1–7 are designated α-helical segments of BR: 1 – A-segment; 2 – B-segment; 3 – C-segment; 4 – D-segment; 5 – E-segment; 6 – F-segment; 7 – G-segment; c) – the spatial structure of the BR molecule: 1 – A-segment; 2 – B-segment; 3 – C-segment; 4 – D-segment; 5 – E-segment; 6 – F-segment; 7 – G-segment.

The mechanism of functioning of BR

BR acts as a light-dependent proton pump, pumping protons across the cell membrane and generates an electrochemical gradient of H^+ on the surface of the cell membrane, which energy is used by the cell for the synthesis of ATP in the anaerobic photosynthetic phosphorylation [24]. The mechanism of ATP synthesis is called "non-chlorophyll photosynthesis", in contrast to the plant photosynthesis with the participation of chlorophyll. In this mechanism, at absorption of a light photon the BR molecule becomes decolorized by entering into the cycle of photochemical reactions, resulting in the release of a proton to the outside of the membrane, and the absorption of proton from intracellular space. The formation of concentration gradient of H^+ leads to the fact that the illuminated halobacteria cells begin to synthesize ATP, i.e. convert light energy into the energy of chemical bonds. Due to this, the pH value inside the cytoplasm keeps the constant value – about 3 units and only slightly dependent on the pH of the exterior medium, which can reach 10–12 units.

The mechanism of subsequent sequential proton transfer of H^+ with the participation of the BR molecule across the cell membrane includes a chain of hydrogen bonds formed by the side residues of hydrophilic amino acids extending through the entire thickness of the protein. This H^+ proton transfer through the protein chain is carried out providing the protein consists of two parts and contains a photochrome functional group capable under the influence of light to change its microenvironment and thereby sequentially "lock" and "unlock" sites of binding of H^+ and its further transfer across the cell membrane. The role of such a "shuttle" mechanism between two conductors of H^+, one of which communicates with the exterior, and the other – with the cytoplasmic surface of the cell membrane plays a retinal residue linked by the aldimine bond (as in the visual pigments of animals) with a lysine-216 residue of the protein. Retinal has a 13-*trans* conformation and is located in the membrane tunnel between protein α-segments of the BR molecule, blocking the flow of protons. By the absorption of a light photon it occurs reversible isomerization of 13-*tras*-BR (λ_{max} = 548 nm) (the quantum yield 0,03 at 20 ^oC) into the 13-*cis*-BR (λ_{max} = 568 nm) [25], initiating a cascade of photochemical reactions lasting from 3 ms to 1 ps with the formation of transitional intermediates J, K, L, M, N, and O, followed by separation of H^+ from the retinal residue of BR and the connection of H^+ from the side of cytoplasm (Figure 3). In this process, the retinal residue is specifically bent in the membrane tunnel forming the transmembrane transport H^+ channel from the cytoplasm to the outside environment, and carries a proton H^+ from the inner cytoplasmic membrane to the outer membrane of the cell. In this case, a proton H^+ from the retinal residue is transferred to the Asp-85-residue, after that the resulting vacancy is filled with a proton H^+ transferred from the residue Asp-96. As a result, between the internal and external surface of the membrane forms a concentration gradient of H^+, which leads that illuminated cells begin to synthesize ATP, i.e. convert light energy into energy of chemical bonds. This process is reversible and in the dark flows in the opposite direction. In this way the BR molecule behaves as a photochromic carrier with a short relaxation time – the transition from the excited state to the ground state. Optical characteristics of BR vary depending on the method of preparation of PM embedded onto the polymer matrix.

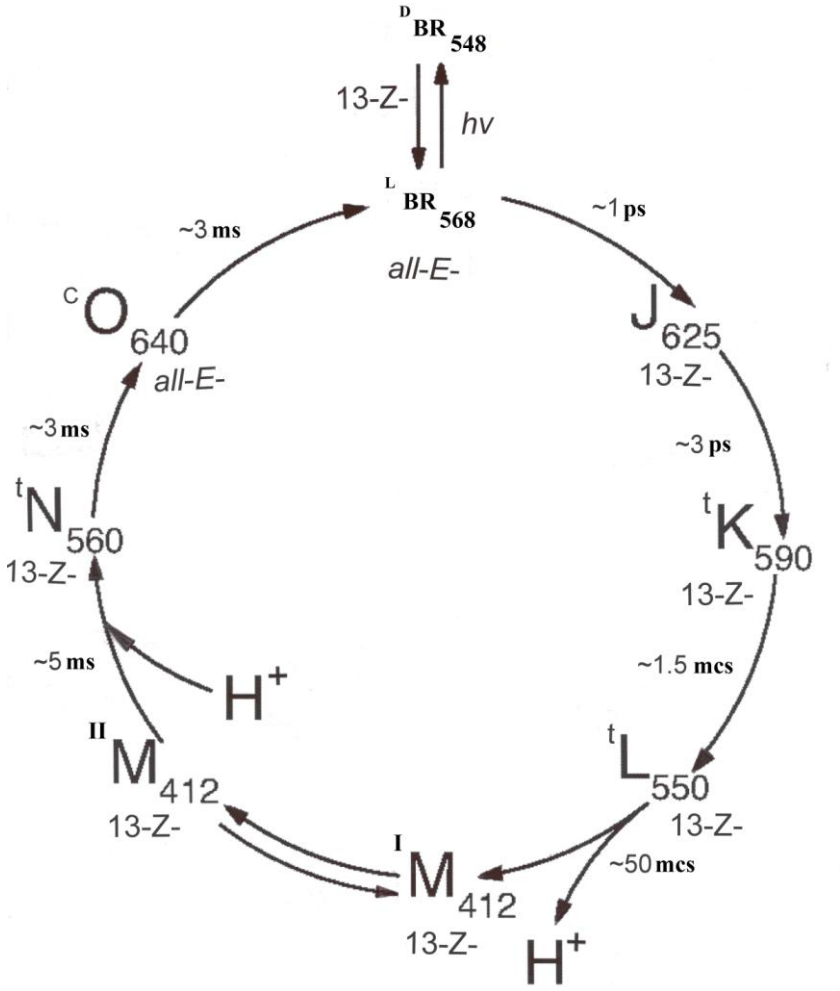

Figure 3. Photocycle scheme of BR (aqueous solution, pH = 7,2; t = 20 °C). Latin numbers J, K, L, M, N, O denote spectral intermediates of BR. [I]M and [II]M represent spectral intermediants of *meta*-bacteriorhodopsin with the protonated ([I]M) and deprotonated ([II]M) aldimine bond. L and D denote dark and light forms of pigments. The subscripts correspond to the position of the absorption maximum in the photocycle intermediates (nm).

An interesting feature of the metabolism of halobacteria is at that the presence of oxygen and the organic compound (amino acids, peptones), which can be used as growth substrates and sources of energy, halophiles can grow in the dark, by switching on a heterotrophic photosynthetic metabolism [26]. However, with a lack or even in the complete absence of oxygen and under the bright light in the cell membrane of halobacteria is synthesized BR, allowing them to use solar energy for growth and ATP synthesis. Thus, halobacteria are capable to carry out the synthesis of ATP molecules as due to chemical energy released in the process of oxidation in the respiratory chain, as well as using the light energy absorbed by BR.

The spheres of practical application of BR in bionanotechnology

BR is the focus of bio-and nanotechnology because of its high sensitivity and resolution, and is used in molecular bioelectronics as natural photochromic material for light-controlled electrical regulated computer modules and optical systems [27]. In addition, BR is very attractive as a model for studies related to the research into the functional activity and structural properties of photo-transforming membrane proteins embedded into the native and photo-converting membranes [28].

Nanofilms produced using the BR-containing PM were first obtained and studied in this country in the framework of the project “Photochrome” [29], when it was demonstrated

effectiveness and prospects for the use of BR as photochromic material for holographic recording (Figure 4).

The main task for the manufacture of BR-containing nanofilms is the orientation of PM between the hydrophobic and hydrophilic media. Typically, to improve the characteristics of the BR-containing films use multiple layers of PM that are applied to the surface of the polymeric carrier and dried up, preserving their natural structure. The best results are achieved in the manufacture of nanofilms embedded onto the gelatin matrix [30]. This allows to achive high concentration of BR (up to 50 %) in nanofilms and avoid aggregation of cell membrane fragments and destruction of BR in the manufacturing process [31].

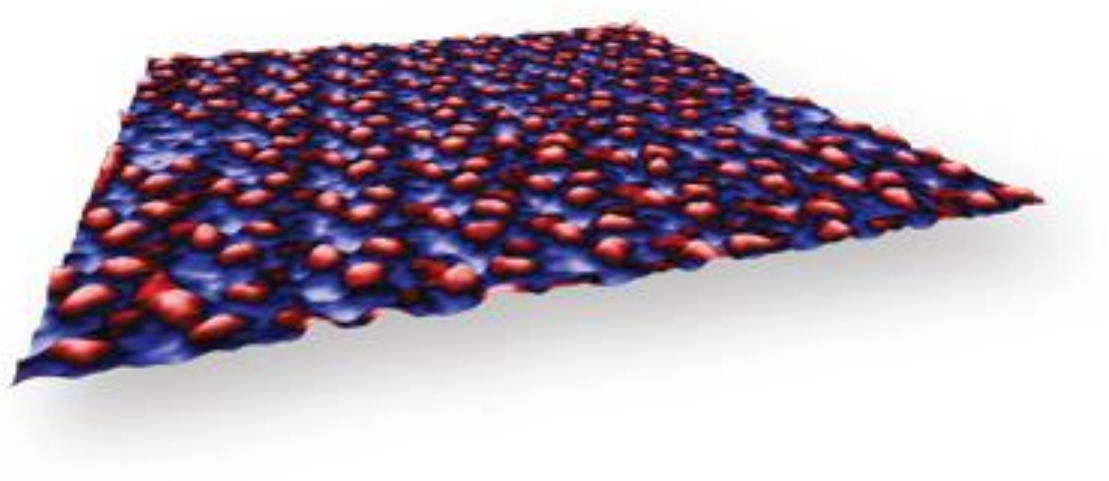

Figure 4. Artificial membrane based on the BR-containing PM in scanning electron microscope (SEM): scanning area – 100×100 mm; resolution – 50 nm; magnification – 100000 times. PM shown in purple, BR – in red color.

Embedded into a gelatin matrix BR-containing PM fragments are durable (~10^4 h) and resistant to solar light, the effects of oxygen, temperatures greater than 80 °C (in water) and up to 140 °C (in air), pH = 1–12, and action of most proteases [32]. The dried PM are stacked on top of each other, focusing in the plane of the matrix, so that a layer with 1 μm thickness contains about 200 monolayers [33]. When being illuminated such nanofilms exert the electric potential at 100–200 mV, which coincides with the membrane potential of living cells [34]. These factors are of great practical importance for integration of PM into polymeric nanomatrix with keeping photochemical properties.

Biosynthesis of BR

The technology of preparation of BR consists in growing of halobacteria on liquid artificial synthetic media with 15–20 % NaCl, containing synthetic amino acids or on natural media with peptones or protein-vitamin concentrate (PVC) of yeast [35].

Artificial synthetic media are represented by mixtures of synthetic essential amino acids (glycine, alanine, arginine, aspartic acid, cysteine, glutamic acid, histidine, isoleucine, leucine, lysine, methionine, phenylalanine, proline, serine, threonine, tyrosine, tryptophan, valine), nucleotides (adenosine-5-monophosphate, uridine-5-monophosphate), inorganic salts and vitamins.

Peptones – are products of partial hydrolysis of animal proteins (milk, meat), consisting of mixtures of different polypeptides; also contain di- and tripeptides, and free amino acids. Peptones are formed by the action of proteolytic enzymes of the gastric and pancreatic juices (pepsin, trypsin) on natural proteins, as well as by mild hydrolysis of animal proteins by acids and alkalis. The source of the peptone protein depends on the species from which it is derived: meat, fish, egg peptones etc.

PVC is a dry biomass of feed yeast of saccharomyces genus of *Saccharomyces cerevisiae*, grown on hydrocarbons - oil paraffins (paprin) or natural gas (gaprin). It contains approx. 50 % of

protein, a full set of vitamins, a large number of trace elements (iron, manganese, iodine, magnesium, sodium, zinc) and amino acids.

Depending on the needs of a particular type of halobacteria in sources of growth substrates use artificial synthetic nutrient media or media prepared on the basis of natural peptons of PVC of yeast.

For the biosynthesis of BR often use the extreme aerobic photo-organotrophic halobacterium *Halobacterium halobium* [36]. This bacterium is grown on the synthetic liquid complex medium containing 18 amino acids (alanine, arginine, aspartic acid, cysteine, glutamic acid, glycine, histidine, isoleucine, leucine, lysine, methionine, phenylalanine, proline, serine, threonine, tyrosine, tryptophan, valine), nucleotides (adenosine-5-monophosphate, uridine-5-monophosphate), inorganic salts of sodium, magnesium, manganese, copper, calcium, zinc, iron, potassium, ammonium, phosphorus) and biotin, folic acid and vitamin B_{12}.

The process of growing the halobacteria is conducted on an orbital shaker in flat-bottomed flasks in condition of intensive aeration under the light of monochrome fluorescent lamps. Bacterial growth was measured by optical density of the cell suspension at λ=620 nm on a spectrophotometer. As is shown in Figure 5 under optimal growing conditions (incubation period 4–5 days, temperature t = 35 °C, illumination with monochromatic light at λ = 560 nm) in cells is synthesized the purple carotenoid pigment, characterized as BR by the spectral ratio of protein and chromophore fragments D_{280}/D_{568} = 1,5:1,0 in the molecule [37]. The subsequent isolation of BR from the PM fraction is carried out by a combination of physical, chemical and enzymatic methods [38].

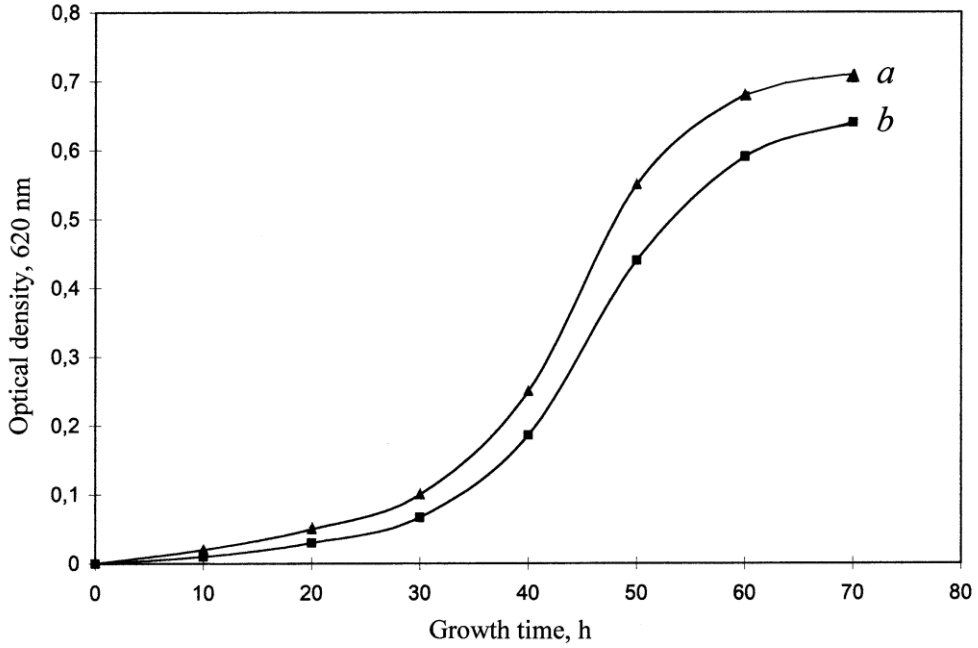

Figure 5. Growth dynamics of *H. halobium* under different conditions: *a)* – the peptone medium; *b)* – complex synthetic medium. Growing conditions: incubation period of 4–5 days at t = 35 °C; illuminating by monochromatic light with a wavelength of λ = 560 nm.

Isolation of BR

Isolation and purification of BR from PM fraction is carried out with using a light-shielding lamp equipped with an orange color filter as BR is very sensitive to light and light isomerization.

The main stages for obtaining BR are:

- Growing the halobacterium *H. halobium* on artificial or natural nutrient media;
- Cell disruption and lysis of cell walls;
- Allocation fraction of PM;
- Cleaning of PM from low- and high molecular weight impurities, cellular RNA and carotenoids;

• Dissolving the PM fraction in a 0,5 % solution of the ionic detergent sodium dodecyl sulfate (SDS-Na) to form a microemulsion;
• Precipitation of BR from the microemulsion by methanol;
• Gel Permeation Chromatography (GPC) on Sephadex G-200;
• Electrophoresis in 12,5 % polyacrylamide (PAGE) gel.

The protein is localized in the PM; the release of low molecular weight impurities and intracellular contents was reached by osmotic shock of cells with distilled water in the cold after the removal of 4,3 *M* NaCl and the subsequent destruction of the cell membrane by ultrasound at 22 kHz. For the destruction of cellular RNA the cellular homogenate was treated with Rnase I. PM fraction along with the desired protein in a complex with lipids and polysaccharides also contained impurity of related carotenoids and proteins. Therefore, it was necessary to use special methods of fractionation of the protein without damaging its native structure and dissociation. That required applying the special methods of purification of carotenoids and lipids, and the subsequent GPC on Sephadex G-200. Removing of carotenoids, consisting in repeated treatment of PM with 50 % (v/v) EtOH at t = 4 °C, was a routine but necessary step, in spite of the significant loss of chromoprotein. It was used five treatments by 50 % (v/v) EtOH to obtain the absorption spectrum of purified from carotenoids PM suspension (4) and (5) (degree of chromatographic purity of 80–85 %), as shown in Figure 6 at various processing stages (*b*) and (*c*) relative to the native BR as a control (*a*). The formation of retinal-protein complex in the BR molecule leads to a bathochromic shift in the absorption spectrum of PM (Figure 6*c*) – the main bandwith (1) with the absorption maximum at λ = 568 nm is caused by the light isomerization of the chromophore by the C13=C14 bond is determined by the presence of 13-*trans*-retinal residue in BR_{568}; additional low-intensity bandwith (2) at λ = 412 nm characterizes a minor impurity of a spectral form of *met*a-bacteriorhodopsin M_{412} (formed in the light) with deprotonated aldimine bond between 13-*trans*-retinal residue and protein; the total bandwith (3) at λ = 280 nm is determined by the absorption of aromatic amino acids in the polypeptide chain of the protein (for the native BR – D_{280}/D_{568} = 1,5:1,0).

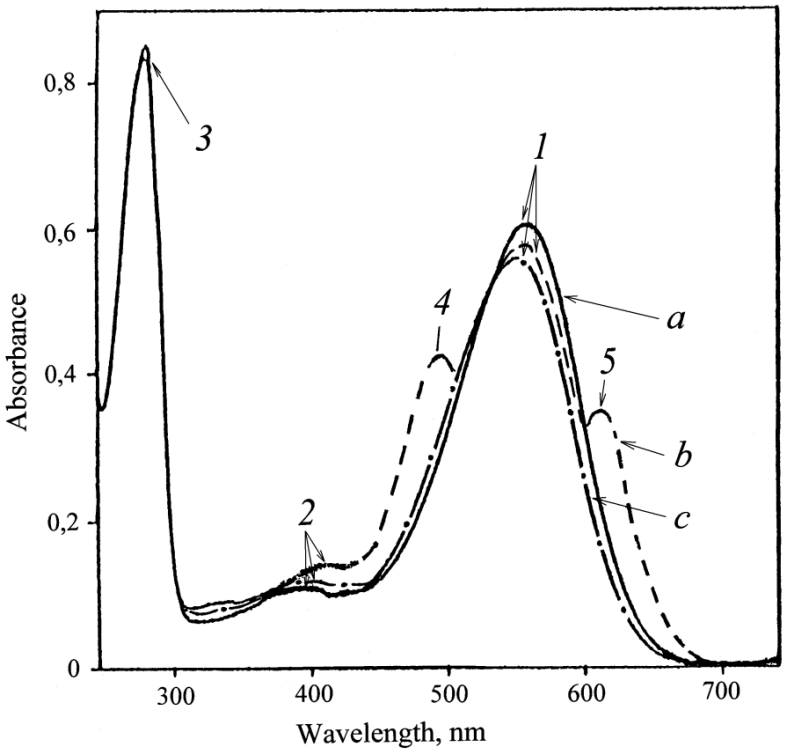

Figure 6. The absorption spectra of the PM (50 % (v/v) EtOH) at various stages of processing: (*a*) – the natural BR (control); (*b*) – PM after intermediate treatment; (*c*) – PM purified from carotenoids. The bandwith (1) is the spectral form of BR_{568}; (2) – impurity of spectral form of *meta*-bacteriorhodopsin M_{412}; (3) – the total absorption bandwith of aromatic amino acids; (4) and (5) – extraneous carotenoids. As a control used the native BR

The fractionation and chromatographic purification of BR

The fractionation and chromatographic purification of the protein was the next necessary step of the research. As BR, being an integral membrane protein intricately penetrates bi-lipid layer in form of seven α-helices, the use of ammonium sulfate and other conventional agents to salting out did not give a positive result for isolation of the protein. The resolving was in the translation of the protein to a soluble form by the colloidal dissolution (solubilization) in an ionic detergent. Using as the ionic detergent SDS-Na was dictated by the need to carry out the solubilization of the protein in a native, biologically active form in complex with 13-*trans*-retinal, because BR solubilized in 0,5 % (v/v) SDS-Na retains a native α-helical configuration [39]. Therefore, there is no need to use organic solvents as acetone, methanol and chloroform for purification of lipids and protein, and precipitation and delipidization is combined into a single step, which significantly simplifies the further fractionation. A significant advantage of this method is that the isolated protein in complex with lipids and detergent molecules was distributed in the supernatant, and other high molecular weight impurities – in unreacted precipitate, easily separated by centrifugation [40]. Fractionation of the protein solubilized in a 0.5% (w/v) SDS-Na and its subsequent isolation in crystalline form was achieved at t = 4 ^{o}C in three steps precipitating procedure with treatment by methanol, reducing the concentration of detergent from 0,5; 0,25 and 0,1 % (w/v) respectively.

The final stage of BR purification involved the separation of the protein from low-molecular-weight impurities by using GPC-method. For this purpose the BR containing fraction was passed twice through a chromatography column with dextran Sephadex G-200 balanced with 0,09 *M* Tris-buffer (pH = 8,35) containing 0,1 % (w/v) SDS-Na and 2,5 *mM* EDTA. The elution was carried out at t = 20±25 ^{o}C with 1 mM Tris-HCl buffer (pH = 7,6) at rate of 10 ml/cm^{2}·h. The data on purification of BR of phospholipids and carotenoids are shown in Table 2. As it is demonstrated in Table 2, 84 % of phospholipids was removed by five washes (65, 70 and 76 % was removed by 1st, 2nd and 3nd wash respectively). The total endogenous phospolipid removal on the BR peak was 92 % relative to the native PM.

Table 2: Summary results for the isolation and purification of BR by various methods

Sample	PM content, mol PM/mol BR	Phospholipid and carotenoid removal, %	BR yield*, %
PM fraction	20,5	–	–
PM washed with EtOH			
1 wash	16,9	65	93
2 wash	15,1	70	90
3 wash	14,5	76	88
4 wash	13,6	81	84
5 wash	13,2	84	80
BR crystallised from MeOH	12,9	86	75
BR from GPC on Sephadex G-200	10,2	92	86

Notes:

* Percentage yield is indicated in mass.% relative to BR solubilized in 0,5 % SDS-Na before concentration.

Conclusions

Haobacteria is a taxonomic group of extreme aerobic microorganisms having great practical bionanotechnological potential. BR synthesized by these microorganisms is the focus of bio-and nanotechnology because of its high sensitivity and resolution, and may be used in molecular bioelectronics as natural photochromic material for light-controlled electrical regulated computer modules and optical systems. The technology of BR biosynthesis allows obtain milligram quantities of pure crystal protein. The main advantage is that BR retains its natural configuration and the ability to undergo photochemical transformations. By this method is possible to obtain similar to

BR transmembrane proteins of halobacteria – sensorodopsin and halorodopsin. The unique properties of these natural bacteriorhodopsins provide a wide range of optical applications in which they can be applied, because the integration of these proteins in the most advanced technical optical systems is very simple.

References:

1. Oren A. Ecology of extremely halophilic microorganisms / in: The Biology of Halophilic Bacteria, R.H. Vreeland & L.I. Hochstein, eds. – Boca Raton, Florida: CRC Press Inc. 1993, P. 25–54.

2. Shammohammadi H.R. Protective roles of bacterioruberin and intracellular KCl in the resistance of *Halobacterium salinarium* against DNA-damaging agents // J. Radiat. Res. 1998. Vol. 39. № 4. P. 251–256.

3. Lake J.A., Clark M.V., Henderson E., Fay S.P., Oakes M., Scheinman A., Thornber J.P., Mah R.A. Eubacteria, halobacteria, and the origin of photosynthesis: The photocytes // Proc. Natl. Acad. Sci. USA. 1985. Vol. 82. № 11. P. 3716–3720.

4. Ignatov I., Mosin O.V. Studying of phototransformation of light signal by photoreceptor pigments – rhodopsin, iodopsin and bacteriorhodopsin // Nanotechnology Research and Practice. 2014. Vol. 2. № 2. P. 80–95.

5. Mosin O.V., Ignatov I. Evolution and metabolism of halophilic microorganisms // Soznanie I phizicheskaja realnost'. M.: Folium Press, 2013. Vol. 17. № 7. P. 9–21.

6. Pfeiffer F., Schuster S.C., Broicher A., Falb M., Palm P., Rodewald K. Evolution in the laboratory: The genome of *Halobacterium salinarum* strain R1 compared to that of strain NRC-1 // Genomics. 2008. Vol. 91. № 4. P. 335–346.

7. Joshia J.G., Guilda W.R., Handlera P. The presence of two species of DNA in some halobacteria // J. Mol. Biol. 1963. Vol. 6. № 1. P. 34–38.

8. Peck R.F., DasSarma S., Krebs M.P. Homologous gene knockout in the archaeon *Halobacterium salinarum* with ura3 as a counterselectable marker // Mol. Microbiol. 2000. Vol. 35. № 3. P. 667–676.

9. Park J.S., Vreeland R.H., Cho B.C., Lowenstein T.K., Timofeeff M.N., Rosenweig W.D. Haloarchaeal diversity in 23, 121 and 419 MYA salts // Geobiology. 2009. Vol. 7. № 5. P. 515–23.

10. Woese. C. The universal ancestor // Proc. Natl. Acad. Sci. USA. 1998. Vol. 95. № 12. P. 6854–6859.

11. Lake J.A. Origin of the eukaryotic nucleus determined by rate-invariant analysis of rRNA sequences // Nature. 1988. Vol. 331. № 6152. P. 184–186.

12. Mosin O.V., Ignatov I. The photo-transforming photochrome protein bacteriorhodopsin derived from photoorganoheterotrophic halobacterium Halobacterium halobium // Nanoengineering. 2013. № 1. P. 14–21 [in Russian].

13. Mosin O.V., Shvez V.I., Skladnev D.A., Ignatov I. Biosynthesis of transmembrane photo transforming protein bacteriorhodopsin labeled with deuterium on residues of aromatic acids [2,3,4,5,6-$^{2}H_5$]Phe, [3,5-$^{2}H_2$]Tyr and [2,4,5,6,7-$^{2}H_5$] // Nauchnoe priborostroenie. 2013. Vol. 23. № 2. P. 14–26 [in Russian].

14. Oesterhelt D., Stoeckenius W. Rhodopsin – like protein from the purple membrane of *Halobacterium halobium* // Nature. 1971. V. 233. № 89. P. 149–160.

15. Oesterhelt D. Bacteriorhodopsin as an Example of a Light-Driven Proton Pump // Angew. Chemie Intern / Ed. Engl. 1976. P. 16–24.

16. Ignatov I., Mosin O.V. Process of perception of light and evolution of sight at the higher animals and humans // Naukovedenie. 2013. № 3. P. 1–19 [in Russian], [Online] Available: URL: http://naukovedenie.ru/PDF/98tvn313.pdf (May-June 2013).

17. Mosin O.V., Ignatov I. The phototransforming photochrome membrane protein bacteriorhodopsin from purple membranes of halobacterium *Halobacterium halobium* // Nanotechnology Research and Practice. 2014. Vol. 1. № 1. P. 43–56.

18. Mosin O.V., Ignatov I., Skladnev D.A., Shvets V.I. The method of preparation of deuterium-labeled transmembrain protein [^{2}H]bacteriorhodopsin from purple membranes of halobacterium *Halobacterium halobium* // Drug Development and Registration. 2014. Vol. 3. № 8. P. 158–167.

19. Mosin O.V., Shvets V.I., Skladnev D.A., Ignatov I. Biosynthesis of transmembrane photo-transforming protein [^{2}H]bacteriorhodopsine, labeled by deuterium at residues of aromatic amino acids [2,3,4,5,6-$^{2}H_5$]PHE, [3,5-$^{2}H_2$]TYR and [2,4,5,6,7-$^{2}H_5$]TRP // Voprosy Biologicheskoi, Meditsinskoi i Farmatsevticheskoi Khimii / Problems of Biological, Medical and Pharmaceutical Chemistry. 2013. № 8. P. 34–45.

20. Lanyi J.K. Understanding structure and function in the light-driven proton pump bacteriorhodopsin // Journal of Structural Biology. 1998. Vol. 124. P. 164–178.

21. Lanyi J.K. X-ray diffraction of bacteriorhodopsin photocycle intermediates // Molecular Membrane Biology. 2004. Vol. 21. № 3. P. 143–150.

22. Jap B.K., Maestre M.F., Hayward S.B., Glaeser R.M. Peptide-chain secondary structure of bacteriorhodopsin // Biophys J. 1983. Vol. 43. № 1. P. 81–89.

23. Grigorieff N. Electron-crystallographic refinement of the structure of bacteriorhodopsin // Journal of Molecular Biology. 1996. Vol. 259. P. 393–421.

24. Haupts U., Tittor J., Bamberg E., Oesterhelt D. General Concept for Ion Translocation by Halobacterial Retinal Proteins: The Isomerization/Switch/Transfer Model // Biochemistry. 1997. Vol. 36. № 2–7. P. 78–85.

25. Zimanyi L., Cao Y., Needleman R., Ottolenghi M., Lanyi J.K. Pathway of photon uptake in the bacteriorhodopsin photocycle // Biochemistry. 1993. Vol. 32. P. 7669–7678.

26. Mosin O.V., Ignatov I. Improved method for isolation of photochrome transmembrane protein bacteriorhodopsin from purple membranes of halobacterium Halobacterium halobium // Journal of Medicine, Physiology and Biophysics. 2014. Vol. 3. P. 71–86.

27. Vought B.W., Birge R.R. (eds.) Molecular electronics and hybrid computers. / in: *Wiley Encyclopedia of Electrical and Electronics Engineering*. – *New York: Wiley-Inter*science, *1999*. P. 477–490.

28. Mosin O.V., Skladnev D.A., Shvets V.I. The inclusion of deuterated aromatic amino acids in the molecule of bacteriorhodopsin of *Halobacterium halobium* // Applied Biochemistry and Microbiology. 1999. Vol. 35. № 1. P. 34–42.

29. Mosin O.V., Karnaukhova E.N., Pshenichnikova A.B., Reshetova O.S. Electron impact mass-spectrometry in bioanalysis of stable isotope labeled bacteriorhodopsin / in: 6th Intern. Conf. on Retinal proteins. Leiden, the Netherlands, 1994. P. 115.

30. Shuguang W.U., Ellerby L.M., Cohan J.S. Bacteriorhodopsin encapsulated in transparent sol-gel glass: a new biomaterial // Chem. Mater. 19993. Vol. 5. P. 115–120.

31. Weetall H. Retention of bacteriorhodopsin activity in dried sol-gel glass // Biosensors & Bioelectronics. 1996. Vol. 11. P. 325–333.

32. Downie J., Timucin D.A., Smithey D.T., Crew M. Long holographic lifetimes in bacteriorhodopsin films // Optics Letters. 1998. Vol. 23. № 9. P. 730–732.

33. Korposh S.O., Sichka M.Y., Trikur I.I. Films based on bacteriorhodopsin in sol-gel matrices // Proc. of SPIE. 2005. Vol. 5956. № 595616. P. 312–320.

34. Seitz A., Hampp N. Kinetic optimization of bacteriorhodopsin films for holographic interferometry // J. Phys. Chem. B. 2000. Vol. 104. № 30. P. 7183–7192.

35. Mosin O.V., Ignatov I. Synthesis of photo-chrome transmembrane protein bacteriorhodopsin by halobacterium *Halobacterium halobium* // Naukovedenie. 2014. № 2. P. 1–15 [in Russian], [Online] Available: URL: http://naukovedenie.ru/PDF/13TVN214.pdf.

36. Mosin O.V., Ignatov I., Skladnev D.A., Shvets V.I. Biosynthetic incorporation of deuterium-labeled aromatic amino acids – [2,3,4,5,6-$^2H_5$]phenylalanine, [3,5-$^2H_2$]tyrosine and [2,4,5,6,7-$^2H_5$]tryptophan into the molecule of transmembrane protein bacteriorhodopsin from halobacterium *Halobacterium halobium* // European Reviews of Chemical Research. 2014. Vol. 2. № 2. P. 92–108.

37. Mosin O.V., Ignatov I. The natural photo-transforming photochrome transmembrane protein nanomaterial bacteriorhodopsin from purple membranes of halobacterium *Halobacterium halobium* // Journal of Nano and Microsystem Technique. 2013. Vol. 7. P. 47–54 [in Russian].

38. Mosin O.V., Ignatov I. Photochrome protein bacteriorhodopsin from purple membranes of *Halobacterium halobium*. Applications in bio- and nanotechnologies // Journal of Medicine, Physiology and Biophysics. 2014. Vol. 6. P. 42–60.

39. Mosin O.V., Ignatov I. Natural photo-transforming nanomaterial bacteriorhodopsin from *Halobacterium halobium* // Nanomaterials and nanotechnologies. 2012. № 2. P. 47–57.

40. Mosin O.V., Ignatov I. Biosynthesis of photochrome transmembrane protein bacteriorhodopsin of *Halobacterium halobium* labeled with deuterium at aromatic amino acids residues of [2,3,4,5,6-$^2H_5$]Phe, [3,5-$^2H_2$]Tyr and [2,4,5,6,7-$^2H_5$]Trp // Chemistry and Materials Research. 2014. V. 6(3). P. 38–48.

Published in the Russian Federation
European Journal of Molecular Biotechnology
Has been issued since 2013.
ISSN: 2310-6255
E-ISSN 2409-1332
Vol. 8, Is. 2, pp. 103-114, 2015

DOI: 10.13187/ejmb.2015.8.103
www.ejournal8.com

UDC 581.54:582.971.1

The Effect of Drought Stress on the Essential Oil Content and Some of the Biochemical Characteristics of Anise Hyssop (*Agastache foeniculum* [Pursh] Kuntze)*

[1] Sajedeh Saeedfar
[2*] Marzieh Negahban
[3] Mohammad Mahmoodi Soorestani

[1] Islamic Azad University, Unit Karaj, Karaj, Iran
[2] Islamic Azad University, Unit Jahrom, Jahrom, Iran
[3] Department of Horticultural science, College of Agriculture, Chamran University, Ahwaz, Iran
* Corresponding author E-mail: marziehnegahban_86@yahoo.com

Abstract

Plot trials were carried out in a research field in Tehran (Iran) to determine the effect of drought stress on the essential oil content and some of the plant biochemical characteristics of Anise Hyssop (*Agastache foeniculum* [Pursh] *Kuntze*), which is a valuable medicinal plant. Drought stress was conducted at different levels including: well-water (100% FC), mild drought stress (85% FC), moderate drought stress (70% FC), severe drought stress (55% FC), 100% FC (vegetative stage) 85% FC (reproductive stage), 100% FC (vegetative stage) 70% FC (reproductive stage), and 85% FC (vegetative stage) 100% FC (reproductive stage). The experiment was arranged as a RCBD with three replications. The output results showed that, water deficit stress significantly (P≤0.05) increased activities of antioxidant enzymes (Superoxide Dismutase, Catalase, Glutathione Peroxidase) as well as Essential Oil yield and Abscisic Acid content. Lipid and protein oxidation (malondialdehyde and dityrosine contents) also increased significantly under severe water deficit stress. According to the results, severe drought conduction (55% FC) is the optimum level of soil moisture to plant Anise Hyssop under water deficit stress.

Keywords: Anise Hyssop, drought stress, anti oxidative enzymes, biochemical characteristics.

Introduction

Iran is located in arid and semi-arid region. Having an average annual precipitation of 250 mm, Iran receives less than one third of global average precipitation (750 mm). In addition, the rainfall distribution pattern over the country is not the same everywhere. Bearing in mind such a climatic condition, many severe or mild droughts are inevitable to come up. Any drought can inflict a severe damage on the agricultural, domestic and industrial sectors of the country. Due to the growth of population and expansion of the agricultural, energy, and industrial sectors, the

[*] **Abbreviations:** EO – Essential Oil; SOD – Superoxide Dismutase; GPO – Glutathione Peroxidase; MDA – Malondialdehyde; Di-Tyr – Dityrosine; ABA – Abscisic Acid; ROS – Reactive Oxygen Species

demand for water has increased extensively, and water scarcity has been occurring almost every year in many parts of the world [39].

Drought is known as a major abiotic factor that limits plant's growth and production. Although the general effects of drought on plant growth are fairly well known, the primary effects of water deficit at the biochemical and molecular levels are not well understood [11]. Furthermore, the physiologic and metabolic responses of crops to dry environments have been well studied, but similar studies are lacking in medicinal and aromatic plant. Stress is a factor outside plant's body which damages plant growth [27]. Among the abiotic stress, drought is the most important one which affects plants periodically in some growth stages, or permanently in all life cycle [46]. Drought stress usually occurs when available water in soil reduces and atmospheric conditions increase water loss through evapotranspiration [24]. A primary symptom of low available water to plants is the loss of turgor pressure and reduction of cell development especially in stems and leaves. Reduction of cell development makes the plant smaller in size, which is the characteristic of drought stressed plants. Moreover, drought stress disturbs nutrient absorption and reduces leaves growth. Lower leaf area means lower light absorption and photosynthesis. All these events finally decrease plant growth and yield [22]. Drought stress in induced when moisture at the rhizosphere falls below the permanent wilting point (PWP). So the plant is not able to take up sufficient water, resulting in cell dehydration. Dehydration is reversible until a certain point (elastic point); however, is irreversible if the water loss is too server (plastic point) [30]. However, the time duration and frequency of drought stress incident, soil properties and so many other factors affect plant tolerance to drought, and different genotypes may also respond differently [50]. Drought stress induces some morpho–physiological responses in plant such as the reduction of leaf area, shoot growth, enhancement of root growth, stomata closure, reduction of growth rate, sudden antioxidants and soluble compounds accumulation, and activation of some enzymes [23].

Stephanie et al. [54] and later, Asadi [6] reported that drought stress reduced stem length and root length of *Salvia splendens*. Lebaschy and Sharifi Ashoorabadi [31] concluded that higher drought stress levels reduced plant high and shoot weight in some medicinal plants such as *Salvia officinalis* and *Achillea millefolium*. Sangwan et al. [49] reported that mild drought stress decreased lemon grass height, leaf area and leaf weight. Finally, Ardakani et al. [5] reported that drought stress affected shoot yield, essential oil percentage and yield, leaf yield, stem yield, height, the number of tillers, leaf area, stem diameter and the length of internodes in balm (*Melissa officinalis*). Water deficit (commonly known as drought) can be defined as the absence of adequate moisture necessary for normal plant grow and to complete the life cycle [60]. The lack of adequate moisture leading to water stress is common occurrence in rain fed areas, brought about by infrequent rains and poor irrigation [56]. In higher plants the oxygen toxicity is more serious under condition of water-deficit conditions. Water stress causes stomatal closure, which reduces the CO_2/O_2 ratio in leaves and inhibits photosynthesis [25, 41]. These conditions increase the rate of reactive oxygen species (ROS) like superoxide radical ($O_2^{\bullet -}$) hydrogen peroxide (H_2O_2), and hydroxyl radical ($OH^{\bullet}$) particularly in chloroplast and mitochondria [40, 45], *via* enhanced leakage of electrons to oxygen. The superoxide radicals and their dismutation product, hydrogen peroxide, can directly attack membrane lipid and inactivate SH containing enzymes [48].

The hydroxyl radical, one of the most reactive oxygen species, is responsible for oxygen toxicity in vivo, causing damage to DNA, protein, lipids, chlorophyll and almost every other organic constituent of the living cell. Plants protect cellular and sub-cellular system from the cytotoxic effects of active oxygen radicals with anti-oxidative enzymes such as SOD, POX and CAT as well as metabolites like glutathione, ascorbic acid, tocopherol and carotenoids [3]. It has been reported which membranes are subject to damage rapidly with increasing water stress. This leakiness of membranes is caused by an uncontrolled increase in free radicals, which cause lipid peroxidation [53]. The stress induced burst in free radicals could also be partially related to the activity of lipoxygenase, which convert C18:2 and C18:3 to the corresponding hydroxyl peroxides [10]. Further damage to fatty acid could then produce small hydrocarbon fragments including malondialdehyde (MDA) [3]. It is hypothesized that modulation of the activities of these enzymes at early growth stage may be important in imparting resistance to a plant against environmental stresses. Therefore, in the present investigation the relative significance of antioxidative enzymes, MDA, H_2O_2 content, PRO, GB accumulation, photosynthetic activity and membrane permeability has been examined at seedling stage in drought-tolerant and susceptible maize cultivars [20].

Plants subjected to environmental stress evolved a complex and efficient antioxidant system, which includes enzymatic antioxidants and non-enzymatic antioxidants to counteract the detrimental effects of active oxygen species [59]. These are toxic intermediates that result from a reduction in molecular O_2, including superoxide anion (O_2^-), hydrogen peroxide (H_2O_2), and hydroxyl radical (OH) [15]. The role of antioxidative defence systems in plant responses to drought stress was comprehensively documented in *Gypsophila aucheri*, which is a xerophytic plant [51]. In another study, antioxidative and physiological responses of 2 sunflower (*Helianthus annuus*) cultivars under drought stress were evaluated, and the efficiency of antioxidative systems in coping with drought effects was clear [9]. It was also shown that a plant's ability to cope with abiotic stress is mainly related to an altered biochemical profile and produces a varied range of secondary metabolites. Secondary metabolite production is a critical part of the defence response to stress conditions. The role of lipid peroxidation in initiation of secondary metabolites has been documented by some researchers. Consequently, the accumulation of secondary metabolites is mainly related to membrane lipid protection from oxidative stress, and reactive oxygen species (ROS) are the mediators in the biosynthesis of particular secondary metabolites [59]. Water stress decreases growth of some medicinal plants, including *Hypericum brasiliense Choisy* [42] and *Bupleurum chinense DC* [59]. On the other hand, many studies have shown that drought enhances the amount of secondary metabolites in a wide variety of plant species, such as *Rehmannia glutinosa* (*Gaertn.) DC.* [14]. Conversely, drought caused a significant reduction in all growth parameters and essential oil yield and percentage in some medicinal plants such as peppermint (*Mentha piperita L.*) [29, 47]. With the looming prospect of global water crisis, the recent laudable success in deciphering the early steps in the signal transduction of the "stress hormone" – abscisic acid (ABA) has ignited hopes that crops can be engineered with the capacity to maintain productivity while requiring less water input. The involvement of ABA in mediating drought stress has been extensively researched. ABA plays a critical role in regulating plant water status through guard cells and growth as well as by induction of genes that encode enzymes and other proteins involved in cellular dehydration tolerance. Early work showed that ABA can act as a long-distance water stress signal in sensing incoming soil drying [58]. The built up of the hormone then triggers diverse adaptive pathways permitting plants to withstand temporary bouts of water shortage [18, 19, 32]. Two lines of evidences support this claim. The first is that ABA mediates many physiological responses that help plants to survive the abiotic stress. The second is that the stress-related production and catabolism of ABA are themselves delicately stress-regulated. Indeed such delicate regulations make it possible for ABA to act as a stress signal [58].

Anise Hyssop (*Agastache foeniculum (Pursh) Kuntze*) is an erect, branched perennial herb with opposite, toothed leaves and square stems. It is a member of the mint family (*Lamiaceae*), and has a pleasant anise-like aroma. The leaves are ovate-triangular, green above and with soft grey hairs below. Flowers are purple-blue, two-lipped, in a dense terminal spike 4–8 cm long. It blooms from June to September and grows up to 1 m tall. Anise Hyssop has been used by North American First Nations people as a breath-freshener, as a tea and as a sweetener. An infusion of the herb was used for chest pains, and the roots were used for coughs. *Agastache foeniculum* is used in Chinese prescriptions for heatstroke, headache, fever, and angina. Leaves are used as poultices for sores. It is used in dried flower arrangement, and the essential oils are used in perfumes and aromatherapy. It is also a good source of nectar. Anise Hyssop is found mostly in moist, open woods, along streams and lakeshores, and in wet ditches and prairies. It prefers sandy, moist, well-drained loam, in full sun or very light shade. The pH value should be 6.0–6.5. It requires lots of moisture, and wilts if it is too hot. Its natural distribution is from BC across the prairies (in MB north to the Porcupine Mountains) and into western Ontario and the adjacent states. It has been introduced into the northeastern North America [36].

The objective of this experiment was to determine the effect of different levels of drought stress on essential oil yield and some of the biochemical characteristics of Anise Hyssop (*Agastache foeniculum (Pursh) Kuntze*).

Material and Methods

The experiment was conducted in Randomized Completely Block Design with three Replications at the research field of Tarbiat Modares University (Peykan Shahr, Tehran, Iran) in April 2009. Average annual precipitation at the site was 122.2 mm, minimum air temperature was -

5°C and maximum air temperature was 40.4°C. The dominant winds at the area blow from Northeast. The properties of soil at the test site are listed in Table 1. Information about test site climate and meteorological data in 2009–2010 is listed in Table 2 and Table 3, respectively.

Table 1: Physical and chemical properties of the test site soil

B	Mn	Cu	Zn	Fe	Mg	Ca	K	P	N	% organic matter	Electrical conductivity	Acidity	Soil texture
ppm	ppm	ppm	ppm	ppm	ppm	ppm	ppm	ppm	%	%	Ds/ms	pH	
0.6	10.63	0.87	3.37	9.08	381	5045	770	140	0.15	1.73	1.04	7.7	Sandy loam

Seeds were obtained from Zardband Company. Each replication consisted of seven treatments. Seeds were sown in rows with distance of 20 cm and depth of 0.5 cm. The distance of rows in each plot was 40 cm. TDR (Time Domain Reflectometry) apparatus was used to to measure volumetric water content in soil. The TDR technique is based on the measure of dielectric constant of a soil to estimate its volumetric water content. Drought stress was conducted according to percentage of weight moisture. The treatment consisted of 7 FC levels. Due to induce the drought stress, 100% of FC was considered as the well water and 85%, 70%, 55% of FC; 100% FC (vegetative stage), 85% FC (reproductive stage); 100% FC (vegetative stage), 70% FC (reproductive stage); 85% FC (vegetative stage), 100% FC (reproductive stage) were considered as the drought stress treatments. Vegetative organs and flowers were harvested in 3 stages (1 – floret formation, 2 – formation of adult florets, 3 – full flowering) to measure content of essential oil and enzymes activity. Leaf samples were frozen in liquid nitrogen (t = -80°C) to determine enzymes activity, biological markers and Abscisic acid content. EO was extracted by subjecting flowers and leaves together (25 g) to hydro-distillation for 4 h using an all glass Clevenger-type apparatus (Goldis, Tehran, Iran), according to the method outlined by the European pharmacopoeia [4]. EO yield was expressed as percentage (w/w) on dry matter basis.

Table 2: Profile of test site climate

Profile of climate research site	
35° 43 ‘ North	Latitude
51° 8 ‘ East	Longitude
1315 m	altitude
Semi-arid	climatic regime

Table 3: Meteorological Data in 2009–2010

2010 Statistics	2009 Statistics	Meteorology factors making up
17.3	17.5	Average Temperature, °C
41	40.4	Absolute maximum, °C
-16.25	-5	Least desirable, °C
41%	36%	Humidity
2685.4	3201.1	Sun Clock
***	2125.5	Evaporation
West	Northeast	Winds side
20 m/s	16 m/s	Wind speed
277.7 mm	122. 2 mm	Rainfall

Antioxidant Enzyme Activity:

Superoxide Dismutase (SOD) Activity

Frozen leaf segments (0.5 g) were homogenized into a fine powder with a mortar and pestle under liquid nitrogen. Soluble proteins were extracted by homogenizing the powder in 10 ml of 50 mM potassium phosphate buffer (pH=7.0) containing 1 mM EDTA and 1% polyvinylpyrrolidone (PVP). The homogenate was centrifuged at 12000×g for 20 min at 4°C and then the supernatant was used for the following enzyme assays. The amount of soluble proteins was quantified according to the Bradford method with bovine serum albumin as standard. Superoxide dismutase activity was measured spectrophotometrically by monitoring the inhibition of the photochemical reduction of nitroblue tetrazolium (NBT), with the modification as follows: the reaction mixture contained 50 mM phosphate buffer (pH=7.8), 0.1 mM EDTA, 130 mM methionine, 750 μM NBT, 20 μM riboflavin and 0.1 ml enzyme extract. Riboflavin was added at last, and the reaction was initiated by placing the glass test tubes under fluorescent lamps. The reaction was terminated after 25 min by removal from the light source. An illuminated blank without protein gave the maximum reduction of NBT, thus, the maximum absorbance at λ=560 nm. In this assay, one unit of SOD was defined as the amount of enzyme inhibiting the photo-reduction of NBT by 50%. The specific activity of SOD was expressed as units g^{-1} FW.

Catalase (CAT) Activity

CAT activity was estimated by the method of Cakmak and Horst[13]. The reaction mixture contained 100 crude enzyme extract, 500 μl of 10 mmol H_2O_2 and 1400 μl of 25 mmol of sodium phosphate buffer. The decrease in the absorbance at λ=240 nm was recorded for 1 min by spectrophotometer; model Cintra 6 GBC (GBC Scientific Equipment, Dandenong, Victoria, Australia). Enzyme activity of the extract was expressed as enzyme units (μmol min^{-1} substrate) per 1 milligram of protein.

Glutathione Peroxidase (GPX) Activity

GPX activity was measured by the Paglia method in which 0.56 mol (pH=7.0) of phosphate buffer, 0.5 mol of EDTA, 1 mmol of $NaNO_3$, and 0.2 mmol of NADPH were added to the extracted solution; GPX catalyses the oxidation of glutathione (GSH) by cumene hydroperoxide. In the presence of glutathione reductase and NADPH, the oxidized glutathione is immediately converted to the reduced form with the concomitant oxidation of NADPH to NADP. The decrease in absorbance at λ=340 nm and t=+30°C was measured with a spectrophotometer.

Estimation of Malondialdehyde Content

Oxidative damage to lipids was estimated by measuring the content of malondialdehyde (MDA) in leaf. Leaf segments (0.3 g) were homogenized in 10 ml of 10% trichloroacetic acid (TCA), and centrifuged at 12000×g for 10 min. Then 2 ml of 0.6% thiobarbituric acid (TBA) in 10% TCA was added to an aliquot of 2 ml from the supernatant. The mixture was heated in boiling water for 30 min, and then quickly cooled in an ice bath. After centrifugation at 10000×g for 10 min, the absorbance of the supernatant at 440, 532 and 600 nm was determined with a spectrometer (Unicam UV-330, Cambridge, UK). MDA content was calculated as described by Hodges et al. [21].

Estimation of Di-Tyrosine Content

Fresh tissue material (1.2 g) were homogenized with 5 ml of ice-cold 50 mM HEPES-KOH, pH=7.2, containing 10 mM EDTA, 2 mM PMSF, 0.1 mM p-chloromercuribenzoic acid, 0.1 mM *D,L*-norleucine and 100 mg Polyclar® AT. The plan tissue homogenate was centrifuged at 5000 g for 60 min to remove debris. *o,o*-di-tyrosine was recovered by gradient elution from the C-18 column (Econosil C18, 250×10 mm) and was analyzed by the reversed-phase HPLC with simultaneous UV-detection (λ=280 nm). A gradient was formed from 10 mM ammonium acetate, adjusted to pH=4.5 with acetic acid, and methanol, starting with 1% methanol and increasing to 10% over 30 min. A standard di-tyrosine sample was prepared according to Amado et al. (1984). Di-tyrosine was quantified by assuming that it's generation from the reaction of tyrosine with horseradish peroxidase in the presence of H_2O_2 was quantitative (using the molar extinction coefficient e_{315} = 4.5 $mM^{-1}{\cdot}cm^{-1}$ at pH=7.5) [38].

Estimation of Abscisic acid (ABA)

Abscisic acid was extracted, purified and assayed following the procedure described by Li et al. [33] with some modifications using GC–MS technique as reported earlier [38, 44].

Chemicals

Tris-Phosphate Buffer, photodynamic phosphate and EDTA were purchased from LabScan (Dubline, Ireland), $NaNO_3$ and NaDPH were purchased from Flula (Buchs, Switzerland), acetone and acetic acid were purchased from Sigma-Aldrich (Buchs, Switzerland).

Hydro-distillation

After recording their fresh biomass, 25 g of each *Agastache foeniculum [Pursh] Kuntze*) organs (leaves, flowers, stems, seeds) were air dried during 15 days. In order to extract their EO, they were subjected to conventional hydrodistillation for 4 h. Then, extraction of all replications belonging to each treatment was mixed, and final extractions were analyzed. The hydrodistillation was performed by a simple laboratory Quikfit apparatus which consisted of a 2000 ml distillation flask, a condenser and a receiving vessel. For the determination of the yield, the EO was weighed on an analytical scale.

Results and Discussion

Effect of drought stress on Essential Oil content (EO)

The data of this investigation (Table 4) showed that drought stress had a significant (P≤0.05) effect on the essential oil content. The most important characteristic of medicinal plants is the EO yield. Fortunately, EO of *Agastache foeniculum [Pursh] Kuntze* in this experiment enhanced significantly (P≤0.05) at 55% FC. The EO yield was 1.84% in well-water treated plants. It peaked 2.30% at 55% FC. In other words, the highest EO content was obtained at 55% FC. On the other hand, the lowest amount of EO was obtained at 100% FC (vegetative stage) and 70% FC (reproductive stage) (1.64%). EO yield decreased gradually from 2.30 at 55% FC to 1.64% at 100% FC (vegetative stage) and 70% FC (reproductive stage). EO yield had a small increase at 85% FC (vegetative stage) and 100% FC (reproductive stage) compared with 100% FC (vegetative stage) and 70% FC (reproductive stage). Generally, drought stress conduction increased the biosynthesis of the EO in the leaves of *Agastache foeniculum [Pursh] Kuntze*.

Drought stress increases the essential oil percentage of more medicinal and aromatic plants, because in case of stress, more metabolites are produce in the plants and substances prevent from oxidization in the cells, but essential oil content reduce under drought stress, because the interaction between the amount of the essential oil percentage and shoot yield is consider important as two components of the essential oil content and by exerting stress, increases the essential oil percentage but shoot yield decreases by the drought stress, therefore essential oil content reduces [1]. The effect of water stress on essential oil was studied in excised leafs of Palmarosa (*Cymbopogon martinii var. motia*) and Citronella Java (*C. winterianus*). Essential oil percentage was increased under water stress and essential oil content was decreased under this condition [17]. An experiment was carried out to study the influence of water deficit stress on essential oil of balm. The results of this experiment showed that essential oil yield was reduced under water deficit stress but essential oil percentage was increased under stress [1]. Also, Khalid [28] evaluated the influence of water stress on essential oil of two species of an herb plant that is *Ocimum basilicum L.* (sweet basil) and *Ocimum americanum L.* (American basil). For both species under water stress, essential oil percentage and the main constituents of essential oil increased. Seventy five percent of field water capacity resulted in the highest yield of herb and essential oil for both species. Also, three parsley cultivars (plain-leafed, curly-leafed and turnip-rooted) were grown under conditions of 35–40% and 45–60% water deficit in order to evaluate the effect of this form of stress on essential oil yield [2].

Table 4: Effect of drought stress on the measured traits*

Treatment	ABA (ppm)	Di-Tyr (mM/mg protein)	MDA (mM/mg protein)	GPX (mg/Unit protein)	CAT (mg/Unit protein)	SOD (mg/Unit protein)	EO Yield, %
1. T1	^{cd}31.07	^{b}11.43	^{c} 24.67	^{b}**36/3**	^{c}84.6	^{c}831.3	^{ab}1.844

2. T2	[bcd]39.9	[b]12.4	[b]39.23	[b]**39/97**	[c]85.27	[c]837	[ab]1.7316
3. T3	[ab]42.73	[b]12.33	[b]39.4	[a]**58/93**	[b]113	[b]1191	[ab]1.8597
4. T4	[a]52.57	[a]29.57	[a]2.47	[a]**60/83**	[a]135.5	[a]1515	[a]2.3077
5. T5	[d]30	[b]11.43	[c]25.53	[b]**37**	[c]89.47	[c]827.7	[ab]1.7249
6. T6	[cd]31.1	[b]11.9	[c]25.7	[b]**36/9**	[c]84.13	[c]839	[b]1.6449
7. T7	[abc]41.93	[b]12.63	[b]38.53	[a]**58/5**	[c]84.17	[c]833	[ab]1.7741

Notes* T1 – 100% FC, T2 – 85%FC, T3 – 70% FC, T4 – 55% FC, T5 – 100% FC (vegetative stage)–85% FC (reproductive stage), T6 – 100% FC (vegetative stage)–70% FC (reproductive stage), T7 – 85% FC (vegetative stage)–100% FC (reproductive stage); means in a column followed by the same letter are not significantly different at P≤0.05.

Effect of drought stress on Superoxide Disesmutase activity (SOD)

Drought stress significantly activated antioxidant system of leaves of Anise Hyssop. As regards SOD activity, it varied widely (Table 4). SOD activity was about 831.3 mg/Unit protein at well-water treatment. Mild water deficit resulted in a slight increase of SOD activity, but it increased significantly (P≤0.05) to 1515 mg/Unit protein when soil water content dropped to 55% FC. However, it decreased remarkably to 827.7 mg/Unit protein at 100% FC (vegetative stage) 85% FC (reproductive stage) compared with well-water treatment.

The activity of superoxide dismutase was assayed as given by Dhindsa et al. [16]. The superoxide dismutase activity enhanced continuously with the increase of drought stress levels. It is known that plants have a well-organized defense system against reactive oxygen species (ROS) under stress conditions and SOD constitutes the first line of defense via detoxification of superoxide radicals [20, 48]. It seems when the intensity of water deficit stresses increase too much in crops, the physiological damages will increase, too. Thus, they can not promote their antioxidant defensive mechanism along with the intense of water deficit in parallel manner. In other words, in severe water deficit stress condition, the antioxidant defensive mechanism of crops will be activated as well and the antioxidants content will increase as compared to the full-irrigated. But, due to the excessive physiological damages resulted of water deficit stress, the antioxidant activities are less than mild water deficit level. These findings can be related as the ability of the crops against different intensities of water deficit stress. Previously, an increase in the level of antioxidants was reported with an increase in stress intensity in maize and soybean by Vasconcelos et al. [55], Jiang and Zhang [26] which might be attributed to inhibitory effects of water stress on protein turnover causing depletion of antioxidants. Moreover, Masoumi et al. [38] reported a positive and significant correlation between SOD and CAT under both conditions of well irrigated and water deficit stress conditions.

Effect of drought stress on Catalase activity

Analysis of variance for catalase content showed that, there were significant differences (P≤0.05) among irrigation levels (Table 4)**.** Drought stress conduction enhanced significantly (P≤0.05) catalase activity (mg/Unit protein). In other words, the enhancement of catalase activity was 1.6-fold when soil moisture reached the lower values of available soil water (55% FC) compared with well-watered plants. However, it showed a wide difference at 100% FC (vegetative stage), 85% FC (reproductive stage) and 100% FC (vegetative stage) 70% FC (reproductive stage) levels (about

89.47 and 84.13 mg/Unit protein, respectively) compared with well-water treatment (84.6 mg/Unit protein).

Nayar and Kaushal [43] also reported that the increased activity of CAT and POX enzymes constitute potential defense mechanism against chilling induced oxidative damage in germinating wheat grains. In other words, drought stress enhanced enzyme activity of Catalase in wheat. The activity of Catalase was determined as described by Siminis et al. [52]. The combined action of CAT and SOD converts the toxic O_2 and H_2O_2 into water and molecular oxygen, averting the cellular damage under unfavorable conditions like water stress.

Masoumi et al. [38] indicated that activities of the antioxidants (CAT) were increased in all levels of water deficit stress in soybean cultivars. Induction of oxidative stress in drought-stressed plants reported in the previous studies [12, 37]. They showed that enzymatic antioxidants content played an important role in scavenging harmful oxygen species and the activities of antioxidant enzymes were altered when plants were subjected to stress. These results are in agreement with findings of Masoumi et al. [38].

Effect of drought stress on Glutathione Peroxidase activity (GPX)

Regarding Glutathione Peroxidase activity (mg/Unit protein), the activity of well-watered plants was 36.3 mg/Unit protein, although the activity enhanced significantly ($P \leq 0.05$) to 58.93 mg/Unit protein under moderate drought stress (Table 4). In fact, the highest activity of Glutathione Peroxidase was obtained under severe drought stress (60.83 mg/Unit protein). At 100% FC (vegetative stage) and 85% FC (reproductive stage) level, Glutathione Peroxidase activity sank significantly to 37 mg/Unit protein.

Activities of various antioxidant enzymes are known to increase in response to drought. The hydrogen peroxide content enhanced linearly with increasing level of water stress in maize cultivars. It is known that H_2O_2 is a toxic compound that is produced as a result of scavenging of superoxide radicals. Its higher concentration is injurious to plant via lipid peroxidation and membrane injury. Water stress increased Glutathione Peroxidase activity in wheat grains [43]. Sairam and Saxsna [48] studies on three wheat cultivars indicated that water stress increased lipid peroxidation and reduced membrane resistance, the chlorophyll, carotenoid, antioxidant enzymes, ascorbate peroxidase, glutathione reductase and peroxidase significantly. The activity of peroxidase was determined according to Macheix and Quessada [35].

Effect of drought stress on Malondialdehyde (MDA) content

The effects of drought stress on the levels of lipid peroxides (i.e., MDA content) in leaves of anis hyssop are shown in Table 4. According to the results, the malondialdehyde levels were found to be significantly ($P \leq 0.05$) higher in the water deficit stress levels (mild, moderate and severe) than optimum condition of irrigation.

In other words, the lowest content of MDA was obtained at well-water treatment (24.67 mM/mg protein). However, it peaked under mild and moderate drought stress (39.23 mM/mg and 39.4 mM/mg proteins respectively). In fact, the highest MDA content was obtained under severe drought stress (62.47 mM/mg protein), but as drought stress levels increased [100% FC (vegetative stage) 85% FC (reproductive stage) and 100% FC (vegetative stage) 70% FC (reproductive stage)], the MDA activity sank significantly to 25.53 mM/mg protein for the former and 25.7 mM/mg protein for the latter. However, at 85% FC (vegetative stage) and 100% FC (reproductive stage), the activity of MDA rose widely to 38.53 mM/mg of protein.

Malondialdehyde (MDA), as a breakdown product resulting from lipid peroxidation, has been used as an index for the occurrence of oxidative stress [38]. The MDA content was significantly higher in maize cultivars both under non-stress and water-stress conditions. The rise in MDA content under stress conditions suggests that water stress could induce membrane lipid peroxidation by means of reactive oxygen species (ROS) [48]. Nayar and Kaushal [43] showed that drought stress enhanced MDA content in wheat grains. Moreover, our results are in agreement with Masoumi et al. [38], which showed drought stress significantly increased MDA content in all soybean cultivars.

Effect of drought stress on Di-Tyrosine (Di–Tyr) content

As regards di-tyrosine content (mM/mg protein), it varied widely (Table 4). In fact, drought stress increased significantly (P≤0.05) Di-Tyr content. The highest content of Di-Tyr was obtained under severe drought stress (29.57 mM/mg protein). However, well-watered plants had the lowest Di-Tyr content (11.43 mM/mg protein). There was a significant difference between Di-Tyr content at under severe drought stress and all other treatments, but there were no significant difference between Di-Tyr content under other drought stress levels. According to Nayar and Kaushal [43] results, Di-Tyr content in wheat grains enhanced under water stress condition. Furthermore, these results agreed with results of Masoumi et al. [38]; di-tyrosine levels were found to be significantly higher in the water deficit stress levels than optimum condition of irrigation in soybean cultivars. The elevation of MDA and di-tyrosine in our experiment could be a direct reflection of an oxidative injury of the cells after water deficit stress.

Effect of drought stress on Abscisic Acid content (ABA)

In this study, the ABA content increased significantly in the leaves of Anise Hyssop with an increase in intensity of water deficit stress. According to the biosynthesis of ABA (ppm), well-watered plants had the lowest ABA content (Table 5). However, ABA content peaked under moderate drought stress (42.73ppm). In other words, ABA content enhanced 1.6-fold under severe drought condition.

On the other hand, ABA content decreased to 30 ppm at 100% FC (vegetative stage) 85% FC (reproductive stage). There was a significant rise (P≤0.05) between ABA content at 100% FC (vegetative stage) 85% FC (reproductive stage) and 85% FC (vegetative stage) 100% FC (reproductive stage) levels (30 ppm and 41.93 ppm respectively).

The amount of abscise acid in plant leaves of maize increased under drought stress [7], 1975). ABA accumulated up 10 to 30-fold in plants under drought stress relative to unstressed conditions [19]. Heidari and Moaveni (2009) reported that, the increase in ABA content is suggested to be associated with maintenance of growth of roots and shoots under water stress due to suppression of ethylene in case of maize. Lobato et al. [34] have been found a positive and significant correlation between content of antioxidants with accumulation of ABA in soybean cultivars. Masoumi [38] reported that there is a positive and significant correlation between ABA, antioxidant enzymes, at the extreme severe deficit stress.

Table 5: Analysis of variance of the effect of drought stress on the measured traits

SOV	DF	EO Yield	SOD	CAT	GPX	MDA	Di-Ty	ABA
Replication	2	0.01^{ns}	1618.857^{ns}	25367.935^{ns}	3.939^{ns}	3.918^{ns}	0.438^{ns}	3.443^{ns}
Drought stress	4	0.142^{**}	203751.667^{**}	24444.241^{**}	440.419^{**}	243.183^{**}	45.593^{**}	222.248^{**}
Error	12	0.006	2179.357	2655.270	17.170	13.103	6.146	1.713
CV%		1.21%	4.93%	12.37%	8.96%	14.67%	19.42%	11.19%

Notes: ns – non significant; * – significant at P≤0.05; ** – significant at P≤0.01

Conclusions

The results showed that, water deficit stress significantly (P≤0.05) increases activities of antioxidant enzymes (Superoxide Dismutase, Catalase, Glutathione Peroxidase) as well as Essential Oil yield and Abscisic Acid content. Lipid and protein oxidation (malondialdehyde and dityrosine contents) also increased significantly under severe water deficit stress. According to the results, severe drought conduction (55% FC) is the optimum level of soil moisture to plant Anise Hyssop under water deficit stress.

Acknowledgements

This work is dedicated to the memory of Dr. Seyed Mehdi Miri for his collaboration and providing figure quality.

References:

1. Aliabadi Farahani H., Valadabadi S.A., Daneshian J., Khalvati M.A. (2009) Evaluation changing of essential oil of balm (*Melissa officinalis* L.) under water deficit stress conditions. *J. Med. Plant. Res.* 3(5), pp. 329–330.

2. Aliabadi Farahani H., Valadabadi S.A., Daneshian J., Shiranirad A.H., Khalvati M.A. (2009) Medicinal and aromatic plants farming under drought conditions. *Journal of Horticulture and Forestry*. 1(6), pp. 86–92.

3. Alscher R.G., Erturk N., Heath L.S. (2002) Role of superoxide dismutase (SODs) in controlling oxidative stress in plants. *Exp. Bot.* 53, pp. 133–141.

4. Anonymous. *European Pharmacopoeia (1996)* 3rd ed. – London: London Publisher, 1996, pp. 137–138.

5. Ardakani M.R., Abbaszadeh B., Sharifi Ashoorabadi E., Lebaschi M.H., Paknejad F. (2007) Plant acclimation to environmental stress. *Iranian Journal of Aromatic and Medicinal Plants*. 23(2) , pp. 251–261.

6. Asadi S., Lebaschy M.H., Khourgami A., Shirani Rad A.M. (2012) Effect of Drought Stress on the Morphology of Three Salvia sclarea Populations. *Ann. Biol. Res.* 3(9) , pp. 4503–4507.

7. Beardsell M.F., Cohen D. (1975) Relation ships between leaf water status, abscisic acid levels, and stomatal resistance in maize and sorghum. *Plant Physiol.* 156, pp. 207–212.

8. Becana M., Moran J.F., Iturbe-Ormaetxe I. (1998) Iron dependent oxygen free radical generation in plants subjected to environmental stresses: Toxicity and antioxidants. *Plant Soil.* 201, pp. 137–147.

9. Baloğlu M.C., Kavas M., Aydın G., Oktem H.A., Yucel A.M. (2012) Antioxidative and physiological responses of two sunflower (Helianthus annuus) cultivars under PEG-mediated drought stress. *Turk J. Bot.* 36, pp. 707–714.

10. Bell E., Mullet J.E. (1991) Lipoxygenase gene expression is modulated in plants by water deficit, wounding and methyl jasmonate. *Mol. Genet.* 230, pp. 456–462.

11. Bhatnagar-Mathur P., Devi M.J., Vadez V., Sharma K. (2009) Differential antioxidative responses in transgenic peanut bear no relationship to their superior transpiration efficiency under drought stress. *J Plant Physiol.* 166, pp. 1207–1217.

12. Borrmann D., Junqueira R., Sinnecker P., Gomes M., Castro I., Marquez U. (2009) Chemical and biochemical characterization of soybean produced under drought stress. *Ciênc Tecnol Aliment.* 29(3) , pp. 676–681.

13. Cakmak I., Horst W.J. (1991) Effect of aluminum on lipid peroxidation, superoxide dismutase, catalase and peroxidase activities in root tip of soybean (*Glycine max*). *J. Plant. Physiol.* 83, pp. 463–468.

14. Chung I.M., Kim J.J., Lim J.D., Yu C.Y., Kim S.H., Hahn S.J. (2006) Comparison of resveratrol SOD activity, phenolic compounds and free amino acids in Rehmannia glutinosa under temperature and water stress. *Environ. Exp. Bot.* 56, pp. 44–53.

15. Dat J., Vandenabeele S., Vranova E., Van Montagu M., Inze D., Van Breusegem F. (2000) Dual action of the active oxygen species during plant stress responses. *Cell Mol. Life Sci.* 57, pp. 779–795.

16. Dhindsa R.S., Plumb-Dhindhsa P., Thorne T.A. (1981) Leaf senescence: correlated with increased level of membrane permeability and lipid peroxidation, and decreased level of superoxide dismutase and catalase. *J. Exp. Bot.* 32, pp. 93–101.

17. Fatima S., Farooqi A.H.A., Sangwan R.S. (2006) Water stress mediated modulation in essential oil, proline and polypeptide profile in palmarosa and citronella java. In *Physiology and Molecular Biology of Plants*. – Lucknow, India: Central Institue of Medicinal and Aromatic Plants, P.O. CIMAP.

18. Fonseca J.M., Rushing J.W., Rajapakse N.C., Thomas R.L., Riley M.B. (2006) Potential Implications of medicinal Plant Production in Controlled Environments: The case of Feverfew (*Tanacetum parthenium*). *Hort. Science.* 41(3) , pp. 531–535.

19. Fonseca J.M., Rushing J.W., Rajapakse N.C., Thomas R.L., Riley M.B. (2005) Parthenolide and Abscisic acid Synthesis in Feverfew are associated but environmental factors affect them dissimilarly. *J. Plant. Physiol.* 162, pp. 485–494.

20. Helal R.M., Samir M.A. (2008) Comparative response of drought tolerant and drought sensitive maize genotypes to water stress. *Aus. J. Crop Sci.* 1(1) , pp. 31–36.

21. Hodges D.M., DeLong J.M., Forney C.F., Prange R.K. (1999) Improving the thiobarbituric acidreactive-substances assay for estimating lipid peroxidation in plant tissues containing anthocyanin and other interfering compounds. *Planta*. 207, pp. 604–611.

22. Hsaio T.C. (1973) Plant responses to water stress. *Ann. Rev. Plant Physiol.* 24, pp. 519–570.

23. Hughes S.G., Bryant J.A., Smirinoff N. (1989) Application to studies tolerance in plants under stress. In: *Molecular biology*. Hamlyn G.J., Flowers T.J. and Jones M.B, eds. – New York: Cambridge university press.

24. Jaleel C.A., Gopi R., Panneerselvam R. (2009) Effect of drought stress on plants. *Plant Omics J.* 2(1), pp. 30–40.

25. Jason J.G., Thomas G.R., Mason-Pharr D. (2004) Heat and drought influence photosynthesis, water relations, and soluble carbohydrates of two ecotypes of redbud (Cercis Canadensis). *J. Am. Soc. Hort. Sci.* 129(4), pp. 497–502.

26. Jiang M.Y., Zhang J.H. (2002) Role of abscisic acid in water stress-induced antioxidant defense in leaves of maize seedlings. *Free Radic. Res.* 36, pp. 1001–1015.

27. Kafi M., Lahuti M., Zand E., Sharifi H.M., Goldani M. (2000) *Plant Physiology. Effect of environmental conditions on biochemical characteristics of plants*. – Mashhad, Iran: Mashhad University Jahad Publications, 3, pp. 36–43.

28. Khalid Kh.A. (2006) Influence of water stress on growth, essential oil, and chemical composition of herbs (*Ocimum sp.*). *Int. Agrophys*. 20(4), pp. 289–296.

29. Khorasaninejad S., Mousavi A., Soltanloo H., Hemmati K.H., Khalighi A. (2011) The effect of drought stress on growth parameters, essential oil yield and constituent of peppermint (*Mentha piperita L.*). *J. Med. Plant Res.* 5, pp. 5360–5365.

30. Kuchaki A., Nasiri Mahallati M. (1992) Relation of water and soil with plant. In *Crop Ecology*. – Tehran, Iran: Gutenberg Publications, Vol. 1, pp. 250–255.

31. Lebaschy M.H., Sharifi Ashoorabadi E. (2004) Effect of different soil moisture levels on morphological and physiological characteristics of *Dracocephalum moldavica*. *Iranian Journal of Medicinal and Aromatic Plants Research*. 20(3), pp. 249–261.

32. Leung J., Valon C., Moreau B., Boeqlin M., Lefoulon C., Joshi-Saha A., Chérel I. (2012) The ABC of Abscisic Acid action in plant drought stress responses. *Biol. Aujourdhui.* 206(4), pp. 301–312.

33. Li X., La Motte C.E., Stewart C.R., Cloud N.P., Wear-Bagnall S., Jiang C.Z. (1999) Determination of IAA and ABA in the same plant sample by a widely applicable method using GC–MS with selected ion monitoring. *J. Plant Growth Regul.* (Suppl.), pp. 11: 55–65.

34. Lobato A.K.S., Costa R.C., Oliveira Neto C.F., Santos Filho B.G., Cruz F.J.R., Freitas J.M.N., Cordeiro FC. (2008) Physiological and biochemical behavior in soybean (*Glycine max L.*) plants under water deficit. *Aus. J. Crop Sci.* 2(1), pp. 25–32.

35. Macheix J.J., Quessada M.P. (1984) Caractérisation d'une peroxydase impliquée spécifiquement dans la lignification, en relation avec l'incompatibilité au greffage chez l'Abricotier. *Physiol. Végét.* 22, pp. 533–540.

36. Mahmoudi Sarvestani M., Omidbeigi R. (2011) Effect of drought stress on physiological characteristics of Anis hyssop (*Agastache foeniculum [Pursh] Kuntze*). *J. Med. Arom. Plants*. 3, pp. 34–45.

37. Manavalan L.P., Guttikonda S.K., Tran L.S.P. (2009) Physiological and molecular approaches to improve drought resistance in Soybean. *Plant Cell Physiol.* 50(7) , pp. 1260–1276.

38. Masoumi H., Darvish F., Daneshian J., Nourmohammadi G., Habibi D. (2011) Chemical and biochemical responses of soybean (*Glycine max L.*) cultivars to water deficit stress. *Aus. J. Crop Sci.* 5(5), pp. 544–553.

39. Mishra A.K., Singh V.P. (2011) A review of drought concepts. *J. Hydrol.* 391: 202–216.

40. Mittler R. (2002) Oxidative stress, antioxidants and stress tolerance. *Trends Plant Sci.* (Suppl.), pp. 405–410.

41. Moussa H.R. (2006) Influence of Exogenous Application of Silicon on Physiological Response of Salt-Stressed Maize (*Zea mays L.*). *Int. J. Agricult. Biol.* 3(8), pp. 293–297.

42. Nacif de Abreu I., Mazzafera P. (2005) Effect of water and temperature stress on the content of active constituents of *Hypericum brasiliense Choisy*. *Plant Physiol. Biochem.* 43, pp. 241–248.

43. Nayar H., Kaushal S.K. (2002) Chilling induced oxidative stress in germinating wheat grains as affected by water stress and calcium. *Biol. Plant.* 45, pp. 601–604.

44. Nayar H., Bains T., Kumar S. (2005) Low temperature induced floral abortion in chickpea: relationship to abscisic acid and cryoprotectants in reproductive organs. *Environ. Exp. Bot.* 53, pp. 39–47.

45. Neill S., Desikan R., Clarke S., Hurs At R.D., Hancock J.T. (2002) Hydrogen peroxide and nitric oxide as signaling molecules in plants. *J. Exp. Bot.* 53, pp. 1237–1247.

46. Reddy P.C.O., Sairanganayakulu G., Thippeswamy M., Reddy P.S., Reddy M.K., Sudhakar C.H. (2008) Antioxidant enzyme activities and gene expression patterns in leaves of Kentucky Bluegrass in response to drought and post-drought recovery. *Plant Science.* pp. 175: 372–384.

47. Saeidnejad A.H., Kafi M., Khazaei H.R., Safikhani F., Pessarakli M. (2013) Effects of drought stress on quantitative and qualitative yield and antioxidative activity of *Bunium persicum*. *Turk. J. Bot.* 37, pp. 930–939.

48. Sairam R.K., Srivastava G.C., Saxena D.C. (2000) Increased antioxidant activity under elevated temperature: a mechanism of heat stress tolerance in wheat genotypes. *Biol. Plant. 43*, pp. 245–251.

49. Sangwan N.S., Farooqi Abad A.H., Sangwan R.S. (1994) Effect of drought stress on fennel. *New Phytol.* 128, pp. 173–179.

50. Sarmadnia G. (1993) Importance of environmental stresses in agronomy. In: *Proceedings of the 1st Iranian Congress of Crop Science*, Karaj, Iran.

51. Sekmen Esen A.H., Ozgur R., Uzilday B., Tanyolac Z., Dinc A. (2012) The response of the xerophytic plant *Gypsophila aucheri* to salt and drought stresses: the role of the antioxidant defense system. *Turk J. Bot.* 36, pp. 697–706.

52. Siminis C.I., Kanellis A.K., Roubelakis-Angelakis K.A. (1994) Catalase is difficially expressed in dividing and non-dividing protoplasts. *Plant Physiol.* 105, pp. 1375–1383.

53. Smirnoff N. (1993) The role of active oxygen in the presence of plant of water deficit and dessiccation. *New Phytol.* 125, pp. 27–58.

54. Stephanie E.B., Svoboda V.P., Paul A.T., Marc W.V.I. (2005) Controlled drought affects morphology and anatomy of *Salvia solendens*. *Soc. Horticulture.* 130, pp. 775–781.

55. Vasconcelos A.C., Zhang X.Z., Ervin E.H., Kiehl J.D. (2009) Enzymatic antioxidant responses to biostimulants in maize and soybean subjected to drought. *Sci. Agricola.* 66(3), pp. 395–402.

56. Wang F.Z., Wang Q.B., Kwon S.Y., Kwak S.S., Su W.A. (2005) Enhanced drought tolerance of transgenic rice plants expressing a pea manganese superoxide dismutase. *J. Plant. Physiol.* 162, pp. 465–472.

57. Xiao X., Xu X., Yang F. (2008) Adaptive Responses to Progressive Drought Stress in Two Populus cathayana Populations. *Silva Fennica J.* 42(5), pp. 705–719.

58. Zhang J., Jia W., Yang J., Abdelbagi M.I. (2006) Role of ABA in integrating plant responses to drought and salt stresses. *J. Field Crops Res.* 97, pp. 111–119.

59. Zhu Z., Liang Z., Han R. (2009) Saikosaponin accumulation and antioxidative protection in drought-stressed *Bupleurum chinense DC* plants. *Environ. Exp. Bot.* 66, pp. 326–333.

60. Zhu J.K. (2002) Salt and drought stress signal transduction in plants. *Ann. Rev. Plant Biol.* 53, pp. 247–273.